ABSTRACT

SLIVKA, RACHEL MARIE. *Clostridium autoethanogenum* Fermentation Using Sugar and Gaseous Carbon Substrates. (Under the direction of Dr. Mari S. Chinn).

Clostridium autoethanogenum is an anaerobic acetogen that is capable of metabolizing both energy-rich xylose and the single carbon gases (CO and CO_2+H_2) found in synthesis gas (syngas). These features are desirable because they enhance the amount of carbon in lignocellulosic biomass that can be converted through hydrolysis, gasification, and fermentation technology to value-added products such as bio-fuels and bio-chemicals. While *C. autoethanogenum* may be among the limited number of microorganisms that can naturally metabolize xylose, its innate ability to utilize the substrate is hindered without optimization of the fermentation conditions. Assessment of the factors which impacted xylose metabolism ranged from initial xylose concentration to nutrient limitation to pH optimization studies. Once it was discovered that *C. autoethanogenum* preferred a growth-optimized pH (~5.8) for sugar metabolism, the bacteria was able to fully consume all fed xylose (up to 30 g/L) and yield an ideal ethanol to acetate ratio of 1:3 (mass-basis). Unlike other acetogens, *C. autoethanogenum* is a pH sensitive organism which co-produces both acetate and ethanol during growth rather than having a distinct growth-associated acetogenic phase followed by non-growth-associated solventogensis. Ethanol formation serves to prevent acidification of the culture by sequestering excess reductant in an electron sink. *C. autoethanogenum* uses the Wood-Ljungdahl pathway to metabolize CO and CO_2+H_2; however, due to the high reductant demand of the pathway, the bioenergetics provided by syngas as the sole substrate is limited. Preadaptation studies were conducted to determine if inoculum adapted to xylose, syngas, or a sugar-gas mixture would provide an energy boost to the bioenergetics of fermentation systems containing syngas as a sole or co-substrate. Surprisingly, the method by which the organism was acclimated to syngas, and

not sugar preadaptation of the organism, had the largest effect on whether *C. autoethanogenum* could metabolize syngas in an effective and timely manner. Cultures which had stagnant preadaptation to syngas experienced long lags in cell growth, while cultures that used reactor agitation during preadaptation to syngas demonstrated ideal growth profiles. Since the gases present in syngas are sparingly soluble, enhanced mass transfer by means of reactor agitation was required to increase the concentrations of CO, CO_2, and H_2 in the liquid phase so that the cells were able to uptake the gaseous substrate. Based on physiology differences observed between *C. autoethanogenum* cultures grown on xylose, syngas, or a mixture of xylose-syngas, a proteomic analysis was used to illustrate how protein expression changes under each substrate condition. The main pathways which showed changes in protein regulation as a result of the carbon source available included those related to sugar transport, carbon fixation, and energy metabolism. Although future optimization work remains, this study has advanced our overall understanding of *C. autoethanogenum* fermentations involving xylose and syngas as substrates.

Clostridium autoethanogenum Fermentation Using Sugar and Gaseous Carbon Substrates

by
Rachel Marie Slivka

A dissertation submitted to the Graduate Faculty of
North Carolina State University
in partial fulfillment of the
requirements for the degree of
Doctor of Philosophy

Biological and Agricultural Engineering

Raleigh, North Carolina
2018

APPROVED BY:

_____	_____
Dr. Mari Chinn Committee Chair	Dr. Amy Grunden
_____	_____
Dr. Praveen Kolar	Dr. Michael Goshe

DEDICATION

This dissertation is dedicated to my three dogs:

- To the memory of Betsy, I asked God to let you stay with me through graduate school and bless your heart you did. You will always be my little dog.
- To Electra, my little red ball of fun.
- To Blue, my special friend.

BIOGRAPHY

Who am I? I am the granddaughter of a Polish immigrant who used every ounce of gumption she had to raise my father and to give him a better life than she had as a child. I am the great-granddaughter of an Irish milkman from Northeast Ohio. I am a proud descendant of a young couple by the name of Slivka who left their homeland in Slovakia and started a family in America in 1908. I am the sister of a veterinarian who lets me think that I am the "smart" one. I am the daughter of two incredibly gifted, intelligent parents – one is a mechanical engineer and the other is a Special Education teacher.

Hello, I am Rachel. I was born in Northeast Ohio, but moved to Danville, VA with my family when I was nine-years-old. Thank goodness because the weather in the South is considerably more pleasant. After spending my school days as "the girl who always ruined the curve", I decided to attend Virginia Tech and pursued a BS in Chemical Engineering. When I wasn't studying during undergrad, I loved to hike the trails in the area surrounding Blacksburg, VA. My younger sister followed me to Virginia Tech, so I also spent many free hours with her in the land of Hokies. After undergrad, I moved to West Virginia for a brief period to work as a Process Engineer in the polymer industry. Although I enjoyed the hiking there, the job just wasn't for me and I decided to return to academia for a PhD. During graduate school at NC State, I majored in Biological and Agricultural Engineering and found my calling doing fermentation research. I love to bake so the ability to mix ingredients together in a lab was fun for me. While living in Raleigh, NC during graduate school, I took up the new hobbies of Zumba and salsa dancing. I also continued my existing hobbies of "making stuff" which included knitting my first afghan and sewing Halloween costumes for several of the dogs in my family (I love dogs).

ACKNOWLEDGMENTS

I wish acknowledge first and foremost my parents, John and Laura Slivka, who raised me to be the person I am today. Without your love and guidance, I would not have had the courage and perseverance to accomplish as much as I have thus far in life. And thank you so very much for supporting me when I decided to get a PhD! Appreciation also goes to my sister, Reba, who is my best friend and has supported me in my endeavors just as much as I have supported her in her own. You are my cheerleader for life!

A big thank you goes to Dr. Mari Chinn who is absolutely the best research advisor. You have been a fantastic role model and mentor and, on the days when I needed it, you treated me like a true friend.

Last of all, I want to acknowledge my research family: Joscelin Diaz, Matt Whitfield, Ed Godfrey, and Ana Zuleta Correa. We have laughed together, vented about crazy things together, and gone on many a road trip to the field or conferences together. Without your help, graduate life would have been considerably more hectic.

TABLE OF CONTENTS

LIST OF TABLES

LIST OF FIGURES

CHAPTER 1

Gasification and Synthesis Gas Fermentation: An Alternative Route to Biofuel Production

Literature Review

Rachel M. Slivka, Mari S. Chinn, Amy M. Grunden

Adapted from Biofuels. (2011) 2(4), 405-419.

Summary

Lignocellulosic biomass has been identified among the renewable energy sources to have the highest potential to minimize dependency on dwindling supplies of fossil fuels. Conversion of this biomass to biofuels by microorganisms through direct hydrolysis and fermentation can be challenging. Alternatively, biomass can be converted to synthesis gas (a mixture of CO, CO_2, N_2, and H_2) through gasification and transformed to fuels using microbial catalysts that can convert the CO, H_2 and CO_2 to fuels such as ethanol, butanol and hydrogen. Biomass gasification-fermentation processing systems have shown promise and companies are now entering the marketplace for commercial-scale ethanol production from synthesis gas. Isolation of new organisms capable of higher product yield, as well as functional implementation of bioreactors that enhance gas solubility for microbial fermentation, make this technology an attractive option for reducing our dependency on fossil fuels.

Introduction

The world around us is dependent on energy from the cars we drive to the electricity we use to light our homes. However, the natural resources (petroleum, coal, natural gas, etc.) we currently use to supply this energy are limited, and as such, there has been an emphasis placed on development of renewable fuel production systems. The concept of using biomass to produce biofuels began gaining widespread attention in the 1970's (Stephanopoulos, 2007) and since then a variety of concerns from greenhouse gas emissions to volatility in the oil market have made the development of biofuels technology a necessity. While the current production and use of biofuels has gradually advanced, it still needs to grow considerably to have an impact on our energy crisis. For example, the United States produced 30 mega-tons of liquid biofuels in 2008, but it consumed 360 mega-tons of automobile gasoline (International Energy Agency, 2010a;

International Energy Agency, 2010b). On the global level, renewable energy (biofuels, wind, solar, etc.) currently only provides 15% of the total energy supply (Lund, 2007).

Gasification-fermentation is the thermochemical and biological conversion of a biomass substrate to end products such as ethanol, butanol, hydrogen, methane, and acetate. It involves the partial or incomplete combustion of hydrocarbons to yield CO, CO_2, H_2, H_2O, CH_4 and impurities (ash, tar, and minor species) (Bridgwater, 1995; McKendry, 2002). After gasification has occurred, the synthesis gas (syngas) is converted to acids and alcohols by select microorganisms during the fermentation process. There are three primary steps required to make biofuels from biomass-derived gas: gasification of the raw feedstock, purification of the resultant syngas, and use of the syngas in either a biological or chemical process to yield the end products (Demirbas, 2007). Biomass resources that are used in the gasification process range from agricultural residues, forestry residues, and dedicated energy crops to domestic waste. Prime examples include wood, corn stover, cotton stalks, nut shells, bagasse, and grasses (Huber et al., 2006; Sun and Cheng, 2002). The use of these non-food feedstocks and lignocellulosic biomass is a major advantage of using gasification and fermentation to produce ethanol, butanol, hydrogen, and other biofuels (Wei et al., 2009).

As opposed to other methods of preparing raw lignocellulosic biomass for the fermentation process, for example steam explosion, ozonolysis, enzymatic hydrolysis and acid/base treatment to unlock the sugar units, the gasification method requires no gross pre-treatment step other than mechanical break-down of the substrate into small chips (Figure 1.1) (Hayes, 2009; Wei et al., 2009). Steam explosion, ozonolysis, enzymatic hydrolysis and acid/base treatment are often energy intensive and require numerous chemicals and catalysts for completion. In comparison, the decreased amount of pretreatment with gasification significantly

cuts down the amount of energy, time, and money required to prepare the biomass for processing (Sun and Cheng, 2002; Wei et al., 2009). Plus, in the process of separating out the cellulose fraction from hemicellulose and lignin, a large percentage of the initial carbon content may be lost as "waste" because it cannot be fully extracted from the bulk biomass (hemicellulose and lignin are interwoven within the crystalline structure of cellulose which makes it hard to break the chemical bonds), the enzymes responsible for saccharification are inhibited by high sugar concentrations and pretreatment byproducts (Lin and Tanaka, 2006) and product loss is often experienced in handling of processed material. Gasification, on the other hand, allows for more efficient capture of the biomass feedstock as there are no issues with separation of the cellulose fraction from hemicellulose and lignin because process temperatures are sufficiently high enough to break the chemical bonds. For most lignocellulosic biomass, the lignin content alone represents 25-30% of the total mass and 35-45% of the stored chemical energy (Hickey et al., 2010).

Fermentation of a gaseous substrate can improve conversion of the biomass feedstock as there is not a requirement for using microbial systems that metabolize both hexose and pentose sugars. A major drawback of traditional fermentation methods is the fact that many of the microorganisms used (ex. *Saccharomyces cerevisiae; Zymomonas mobilis*) cannot naturally metabolize xylose and other pentose sugars (Jeffries and Jin, 2004). Finally, the use of a gaseous substrate as opposed to dissolved sugars during fermentation permits the decoupling of hydraulic retention time from the amount of available substrate (Henstra et al., 2007). Compared to hydrolysis-fermentation, gasification-fermentation is a more efficient process because it yields at minimum 75% conversion of reactants to products in the gasification stage and over 90% conversion in the fermentation stage (Hickey et al., 2010). On a pound for pound basis,

gasification-fermentation yields almost 60% more ethanol from a unit mass of hardwood than the hydrolysis-fermentation process outputs (Wei et al., 2009). However, with any given process there are technological challenges that need to be addressed. These challenges are discussed further throughout the review.

Gasification

Three transformation and temperature regimes are observed during gasification. In the primary regime, biomass is converted to gaseous H_2O, CO_2, and oxygenated vapors and liquids. Throughout the secondary regime, the oxygenated vapors and liquids react to produce gaseous olefins, aromatics, oils, CO, CO_2, H_2, and H_2O. The temperature during the secondary regime ranges from 700-850°C. Finally, in the tertiary regime, the secondary reaction products are converted to CO, CO_2, H_2, and H_2O at 850-1000°C (Evans and Milne, 1987). Any inorganic compounds present in the feedstock will react to form ash during gasification (Babu, 2005). Gasification is an endothermic process which requires thermal energy to drive its reactions (Munasinghe and Khanal, 2010). Primary reactions that occur during gasification include partial oxidation (Eq. 1), complete oxidation (Eq. 2), and a water gas reaction (Eq. 3).

$$C + \frac{1}{2}O_2 \leftrightarrow CO \qquad (1)$$

$$C + O_2 \leftrightarrow CO_2 \qquad (2)$$

$$C + H_2O \leftrightarrow CO + H_2 \qquad (3)$$

Carbon monoxide, hydrogen, and water vapor from the above reactions also participate in the water gas shift reaction (Eq. 4) and methane formation (Eq. 5) inside the gasifier (McKendry, 2002).

$$CO + H_2O \leftrightarrow CO_2 + H_2 \quad (4)$$

$$CO + 3H_2 \leftrightarrow CH_4 + H_2O \quad (5)$$

Gasification typically occurs under oxygen limited, fuel-rich conditions with an equivalence ratio (mass O_2/ stoichiometric mass O_2) of 0.25 (Kuo, 2005; Reed and Das, 1988). The oxidation reactions occur within the combustion (oxidation) zone of the gasifier, while the remaining reactions occur within the reduction zone. Location of these zones (Figure 1.2) is dependent on the configuration of the gasifier, but regardless of the design, both zones are preceded by a pyrolysis region where the biomass interacts with hot gas and undergoes thermal decomposition (Reed and Das, 1988). High moisture levels in the biomass lower the temperature in the combustion zone of the gasifier which deters the degradation of heavier hydrocarbons. However, when high water content coincides with the presence of CO, this leads to increased production of H_2 and subsequently increased production of methane (McKendry, 2002). Feedstock properties such as moisture content and the presence of ash, alkali, and volatile compounds and feedstock preparation (drying and reduction in particle size) are both vital parameters which have an impact on the ability to achieve proper gasification and to produce the desired products (McKendry, 2002).

Currently there are two types of gasifier designs used: fixed bed and fluidized bed. Fixed bed gasifier configurations can include updraft, downdraft, and cross-flow units, while fluidized bed configurations are either circulating fluidized beds or bubbling beds. Key differences between each gasifier configuration are outlined in Table 1.1 and Figure 1.3 (Bridgwater, 1995; Huber et al., 2006; McKendry, 2002). Fluidized bed gasifiers tend to generate more particulate matter (char and ash) than fixed bed gasifiers. The principles of fluidized bed technology allow these gasifiers to operate at a homogeneous temperature; however, the constant intermixing of the bed material with biomass also allows ash to build up which can lead to slagging (a.k.a. ash melting) (McKendry, 2002; Reed and Das, 1988).

Coal gasification systems have been used since the mid-1800's to produce energy, steam, and heat (Kaupp et al., 1984; Turare, 1997). The two main differences between biomass and coal gasification are the process temperature and the presence of impurities. Biomass has a higher reactivity than coal, and as a result, the gasification temperatures used with biomass are lower than those used with coal. A process that functions at lower temperatures means that less heat is needed to feed the endothermic gasification system for efficient reaction, and the product gas requires less cooling before storage or use in downstream processes. Despite the benefit of being a renewable feedstock, the use of biomass requires additional attention in process development than coal as the presence of potassium, sodium and alkali compounds results in higher rates of slagging and fouling in the gasifier and downstream equipment (Huber et al., 2006). A representative component profile for synthesis gas produced from biomass is shown in Table 1.2. The composition of the product gas obtained from biomass gasification is dependent on the type of oxidant (air or oxygen) used and the reactor geometry (Bridgwater, 1995).

Purification of syngas streams for subsequent use in microbial fermentation systems is necessary because the gas is contaminated with particulates, tars, alkali metals, and trace amounts of chlorine. Without removal of the contaminants, corrosion, erosion, and plugging can occur in downstream equipment and pipes (Bridgwater, 1995). Equipment that can be used to clean processed syngas includes scrubbers, filters, cyclones, and spray towers (Bhattacharya et al., 2001).

Tar levels are dependent on the gasification temperature and the feedstock used (Bridgwater, 1995). At temperatures below 450°C, tar in the product gas can condense in downstream equipment. Tar content is removed by either cooling the product gas to 60-80°C and collecting the particles with electrostatic precipitators or degrading the content into lower

molecular weight compounds through thermal (900-1100°C) or catalytic (800-900°C) cracking. In order to yield product gas with minimal tar content, the recommended configuration is a fixed-bed downdraft gasifier (McKendry, 2002). If cleaning operations are minimal downstream, tar content can also be reduced by using solid catalysts (ex. Ni supported on CeO_2/SiO_2) inside the gasifier (Tomishige et al., 2004).

Microorganisms that can convert synthesis gas components to biofuels

Clostridium is a genus of anaerobic bacteria which is usually found in soils, sewage, and the intestinal tract of animals. These microorganisms are known for their ability to produce ethanol, butanol, acetate, and butyrate during fermentation (Ezeji et al., 2007). The primary bacterium used to determine the mechanism of syngas metabolism, *Moorella thermoacetica* (formerly called *Clostridium thermoaceticum*), belongs to this group (Drake, H. L. et al., 2008; Pierce et al., 2008), and by extension other *Clostridium* are considered to be viable targets for current and future syngas fermentation research. Examples of two ethanol producing species which have been studied in the context of syngas fermentation are *Clostridium autoethanogenum* and *Clostridium ljungdahlii*.

Clostridium autoethanogenum was isolated by Abrini *et al.* (1994) who classified it as an anaerobic, acetogenic bacterium that can metabolize CO, CO_2+H_2, xylose, and other sugars to yield a source of carbon and energy and to produce ethanol and acetate. Its optimal growth is attained at a temperature of 37°C and pH of 5.8-6.0. *Clostridium ljungdahlii* is another acetogenic bacterium which consumes CO, CO_2+H_2, fructose, and xylose and produces ethanol and acetate (Tanner et al., 1993). With optimal growth at 37°C and pH 6.0 (Tanner et al., 1993), *C. ljungdahlii* has been described as having fermentation characteristics similar to that of *C. autoethanogenum* (Abrini et al., 1994). The recent sequencing of *C. ljungdahlii*'s complete

genome has reinforced prior discoveries about the organism and also brought to light several new features (Köpke et al., 2010). The genome confirms that *C. ljungdahlii* has the necessary enzymes for hexose metabolism via the Embden-Meyerhof-Parnas pathway, pentose metabolism via the pentose-phosphate pathway, syngas metabolism via the acetyl-CoA pathway, and ethanol generation. It has genes for three modes of nitrogen incorporation: assimilation of nitrate, direct assimilation of ammonia into amino acids, and the fixing of molecular nitrogen. Finally, the genome shows that rather than using sodium ions or cytochromes and quinones to create a proton gradient, *C. ljungdahlii* uses an Rnf complex which is a series of integral and peripheral membrane proteins used for proton translocation to generate energy (Köpke et al., 2010). Other species that metabolize synthesis gas components are listed in Table 1.3 with their reported values for ethanol, butanol and/or hydrogen production.

Mechanisms of microbial synthesis gas utilization

Depending on the reaction conditions and the concentration of species present, syngas metabolism can be driven towards ethanol, butanol, acetate, and/or butyrate production. The bacteria which catalyze syngas (CO and CO_2+H_2) fermentation to ethanol and acetate are hypothesized to follow the reactions represented by Equations 6-9 (Vega et al., 1989; Vega et al., 1990):

$$6CO + 3H_2O \rightarrow C_2H_5OH + 4CO_2 \quad (6)$$

$$4CO + 2H_2O \rightarrow CH_3COOH + 2CO_2 \quad (7)$$

$$2CO_2 + 6H_2 \rightarrow C_2H_5OH + 3H_2O \quad (8)$$

$$2CO_2 + 4H_2 \rightarrow CH_3COOH + 2H_2O \quad (9)$$

These obligate, anaerobic bacteria are able to transform syngas by means of the Wood-Ljungdahl or acetyl-CoA pathway (Figure 1.4). Lars Ljungdahl completed much of the work to resolve

how CO_2 was reduced to a methyl group, while Harland Wood focused on the transformation of CO_2 into the carbonyl group on acetyl-CoA (Drake et al., 2008). As a result this pathway is broken up into an Eastern methyl branch and a Western carbonyl branch (Ragsdale, 1997; Ragsdale, 2008; Ragsdale and Pierce, 2008). A single CO_2 molecule is reduced by six electrons to CH_3-H_4folate in the methyl branch, while a second CO_2 molecule undergoes reduction to carbon monoxide in the carbonyl branch; at this point a condensation reaction occurs between CO, the methyl group, and coenzyme A to produce acetyl-CoA (Ragsdale, 1997). Acetyl-CoA synthase (ACS) catalyzes the reduction of CO_2 to CO. If acetogenesis is initiated by CO (Eq. 7), three of the CO molecules are oxidized to CO_2 which makes available the six electrons to reduce CO_2 to a methyl group, and the fourth CO molecule assimilates into the pathway as a carbonyl group (Drake et al., 2008; Ragsdale and Pierce, 2008). Acetyl-CoA synthase also catalyzes the oxidation of CO to CO_2, but in this sense it is usually called CO dehydrogenase (CODH) (Drake et al., 1980).

The H_2 component of syngas can provide the source of electrons in these reduction reactions as indicated in equations 8 and 9. For example, *C. ljungdahlii* expresses assimilatory hydrogenases that allow the microbe to uptake H_2 to provide electrons (Köpke et al., 2010). However, the bioenergetics of the microbes can influence the source of electrons used. This is often dictated by the media composition, where the preferential source of electrons can be CO rather than H_2. We have observed use of only CO during batch growth of *C. ljungdahlii* in minimal media when provided syngas components (CO, CO_2 and H_2), whereas in batch growth on complex media components (yeast extract, beef extract and peptone) with syngas, CO, CO_2 and H_2 were all completely utilized.

The acetyl-CoA pathway is the primary route used by acetogenic bacteria to generate fixed carbon and acetyl-CoA and to store energy (Drake et al., 2008; Müller et al., 2004; Ragsdale and Pierce, 2008). If sufficient CO_2 is not provided to acetogens through their external environment, decreased growth may be observed. (Hsu et al., 1990; Savage et al., 1987). Elevated proton and acetate levels also hinder growth because they negatively impact the cell's ability to maintain a proton motive force and transmembrane electrical potential (Baronofsky et al., 1984). The substrate level phosphorylation that occurs during the transition from acetyl-CoA to acetate enables energy storage via ATP generation (Drake et al., 2008).

Unless a catalyst is present, CO and CO_2 are not reactive (Ragsdale, 2008). As described above, the enzyme ACS/CODH catalyzes the conversion of CO_2 to CO and vice versa. The CODH mechanism operates through a "ping-pong" action in which CO reduces CODH, and the reduced protein transfers electrons to an external redox agent that couples to either reduced NAD(P)H or ferredoxin dependent processes (Ragsdale, 2007). ACS also initiates the condensation reaction between CO, the methyl group bound to a corrinoid iron-sulfur protein (CFeSP), and coenzyme A to produce acetyl-CoA (Menon and Ragsdale, 1996). Formate dehydrogenase catalyzes the production of formate from CO_2. Enzymes related to the tetrahydrofolate based reaction steps are (in order of utilization): formyl-H_4folate synthase, formyl-H_4folate cyclohydrolase, methylene-H_4folate dehydrogenase, methylene-H_4folate reductase, and methyltransferase (Pierce et al., 2008). The methyl group of methyl-H_4folate is transported to the cobalt center of a CFeSP by means of methyltransferase (MeTr) catalysis. This action is part of a sequence of unique reactions in the acetyl-CoA pathway which form enzyme-bound bioorganometallic intermediates (Ragsdale, 2008; Ragsdale and Pierce, 2008). The synthesis of acetate from acetyl-CoA is catalyzed by phosphotransacetylase to create acetyl-

phosphate and then acetate kinase to yield acetate (Ragsdale and Pierce, 2008). In a similar fashion, the solventogenesis of ethanol via acetyl-CoA is catalyzed by acetaldehyde dehydrogenase to yield acetaldehyde and then ethanol dehydrogenase to produce ethanol (Ezeji et al., 2007). The acetyl-CoA pathway is linked to sugar metabolism by means of pyruvate ferredoxin oxidoreductase (PFOR) which catalyzes the oxidative decarboxylation of pyruvate to form acetyl-CoA and CO_2 and the reductive carboxylation of acetyl-CoA to yield pyruvate (Furdui and Ragsdale, 2000; Ragsdale, 2003).

Synthesis gas fermentation

Based on the mechanics of the acetyl-CoA pathway, acetate production results in an additional ATP synthesis. However, the production of ethanol does not provide the opportunity for additional ATP production (Klasson et al., 1992). This leads to the assumption that acetate production is growth related, while ethanol production is non-growth related and higher ethanol productivity can be attained if growth is purposely regulated. Cotter *et al.* (2009a) took this concept to the next level and tested the ability to induce resting cultures of *C. autoethanogenum* and *C. ljungdahlii* by removing sources of nitrogen from the liquid media (headspace: inert and batch; carbon: sugar). In media with only yeast extract removed, *C. autoethanogenum* cells showed higher levels of ethanol production and a more desirable ethanol to acetate ratio compared to cells grown under normal, unadulterated conditions. However, with all sources of nitrogen absent, *C. autoethanogenum* was neither able to sustain a stable culture density nor was it able to achieve a genuine resting state. *C. ljungdahlii* cells were able to sustain a stable density with all sources of nitrogen removed, but neither ethanol nor acetate could be produced under these conditions. The lack of significant substrate to product conversion might suggest disrupted metabolic activity. Overall, the study could not confirm the growth related assumption.

Ramachandriya *et al.* (2010) also tried to alter the metabolic state of cell cultures by heat shocking *Clostridium* strain P11 cells to induce sporulation and trigger increased solventogenesis. Cells heat shocked at 92°C consumed more synthesis gas (headspace gas was replenished every 24 hours, biomass-derived (BD) syngas), and had higher ethanol yields, ethanol to acetate ratios, and cell densities than control cultures. Furthermore, the heat shocked cells transitioned from acid to solvent production a full day earlier than the control cells.

Efforts to increase the ethanol yield over acetate in Clostridia include supplementing the media, nutrient limiting conditions (ex. nitrogen limitation), addition of a reducing agent, pH shifts, and addition of hydrogen (Cotter et al., 2009a; Cotter et al., 2009b; Heiskanen et al., 2007; Hu et al., 2010; Kundiyana et al., 2010; Munasinghe and Khanal, 2010). The availability of reducing agents is important because they lower the reduction-oxidation (redox) levels of the microbial environment and impact the solubility of nutrients. Anaerobic microorganisms are capable of greater metabolic activity at more negative redox potentials (-200 to -500 mV) (Hickey et al., 2010). Reducing agents can be supplied to change the flow of electrons so that carbon flow and acid intermediates can be directed towards the production of ethanol (Klasson et al., 1992). Frankman (2009) found that the reducing agent cysteine sulfide had a bigger influence on redox potential than the composition of the syngas used in the fermentation vessel during growth of *C. carboxydivorans* for ethanol production. In fact, Hu *et al*. (2010) found that higher cysteine sulfide concentrations in the media during growth of *Clostridium* strain P11 on synthetic-mixed (SM) syngas led to enhanced ethanol production while lower concentrations triggered acetogenesis. Another approach used to raise the overall ethanol yield obtained from syngas fermentation is conversion of the acetate fraction from the product broth to H_2 and CO_2

with microbial oxidation. The newly formed gases are then fed back into the fermentation vessel to undergo reaction again (Simpson et al., 2009).

Culture medium formulations are key to establishing stable bacterial cultures that can effectively ferment synthesis gas. Media for acetogenic bacteria usually consist of reducing agents, a protein source, trace elements, minerals, and vitamins to produce a healthy cell culture. Phillips *et al*. (1993) found that nutritional factors affected cell concentrations which influenced ethanol and acetate yields for *C. ljungdahlii* grown on SM syngas. Since growth of *C. ljungdahlii* in Pfennig's basal medium yields low cell concentrations (<500 mg/L), it was thought that enriching the medium would provide higher cell yields. However, the doubling of medium component concentrations resulted in severe growth inhibition, likely due to osmotic effects on the cells. Limiting B-vitamin concentrations and elimination of yeast extract were shown to slightly reduce cell growth, but enhance ethanol to acetate ratios. Iron was also determined to be a limiting trace metal (which may be related to the fixation of CO and CO_2 by carbon monoxide dehydrogenase). An elemental analysis of macronutrients and micronutrients from this media formulation study indicated that many of the elements were provided in excess. Therefore, further medium optimization studies are warranted as it is known that the presence of nutrients in excess can be growth limiting.

In a recent study by Guo *et al.* (2010), an attempt was made to improve the fermentation media used with *C. autoethanogenum*. Rather than using the standard DSMZ 640 basal medium for *C. autoethanogenum*, the medium formulation defined by Rajagopalan *et al.* (2002) was used as a starting point and then certain ingredients were optimized. Their new medium formulation uses an initial pH of 4.8 and adjusts components to the following amounts: 0.15 g/L yeast extract, 1.69 g/L NH_4Cl, 1.0 g/L NaCl, 0.1 g/L KH_2PO_4, 0.12 g/L $MgSO_4$, and 0.02 g/L $CaCl_2$.

In experimental trials, the new medium generated a maximum ethanol yield of 260 mg/L (a fairly high value for *C. autoethanogenum* cells) with CO (batch headspace, SM) used as the only source of carbon. In a similar study, all or part of the growth media was replaced with cotton seed extract during fermentation with *Clostridium* strain P11. The results under both batch and continuous flow (100 ccm) SM syngas conditions were positive and suggest the possibility of using cotton seed extract in place of more expensive media components to make the fermentation process more economical (Kundiyana et al., 2010).

Syngas is the central component in gasification-fermentation as it requires successful production and consumption in order to make the overall process work. In an effort to define the best mixture of gases, Heiskanen *et al.* (2007) studied the effect of syngas composition (batch headspace; SM) on a strain of *Butyribacterium methylotrophicum* that was acclimated to grow solely on carbon monoxide. When both carbon monoxide and carbon dioxide (70:30%) were used during fermentation, the growth rate and the product concentrations were significantly higher than with carbon monoxide alone. A possible cause for this shift is the fact that acetyl-CoA, and hence acetate/alcohol, production requires carbon dioxide. With carbon monoxide and hydrogen (70:30%) in the fermentation vessel, there were increased levels of butyric acid, but nearly all of the carbon monoxide was consumed before hydrogen consumption began due to initial inhibition of the hydrogenase enzyme by carbon monoxide. Finally, a fermentation headspace which incorporated all three of the main components in syngas (40:35:25% ratio of H_2:CO:CO_2) gave rise to near perfect carbon yields (Heiskanen et al., 2007). This indicates that all three gases are vital for efficient reactant to product conversion.

Along with media composition, proper reactor conditions are crucial to the sustainability and the efficiency of a fermentation run. A syngas flow rate study with *C. autoethanogenum* and

C. ljungdahlii under continuous gas (5, 7.5, and 10 ccm; SM) and batch liquid conditions showed that higher flow rates can lead to higher growth rates and total product levels, and in some cases, a more optimal ethanol to acetate ratio (Cotter et al., 2009b). The individual rates of gas consumption as a function of the gas feed rate for each syngas component were comparable across all three flow rates for the *C. autoethanogenum* fermentations, but the *C. ljungdahlii* results showed a decrease in CO use at 7.5 ccm versus 5 ccm. This effect was attributed to the reduced gas availability in the media as a result of higher cell densities observed and correlated decrease in dissolved CO in the 7.5 ccm treatments. This study also showed that flow rate impacted the rate of net CO_2 production by the cells and a more acidic initial media pH (5.5 versus 6.8) led to decreased levels of acetate production by *C. ljungdahlii* (Cotter et al., 2009b). Studies have also shown that the optimal pH for syngas fermentation ranges between 5.8 and 7.0 (Munasinghe and Khanal, 2010), however adjustment to media pH over the course of the fermentation can affect final product ratios. Lowering and controlling the media pH (4.0-4.5) in a continuously stirred tank reactor with cell recycle using cells initially grown up in batch (SM; 30 ccm) resulted in ethanol concentrations as high as 48 g/L and acetate concentrations as low as 3 g/L (560 h) (Phillips et al., 1993).

Higher gas pressures increase the solubility of gas in the liquid phase thus enabling higher rates of mass transfer and bioconversion (Hickey et al., 2010). Work by Younesi *et al.* and Najafpour and Younesi (Najafpour and Younesi, 2006; Younesi et al., 2005) supports this claim as maximum values for ethanol production, ethanol to acetate ratio, CO_2+H_2 consumption, and CO conversion using SM gases were all observed at the highest test pressures used during experimental treatments in batch reactors. This also agrees with a prior *Peptostreptococcus productus* study which modeled the results of CO consumption at various gaseous substrate flow

rates and found that higher total operating pressures were conducive to increased reactor productivity (Vega et al., 1990). *P. productus* is an acetogen which metabolizes CO and CO_2 plus H_2 primarily to acetic acid and CO_2 (Lorowitz and Bryant, 1984). Besides increasing the mass transfer rates, higher pressure also decreased the gas volume which allowed the use of a smaller reactor (Henstra et al., 2007). An analysis of reactor size (50 mL versus 100 mL bottles, both at 1.4 atm) found that although similar mass transfer rates were exhibited, smaller bottles had twice the growth rate because the headspace difference allowed a greater quantity of CO per liter (Frankman, 2009).

In order for a microorganism to convert syngas, the gas molecules must cross the gas-liquid interface and then diffuse through the liquid medium to the cell surface where it can be incorporated into the cell. Mass transfer can be optimized by maximizing the mass transfer coefficient or the motive driving force (Vega et al., 1989). For marginally soluble gases (ex. CO), the magnitude of absorption across the gas-liquid interface is defined by Equation 10 (Klasson et al., 1992).

$$moles\ transported = \frac{H(P_G - P_L)}{K_L a} \qquad (10)$$

H = Henry's law constant

P_G = partial pressure of the substrate in the gas phase

P_L = partial pressure of the substrate in the liquid phase

$K_L a$ = mass transfer coefficient

For *C. carboxidivorans* P7 syngas (SM) fermentations with a continuous gas flow rate of 10 ccm, as the partial pressure of CO increased, the maximum carrying capacity of the cell population also rose (Hurst and Lewis, 2010). The same effect was observed for the amount of ethanol produced during cellular growth of *C. carboxidivorans* P7 (Hurst and Lewis, 2010).

This occurred because higher operating pressures led to higher rates of CO uptake. On the downside is the fact that CO also inhibits growth and CO uptake at dissolved CO tensions of 0.8-1.0 atm, but this accumulation may be avoided at higher pressures by maintaining a high cell density which can absorb greater quantities of CO (Vega et al., 1990).

According to Vega *et al*. (1990), the relationship between mass transfer, kinetics, cell growth, and end product creation can be explained as follows. At low cell densities, there is an overabundance of gaseous species in the liquid phase because there are few cells to consume the substrate. As a consequence, the driving force to produce products is dependent on the kinetic affinity of the reactants in the system (in this case, the metabolic pathway of the cells). However, as the density of cells increases, the concentration of gaseous species in the liquid phase gradually decreases and eventually a point is reached at which the substrate concentration becomes limited and product inhibition may occur. At this point, the driving force behind the rate of reaction shifts and is now associated with the speed of interfacial mass transfer. In short, at the beginning of fermentation, reaction kinetics controls the rate of product (acid, alcohol, or cell) generation. Then as the fermentation progresses, product synthesis becomes dependent on mass transfer rates.

Datar *et al.* (2004) was the first group to demonstrate success in fermenting true biomass derived synthesis gas with *C. carboxidivorans* P7 as the biocatalyst. In trials, which used a continuous gas flow rate of 180 ccm, they noted that the processed synthesis gas caused the cells to stop growing, but growth resumed once the cells were transitioned to a pure gas mixture of CO, CO_2, H_2 and balance N_2. The period of non-growth showed signs of processed syngas metabolism to ethanol, which was consistent with the common assumption that solventogenesis is induced by non-growth related metabolism in acetogenic bacteria. In a follow up study to

Datar *et al.*, Ahmed *et al.* (2006) hypothesized that tar was the growth inhibitor and overcame stunted cell growth by using a 0.025 µm filter to remove contaminant from the processed gas (160 ccm feed flow rate; BD). Another issue that arose during *C. carboxidivorans* P7 trials was inhibition of the hydrogenase enzyme by nitric oxide (Ahmed et al., 2006; Ahmed and Lewis, 2007; Datar et al., 2004). However, provided that nitric oxide levels were kept below 40 ppm, this inhibition was avoided during experimental trials with a processed (BD) gas flow rate of 10 ccm. (Ahmed and Lewis, 2007). The overall significance of this *C. carboxidivorans* P7 work is the illustration of how acetogenic bacteria interact with biomass derived synthesis gas and the types of obstacles that must be dealt with and overcome in order to successfully use this form of the gaseous feedstock. Tar and nitric oxide are both synthesis gas contaminants which are produced during the gasification and/or combustion process. In order for biomass gasification and syngas fermentation to work as a unified concept, each part of the hybrid process chain must be optimized such that the two can fit together effectively and produce maximal results.

Although there is no optimal bioreactor design due to the various characteristics of the microorganisms used in fermentation, the reactor vessel has a big impact on the success or failure of the fermentation process (Kadic, 2010). Aside from the batch reactor, the most common reactor design is a continuous-stirred tank reactor (CSTR) (Figure 1.5) which allows continual gas flow into an agitated reactor with a fixed liquid volume (Klasson et al., 1992; Vega et al., 1990). CSTR's often yield the highest mass transfer rates; however, high shear rates from excessive agitation speeds can be prohibitive to cell growth (Kadic, 2010). Higher impeller speeds break gas bubbles into finer ones which allow the microorganisms greater access to the substrate gas. Finer bubbles also have a slower rising velocity that enables longer gas retention in the liquid medium and higher mass transfer rates (Munasinghe and Khanal, 2010). Younesi *et*

al. (Younesi et al., 2006) affirmed this point through *C. ljungdahlii* fermentation studies in a CSTR as it was found that higher flow rates (ex. 14 ccm), an impeller speed of 550 rpm versus 400 rpm, and pure CO in the headspace led to the highest mass transfer (K_La=135 h^{-1}).

The bubble column reactor is desirable if a long liquid retention time or a sizeable liquid holdup volume is required. These reactors have a simple design, no moving parts, and require minimal upkeep. They also exhibit large mass transfer coefficients and a large area at the gas-liquid interface. On the downside, particles tend to stick together or coalesce in bubble columns along with the occurrence of substantial back-mixing, but these issues can be avoided with the use of inert materials to disrupt bubble coalescence (Charpentier, 1981; Kadic, 2010; Klasson et al., 1992; Vega et al., 1990).

When there is minimal heat exchange, packed columns are often used to achieve small pressure changes and a minimal liquid holdup volume. On an industrial scale, if any of the reactants or products is corrosive, the packed column is a good choice as it is much easier to replace the packing than an agitator or custom made reactor components (Charpentier, 1981; Klasson et al., 1992). Packed column reactors also readily sustain the microorganisms since the microbes can form a biofilm on the packing pieces which offer a high surface area. However, compared to other reactors, the packed column exhibits poor gas and liquid flow rates (Kadic, 2010).

Future perspective

Combined gasification-fermentation technologies offer a unique approach to biofuel production from renewable, non-food biomass. As with every developing technology there are process challenges linked to each unit operation that need to be addressed and solutions integrated for viable commercial implementation. Gasification technology from coal has an

established history, yet the use of biomass resources as a feedstock has new implications on material handling and transport, operational parameters and variability in gas products and impurities. The use of a subsequent fermentation processing step in conjunction with gasification necessitates having gas streams compatible with robust microbial growth, and gas purification methods that are efficient and not cost prohibitive.

The metabolic capacity of microbes to fix single carbon gases and convert them to biofuels is fairly uncommon and is restricted to a distinct group of microorganisms. These microbes are obligate anaerobes and are typically slow-growing, yield low cell densities, and can have complex nutritional requirements. Because of these growth challenges in combination with mass transfer limitations of the gaseous substrate, research to enhance autotrophic culture performance is critical to development of commercial-scale biofuel production using the gasification-fermentation approach.

White *et al.* (2007) have stated that they can maintain bacterial cultures on syngas (both batch and continuous gas flow) for over two months without any replenishment of the initial liquid media components. During fermentation, the ethanol concentration was reported to increase at a constant rate while the acetic acid concentration decreased. Kundiyana *et al.* (2010) witnessed similar results with biomass-derived syngas and a pilot scale fermenter run in batch liquid medium with continuous gas sparging at 900 sccm. Using *Clostridium* strain P11 as their microorganism of choice, they observed a 24 day acetogenesis phase followed by a 35 day solventogenic phase which was dominated by ethanol production. Such advances are required in order for gasification-fermentation to be considered a feasible technology for larger scale operations.

Currently one of the outstanding questions for syngas fermentation is what aspect of the process is most limiting for solvent production. The microbial catalysts are genetically programmed to produce energetically favored products (acids) and limit solvent production that can be inhibiting to cell structure integrity and intracellular enzyme activities. To overcome the innate physiology of these microbes and advance the technology, particular growth conditions and/or genetic modification designed to redirect metabolism towards solventogenesis and manage BD syngas toxicity are critical. Low molecular weight gases such as those required for syngas fermentation have poor solubility in the liquid phase, and therefore can limit substrate availability to the microbes. Enhancing gas-cell interactions through reactor design/configurations, operating parameters, and immobilization techniques are also important to defining an improved process. A combination of research focused on developing better solvent-producing strains and improved microbial gas consumption will help elucidate the most significant factors limiting the process.

Recent advances in these areas have likely enabled technology development centered on the acetogen strains *C. carboxidivorans* and *C. ljungdahlii* to reach the stage where companies are licensing their applications. Coskata, Inc. uses *C. carboxidivorans* as the bacterial biocatalyst in their semi-commercial scale plant which is designed to allow easy scale-up to facilities capable of producing 50 million gallons of cellulosic ethanol a year (Coskata, 2011; Pinatti et al., 2010). In a similar fashion, INEOS Bio is designing a commercial process for *C. ljungdahlii* syngas fermentation (Green Car Congress, 2008; INEOS Bio,. 2011b; Pinatti et al., 2010; Wei et al., 2009) and, in a joint venture with New Planet Energy, has recently begun construction on a commercial-scale ethanol biorefinery that is slated to produce 8 million gallons of ethanol per year (Hayes, 2009; INEOS Bio., 2011a; Layden, 2008). A third company focused

on bringing syngas fermentation technology to the commercial scale is LanzaTech which uses these methods to produce ethanol from both syngas and CO-rich steel mill off gases (Lanza Tech, 2011a; Lanza Tech, 2011b).

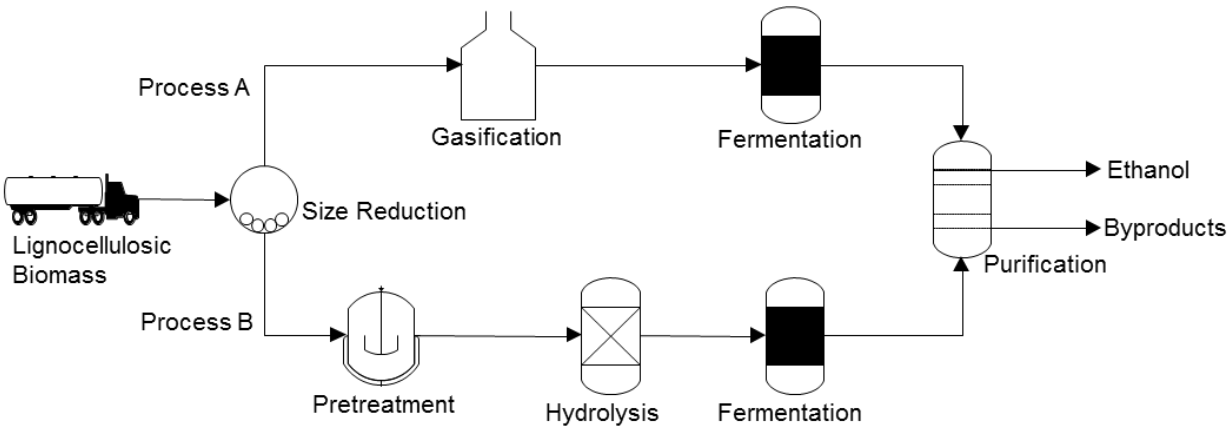

Figure 1.1. Ethanol production process from lignocellulosic biomass. a) Using gasification-fermentation. b) Using traditional methods – pretreatment-hydrolysis-fermentation.

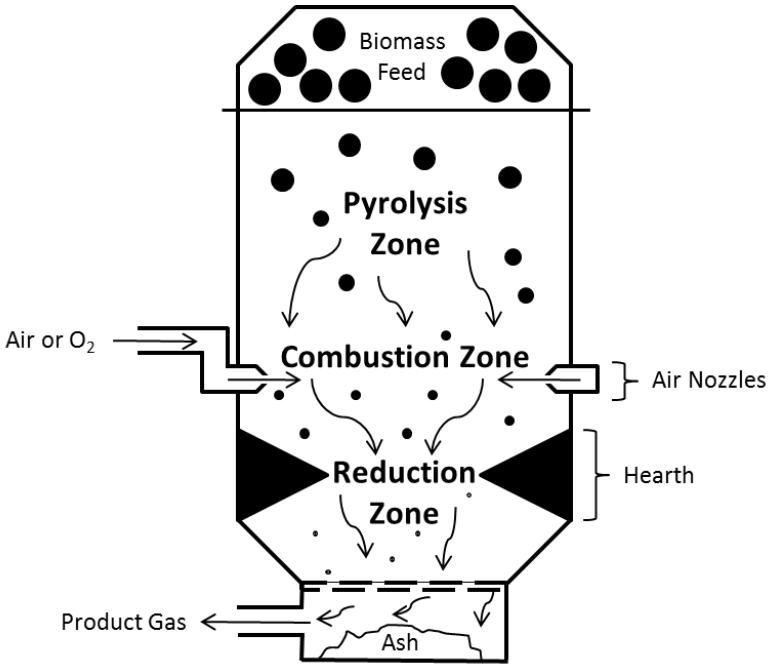

Figure 1.2. Gasification zones in a downdraft gasifier.

Table 1.1. Gasifier configurations.

Type	Biomass/Air Movement
Fixed bed	
Updraft gasifier	• Feed movement is directed downward while air is injected in the upward direction from the bottom of the unit.
Downdraft gasifier	• Feed and air movement are directed downward in the same direction.
Cross-flow gasifier	• Feed movement is directed downward while air is injected in the transverse direction.
Fluidized bed	
Circulating fluidized bed gasifier	• Bed material is circulated from the gasifier to a separation apparatus to remove debris and then back to the gasifier.
Bubbling bed gasifier	• Air is injected at the bottom of the apparatus and bubbled up through the bed material to induce movement.

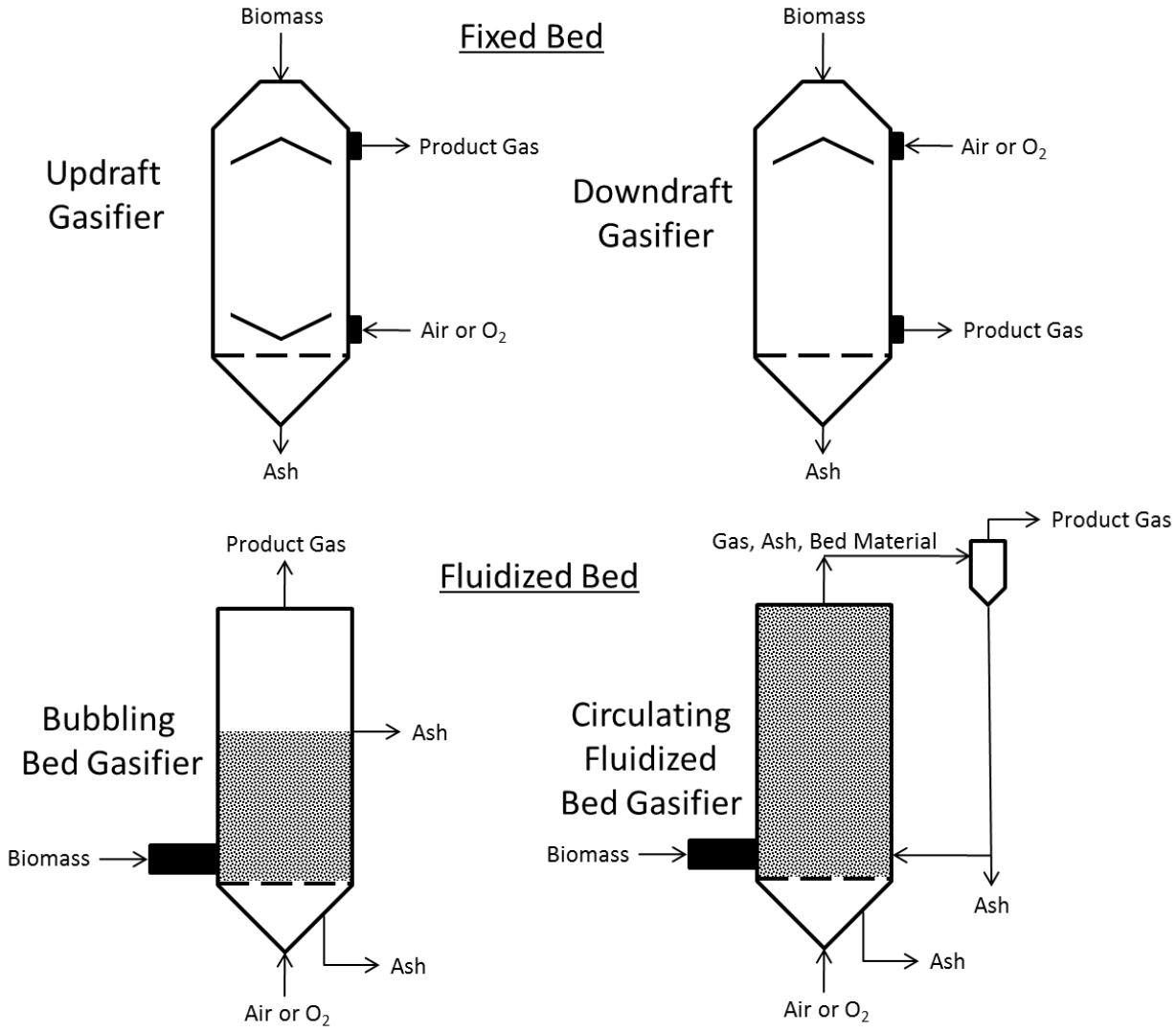

Figure 1.3. Gasification reactor types.

Table 1.2. Composition of synthesis gas from biomass gasification.

Gasifier	Biomass	Component (% Volume, dry)							Reference
		CO	H_2	CO_2	CH_4	C_2H_4	C_2H_6	N_2	
Downdraft	Switchgrass	12-18	7-12	10-17	-	-	-	60	(Kundiyana, Huhnke, and Wilkins, 2010)
Downdraft	95% Hardwood chips	23.9	17	11	1.4	-	-	46.7	(Yang et al., 2009)
Downdraft (air)	n/a	21	17	13	1	-	-	48	(Bridgwater, 1995)
Downdraft (O_2)	n/a	48	32	15	2	-	-	3	(Bridgwater, 1995)
Downdraft	n/a	22.1	15.2	10.2	1.7	-	-	50.8	(Reed and Das, 1988; Reed, 1981)
Updraft (air)	n/a	21	11	9	3	-	-	53	(Bridgwater, 1995)
Multi-stage hybrid	Coconut shell & charcoal	17-22	11-14	10-15	1-3	-	-	50-60	(Bhattacharya et al., 2001)
Bubbling fluidized bed	Empty palm fruit husks	16.6	5.6	19.2	4.3	-	-	54	(Lahijani and Zainal, 2011)
Fluidized bed	Switchgrass	14.7	4.4	16.5	4.2	2.4	-	56.8	(Datar et al., 2004)
Fluidized bed	n/a	14	9	20	7	-	-	50	(Bridgwater, 1995)

Table 1.3. Reported product profiles for microbial species that metabolize syngas to solvents.

Organism	Substrate	Solvent Production	Ethanol: Acetate Molar Ratio	Product Yield	Gas Flow During Reaction	Reference
Ethanol production						
C. ljungdahlii	SM: H_2, CO, CO_2	-	1:9-22	-	Batch (0.088-2.53 atm)	(Vega et al., 1989)
C. ljungdahlii	SM: H_2, CO, CO_2	0.2-2.8 g/L	1:0.8-5	-	Continuous (3.5 ccm)	(Vega et al., 1989)
C. ljungdahlii	Fructose; SM: H_2, CO, CO_2	0.55 g/L	1:1.85	0.41 mg net products/mg CO	Batch (0.08-1.8 atm)	(Younesi et al., 2005)
C. ljungdahlii	Fructose; SM: H_2, CO, CO_2	-	1:0.7-1	1.45-3.25 mmol EtOH/mmol CO	Continuous (8-14 ccm)	(Younesi et al., 2006)
C. ljungdahlii	Fructose; SM: H_2, CO, CO_2	73-175 mg/L	1:8	-	Continuous (5-10 ccm)	(Cotter et al., 2009b)
C. autoethanogenum	Xylose; SM: H_2, CO, CO_2	38-67 mg/L	1:13	-	Continuous (5-10 ccm)	(Abrini et al., 1994; Cotter et al., 2009b)
C. autoethanogenum	SM: CO	260 mg/L	-	-	Batch (1 atm)	(Guo et al., 2010)
C. autoethanogenum	SM: CO	70-355 mg/L	1:1.03-3.6	0.044-0.074 mmol EtOH/mmol CO	Batch (1.97 atm)	(Abrini et al., 1994)
Clostridium strain P11	BD: H_2, CO, CO_2	1.2 g/L	1:1.4	0.055 mol EtOH/mol CO	Fed-batch replenished every 24h (2.56 atm)	(Ramachandriya et al., 2010)
Clostridium strain P11	Cotton seed extract; SM: H_2, CO, CO_2	1.2-2.6 g/L	1:0.09-4	-	Fed-batch replenished every 24h (2.36 atm)	(Kundiyana et al., 2010)
Clostridium strain P11	Cotton seed extract; SM: H_2, CO, CO_2	2-3 g/L	~1:1	-	Continuous (100 ccm)	(Kundiyana et al., 2010)

Table 1.3. (continued).

Clostridium strain P11	Corn steep liquor; BD: H_2, CO, CO_2	25.2 g/L	1:0.15	-	Continuous (900 ccm)	(Kundiyana, Huhnke, and Wilkins, 2010)
C. carboxidivorans P7	SM: CO, CO_2	-	1:0.17	0.075 mol EtOH/mol CO	Continuous (200 ccm)	(Rajagopalan et al., 2002)
C. carboxidivorans P7	BD: H_2, CO, CO_2	1.6 g/L	1:0.19	-	Continuous (180 ccm)	(Datar et al., 2004; Liou et al., 2005)
C. carboxidivorans P7	SM: CO, CO_2	0.5-2.5 g/L	1:0.96	-	Continuous (10 ccm)	(Hurst and Lewis, 2010)
C. carboxidivorans P7	SM: CO	-	1:0.125	0.16 mmol EtOH/mmol CO	Batch (2.27 atm)	(Liou et al., 2005)
Moorella sp. HUC22-1	SM: H_2, CO_2	710 mg/L	1:43	-	Batch (1.97 atm)	(Sakai et al., 2004; Sakai et al., 2005)
Butanol production						
Butyribacterium methylotrophicum	SM: H_2, CO, CO_2	-	-	0.9-1.1 mg net products/mg CO	Batch (1atm)	(Heiskanen et al., 2007; Zeikus et al., 1980)
C. carboxidivorans P7	SM: CO, CO_2	-	1:0.17	0.018 mol BuOH/mol CO	Continuous (200 ccm)	(Rajagopalan et al., 2002)
C. carboxidivorans P7	SM: CO	-	1:0.125	0.04 mmol BuOH/mmol CO	Batch (2.27 atm)	(Liou et al., 2005)
Hydrogen production						
Rhodospirillum rubrum	SM: H_2, CO, CO_2	-	-	0.6-0.7 mmol H_2/mmol CO	Continuous (5-14 ccm)	(Younesi et al., 2008)

SM: synthetic-mix, BD: biomass-derived

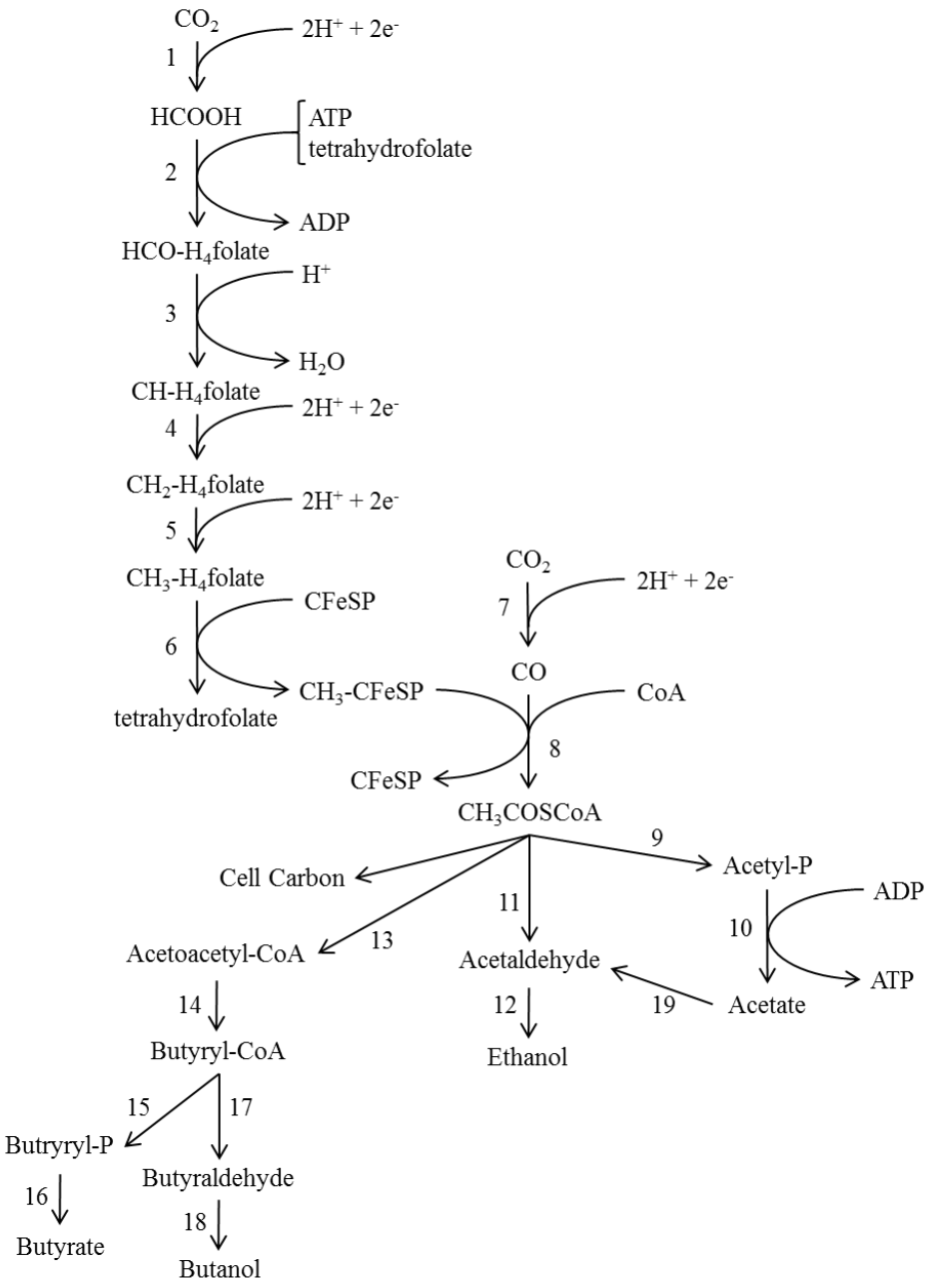

Figure 1.4. Wood-Ljungdahl pathway. 1) formate dehydrogenase; 2) formyl-H_4folate synthase; 3) formyl-H_4folate cyclohydrolase; 4) methylene-H_4folate dehydrogenase; 5) methylene-H_4folate reductase; 6) methyltransferase; 7) CO dehydrogenase; 8) acetyl-CoA synthase; 9) phosphotransacetylase; 10) acetate kinase; 11) acetaldehyde dehydrogenase; 12) ethanol dehydrogenase; 13) thiolase; 14) 3-hydroxybutyryl-CoA dehydrogenase, crotonase, and butyryl-CoA dehydrogenase; 15) phosphate butyltransferase; 16) butyrate kinase; 17) butyraldehyde dehydrogenase; 18) butanol dehydrogenase; 19) aldehyde oxidoreductase. Adapted from (Drake, H. L. et al., 2008; Ezeji et al., 2007; Köpke et al., 2010; Pierce et al., 2008).

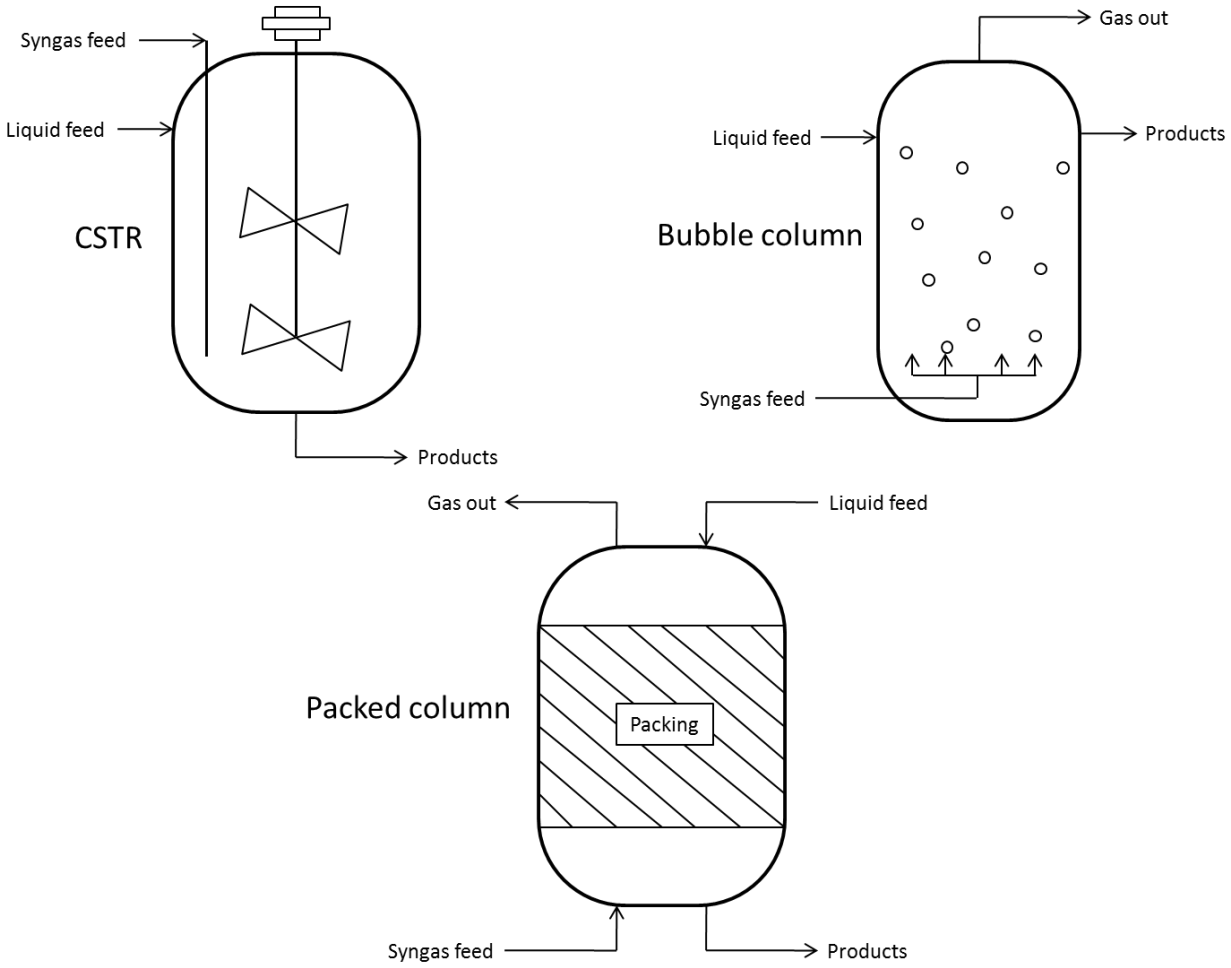

Figure 1.5. Continuous flow bioreactors.

REFERENCES

Abrini, J., Naveau, H., and Nyns, E.J. (1994). *Clostridium autoethanogenum*, sp. nov., an anaerobic bacterium that produces ethanol from carbon monoxide. Arch. Microbiol. *161,* 345-351.

Ahmed, A., Cateni, B.G., Huhnke, R.L., and Lewis, R.S. (2006). Effects of biomass-generated producer gas constituents on cell growth, product distribution and hydrogenase activity of *Clostridium carboxidivorans* P7T. Biomass Bioenergy *30,* 665-672.

Ahmed, A., and Lewis, R.S. (2007). Fermentation of biomass-generated synthesis gas: Effects of nitric oxide. Biotechnol. Bioeng. *97,* 1080-1086.

Babu, S.P. (2005). Observations on the current status of biomass gasification. Biomass & Bioenergy *29,* 1-12.

Baronofsky, J.J., Schreurs, W.J.A., and Kashket, E.R. (1984). Uncoupling by acetic acid limits growth of and acetogenesis by *Clostridium thermoaceticum*. Appl. Environ. Microbiol. *48,* 1134-1139.

Bhattacharya, S., Shwe Hla, S., and Pham, H.L. (2001). A study on a multi-stage hybrid gasifier-engine system. Biomass Bioenergy *21,* 445-460.

Bridgwater, A.V. (1995). The technical and economic feasibility of biomass gasification for power generation. Fuel *74,* 631-653.

Charpentier, J.C. (1981). Mass-transfer rates in gas-liquid absorbers and reactors. Advances in Chemical Engineering *11,* 1-133.

Coskata, Inc. Semi-Commercial Facility. (2011) http://www.coskata.com/facilities/index.asp?source=568A3D3C-AACF-4D95-B297-7264DD2C17B5

Cotter, J.L., Chinn, M.S., and Grunden, A.M. (2009a). Ethanol and acetate production by *Clostridium ljungdahlii* and *Clostridium autoethanogenum* using resting cells. Bioprocess and Biosystems Engineering *32,* 369-380.

Cotter, J.L., Chinn, M.S., and Grunden, A.M. (2009b). Influence of process parameters on growth of *Clostridium ljungdahlii* and *Clostridium autoethanogenum* on synthesis gas. Enzyme Microb. Technol. *44,* 281-288.

Datar, R.P., Shenkman, R.M., Cateni, B.G., Huhnke, R.L., and Lewis, R.S. (2004). Fermentation of biomass-generated producer gas to ethanol. Biotechnol. Bioeng. *86,* 587-594.

Demirbas, A. (2007). Progress and recent trends in biofuels. Progress in Energy and Combustion Science *33,* 1-18.

Drake, H.L., Gößner, A.S., and Daniel, S.L. (2008). Old acetogens, new light. Ann. N. Y. Acad. Sci. *1125,* 100-128.

Drake, H., Hu, S., and Wood, H. (1980). Purification of carbon monoxide dehydrogenase, a nickel enzyme from *Clostridium thermocaceticum*. J. Biol. Chem. *255,* 7174-7180.

Evans, R.J., and Milne, T.A. (1987). Molecular characterization of the pyrolysis of biomass. Energy Fuels *1,* 123-137.

Ezeji, T.C., Qureshi, N., and Blaschek, H.P. (2007). Bioproduction of butanol from biomass: from genes to bioreactors. Curr. Opin. Biotechnol. *18,* 220-227.

Frankman, A.W. (2009). Redox, Pressure and Mass Transfer Effects on Syngas Fermentation. Brigham Young Univeristy.

Furdui, C., and Ragsdale, S.W. (2000). The role of pyruvate ferredoxin oxidoreductase in pyruvate synthesis during autotrophic growth by the Wood-Ljungdahl pathway. J. Biol. Chem. *275,* 28494-28499.

Green Car Congress. INEOS Bio to Commercialize BRI Thermochemical/Biochemical Waste-to-Ethanol Process. (2008) http://www.greencarcongress.com/2008/07/ineos-bio-to-co.html

Guo, Y., Xu, J., Zhang, Y., Xu, H., Yuan, Z., and Li, D. (2010). Medium optimization for ethanol production with *Clostridium autoethanogenum* with carbon monoxide as sole carbon source. Bioresour. Technol. *101,* 8784-8789.

Hayes, D.J. (2009). An examination of biorefining processes, catalysts and challenges. Catalysis Today *145,* 138-151.

Heiskanen, H., Virkajärvi, I., and Viikari, L. (2007). The effect of syngas composition on the growth and product formation of *Butyribacterium methylotrophicum*. Enzyme Microb. Technol. *41,* 362-367.

Henstra, A.M., Sipma, J., Rinzema, A., and Stams, A.J.M. (2007). Microbiology of synthesis gas fermentation for biofuel production. Curr. Opin. Biotechnol. *18,* 200-206.

Hickey R, Basu R, Datta R, Tsai SP. Method of Conversion of Syngas Using Microorgamism of Hydrophilic Membrane. US2010/0047886A1 (2010).

Hsu, T., Daniel, S.L., Lux, M.F., and Drake, H.L. (1990). Biotransformations of carboxylated aromatic compounds by the acetogen *Clostridium thermoaceticum*: generation of growth-supportive CO_2 equivalents under CO_2-limited conditions. J. Bacteriol. *172,* 212-217.

Hu, P., Jacobsen, L.T., Horton, J.G., and Lewis, R.S. (2010). Sulfide assessment in bioreactors with gas replacement. Biochem. Eng. J. *49,* 429-434.

Huber, G.W., Iborra, S., and Corma, A. (2006). Synthesis of transportation fuels from biomass: chemistry, catalysts, and engineering. Chem. Rev. *106,* 4044-4098.

Hurst, K.M., and Lewis, R.S. (2010). Carbon monoxide partial pressure effects on the metabolic process of syngas fermentation. Biochem. Eng. J. *48,* 159-165.

INEOS Bio. INEOS Bio JV Breaks Ground on 1st Advanced Waste-to-Fuel Commercial Biorefinery in U.S. (2011a) http://www.ineosbio.com/76-Press_releases-15.htm

INEOS Bio. Technology Platform. (2011b) http://www.ineosbio.com/60-Technology_platform.htm

International Energy Agency. IEA Energy Statistics - Oil for United States. (2010a) http://www.iea.org/stats/oildata.asp?COUNTRY_CODE=US

International Energy Agency. IEA Energy Statistics - Renewables for United States. (2010b) http://www.iea.org/stats/renewdata.asp?COUNTRY_CODE=US

Jeffries, T., and Jin, Y.S. (2004). Metabolic engineering for improved fermentation of pentoses by yeasts. Appl. Microbiol. Biotechnol. *63,* 495-509.

Kadic, E. (2010). Survey of gas-liquid mass transfer in bioreactors. Iowa State University.

Kaupp, A., Goss, J.R., and United States. Agency for International Development. (1984). Small scale gas producer-engine systems. Vieweg, Wiesbaden, Germany.

Klasson, K.T., Ackerson, M.D., Clausen, E.C., and Gaddy, J.L. (1992). Bioconversion of synthesis gas into liquid or gaseous fuels. Enzyme Microb. Technol. *14,* 602-608.

Köpke, M., Held, C., Hujer, S., Liesegang, H., Wiezer, A., Wollherr, A., Ehrenreich, A., Liebl, W., Gottschalk, G., and Dürre, P. (2010). *Clostridium ljungdahlii* represents a microbial production platform based on syngas. Proceedings of the National Academy of Sciences *107,* 13087-13092.

Kundiyana, D.K., Huhnke, R.L., Maddipati, P., Atiyeh, H.K., and Wilkins, M.R. (2010). Feasibility of Incorporating Cotton Seed Extract in *Clostridium* strain P11 Fermentation Medium During Synthesis Gas Fermentation. Bioresour. Technol. *101,* 9673-9680.

Kundiyana, D.K., Huhnke, R.L., and Wilkins, M.R. (2010). Syngas fermentation in a 100-L pilot scale fermentor: Design and process considerations. Journal of Bioscience and Bioengineering *109,* 492-498.

Kuo, K.K. (2005). Principles of Combustion. John Wiley & Sons, Inc., Hoboken, New Jersey.

Lahijani, P., and Zainal, Z.A. (2011). Gasification of palm empty fruit bunch in a bubbling fluidized bed: A performance and agglomeration study. Bioresour. Technol. *102,* 2068-2076.

LanzaTech. Construction Begins on Steel Mill Off-Gases to Ethanol Demo Plant. (2011a) http://www.lanzatech.co.nz/sites/default/files/imce_uploads/lanzatech_demo_plant.pdf

LanzaTech. The LanzaTech Process. (2011b) http://www.lanzatech.co.nz/content/lanzatech-process

Layden L. Alico won't build Southwest Florida ethanol plant. (2008) http://www.naplesnews.com/news/2008/jun/03/alico-wont-build-southwest-florida-ethanol-plant/

Lin, Y., and Tanaka, S. (2006). Ethanol fermentation from biomass resources: current state and prospects. Appl. Microbiol. Biotechnol. *69,* 627-642.

Liou, J.S.C., Balkwill, D.L., Drake, G.R., and Tanner, R.S. (2005). *Clostridium carboxidivorans* sp. nov., a solvent-producing clostridium isolated from an agricultural settling lagoon, and reclassification of the acetogen *Clostridium scatologenes* strain SL1 as *Clostridium drakei* sp. nov. Int. J. Syst. Evol. Microbiol. *55,* 2085-2091.

Lorowitz, W.H., and Bryant, M.P. (1984). *Peptostreptococcus productus* strain that grows rapidly with CO as the energy source. Appl. Environ. Microbiol. *47,* 961-964.

Lund, H. (2007). Renewable energy strategies for sustainable development. Energy *32,* 912-919.

McKendry, P. (2002). Energy production from biomass (part 3): Gasification technologies. Bioresour. Technol. *83,* 55-63.

Menon, S., and Ragsdale, S.W. (1996). Evidence That Carbon Monoxide Is an Obligatory Intermediate in Anaerobic Acetyl-CoA Synthesis. Biochemistry (N.Y.) *35,* 12119-12125.

Müller, V., Imkamp, F., Rauwolf, A., Küsel, K., and Drake, H.L. (2004). Molecular and cellular biology of acetogenic bacteria. Strict and Facultative Anaerobes: Medical and Environmental Aspects. Horizon Bioscience, Norfolk, UK. 251–281.

Munasinghe, P.C., and Khanal, S.K. (2010). Biomass-derived syngas fermentation into biofuels: Opportunities and challenges. Bioresour. Technol. *101,* 5013-5022.

Najafpour, G., and Younesi, H. (2006). Ethanol and acetate synthesis from waste gas using batch culture of *Clostridium ljungdahlii*. Enzyme Microb. Technol. *38,* 223-228.

Phillips, J.R., Klasson, K.T., Clausen, E.C., and Gaddy, J.L. (1993). Biological production of ethanol from coal synthesis gas: Medium development studies. Applied Biochemistry and Biotechnology *39/40,* 559-571.

Pierce, E., Xie, G., Barabote, R.D., Saunders, E., Han, C.S., Detter, J.C., Richardson, P., Brettin, T.S., Das, A., and Ljungdahl, L.G. (2008). The complete genome sequence of *Moorella thermoacetica* (f. *Clostridium thermoaceticum*). Environ. Microbiol. *10,* 2550-2573.

Pinatti, D.G., Conte, R.A., Soares, ÁG., Pereira, M.L.G., Romão, ÉL., Ferreira, J.C., Oliveira, I., and Marton, L.F.M. (2010). Biomass Refinery as a Renewable Complement to the Petroleum Refinery. International Journal of Chemical Reactor Engineering *8,* 1-16.

Ragsdale, S.W. (2008). Enzymology of the Wood–Ljungdahl pathway of acetogenesis. Ann. N. Y. Acad. Sci. *1125,* 129-136.

Ragsdale, S.W. (2007). Nickel and the carbon cycle. J. Inorg. Biochem. *101,* 1657-1666.

Ragsdale, S.W. (2003). Pyruvate Ferredoxin Oxidoreductase and Its Radical Intermediate. Chem. Rev. *103,* 2333-2346.

Ragsdale, S.W. (1997). The Eastern and Western branches of the Wood/Ljungdahl pathway: how the East and West were won. Biofactors *6,* 3-11.

Ragsdale, S.W., and Pierce, E. (2008). Acetogenesis and the Wood-Ljungdahl pathway of CO_2 fixation. Biochimica Et Biophysica Acta (BBA)-Proteins & Proteomics *1784,* 1873-1898.

Rajagopalan, S., P. Datar, R., and Lewis, R.S. (2002). Formation of ethanol from carbon monoxide via a new microbial catalyst. Biomass Bioenergy *23,* 487-493.

Ramachandriya, K.D., DeLorme, M.J., and Wilkins, M.R. (2010). Heat shocking of *Clostridium* strain P11 to promote sporulation and ethanol production. Biological Engineering *2,* 115-131.

Reed, T.B., and Das, A. (1988). Handbook of Biomass Downdraft Gasifier Engine Systems. Solar Energy Research Institute: Golden, Colorado. 1-140.

Reed, T. (1981). Biomass gasification principles and technologies. Energy Technology Review No. 67. Solar Energy Research Institute Golden, Colorado: Park Ridge, NJ.

Sakai, S., Nakashimada, Y., Inokuma, K., Kita, M., Okada, H., and Nishio, N. (2005). Acetate and ethanol production from H_2 and CO_2 by *Moorella* sp. using a repeated batch culture. Journal of Bioscience and Bioengineering *99,* 252-258.

Sakai, S., Nakashimada, Y., Yoshimoto, H., Watanabe, S., Okada, H., and Nishio, N. (2004). Ethanol production from H_2 and CO_2 by a newly isolated thermophilic bacterium, *Moorella* sp. HUC22-1. Biotechnol. Lett. *26,* 1607-1612.

Savage, M.D., Wu, Z., Daniel, S., Lundie Jr, L., and Drake, H. (1987). Carbon monoxide-dependent chemolithotrophic growth of *Clostridium thermoautotrophicum*. Appl. Environ. Microbiol. *53,* 1902-1906.

Simpson SD, Forster RLS, Rowe M. Microbial Fermentation of Gaseous Substrates to Produce Alcohols. US2009/0203100A1 (2009).

Stephanopoulos, G. (2007). Challenges in engineering microbes for biofuels production. Science *315,* 801-804.

Sun, Y., and Cheng, J. (2002). Hydrolysis of lignocellulosic materials for ethanol production: a review. Bioresour. Technol. *83,* 1-11.

Tanner, R.S., Miller, L.M., and Yang, D. (1993). *Clostridium ljungdahlii* sp. nov., an acetogenic species in clostridial rRNA homology group I. Int. J. Syst. Evol. Microbiol. *43,* 232-236.

Tomishige, K., Asadullah, M., and Kunimori, K. (2004). Syngas production by biomass gasification using $Rh/CeO_2/SiO_2$ catalysts and fluidized bed reactor. Catalysis Today *89,* 389-403.

Turare, C. (1997). Biomass gasification technology and utilization. Artes Institute, University of Flensburg, Germany.

Vega, J., Clausen, E., and Gaddy, J. (1990). Design of bioreactors for coal synthesis gas fermentations. Resour. Conserv. Recycling *3,* 149-160.

Vega, J., Prieto, S., Elmore, B., Clausen, E., and Gaddy, J. (1989). The biological production of ethanol from synthesis gas. Appl. Biochem. Biotechnol. *20,* 781-797.

Wei, L., Pordesimo, L.O., Igathinathane, C., and Batchelor, W.D. (2009). Process engineering evaluation of ethanol production from wood through bioprocessing and chemical catalysis. Biomass Bioenergy *33,* 255-266.

White, A., Ahmed, A., Hu, P., Broderick, A., Sarager, L., Ralston, T., and Lewis, R. Fermentation of syngas to ethanol without media replacement. Paper presented at The 29th Symposium on Biotechnology for Fuels and Chemicals. Denver, CO, 29 April-2 May 2007.

Yang, P., Columbus, E., Wooten, J., Batchelor, W., Buchireddy, P., Ye, X., and Wei, L. (2009). Evaluation of Syngas Storage Under Different Pressures and Temperatures. Appl. Eng. Agric. *25,* 121-128.

Younesi, H., Najafpour, G., and Mohamed, A.R. (2006). Liquid fuel production from synthesis gas via fermentation process in a continuous tank bioreactor (CSTBR) using *Clostridium ljungdahlii*. Iranian Journal of Biotechnology *4,* 45-53.

Younesi, H., Najafpour, G., and Mohamed, A.R. (2005). Ethanol and acetate production from synthesis gas via fermentation processes using anaerobic bacterium, *Clostridium ljungdahlii*. Biochem. Eng. J. *27,* 110-119.

Younesi, H., Najafpour, G., Ku Ismail, K.S., Mohamed, A.R., and Kamaruddin, A.H. (2008). Biohydrogen production in a continuous stirred tank bioreactor from synthesis gas by anaerobic photosynthetic bacterium: *Rhodopirillum rubrum*. Bioresource Technology *99,* 2612-2619.

Zeikus, J., Lynd, L.H., Thompson, T., Krzycki, J., Weimer, P., and Hegge, P. (1980). Isolation and characterization of a new, methylotrophic, acidogenic anaerobe, the Marburg strain. Curr. Microbiol. *3,* 381-386.

CHAPTER 2

Influence of Carbon Source Preadaptation on *Clostridium autoethanogenum*

Rachel M. Slivka, Mari S. Chinn, and Amy M. Grunden

Abstract

Preadaptation of the anaerobic acetogen, *Clostridium autoethanogenum*, to xylose, synthesis gas (CO, CO_2, H_2, and N_2; syngas), and a xylose-syngas mix was conducted to determine if subsequent inoculation of these cells into either a syngas or a xylose-syngas fermentation system could create a bio-energetically superior culture. The presence of xylose during inoculum pre-adaptation had no significant impact on the subsequent fermentations, possibly due to the mechanics of pentose metabolism. However, the manner in which the inocula were pre-adapted to syngas affected whether or not the cultures experienced delayed metabolism in both the syngas and xylose-syngas fermentations. If the inoculum was subjected to agitation during its preadaptation to syngas, then the cells did not experience grow delays during fermentations with syngas present as a substrate. Though, if the inoculum was stationary for the preadaptation to syngas, the inoculum experienced minimal mass transfer of gases into the liquid phase and behaved as if it was not acclimated to syngas as a substrate. Both the xylose pre-adapted and the stationary-xylose-syngas pre-adapted inocula showed a lag in biomass and metabolite (acetate and ethanol) production of 32-48 hours regardless of whether the terminal fermentation had xylose-syngas or syngas as the substrate. Meanwhile, the agitated-syngas pre-adapted and the agitated-xylose-syngas pre-adapted inocula did not exhibit initial delays in growth and substrate utilization. Overall, the xylose-syngas treatment fermentations performed better (410-450 mg dry cells/L) than the syngas treatment fermentations (~100 mg dry cells/L) as a result of the greater availability of carbon and energy provided by the sugar addition. The greater biomass accumulation in the xylose-syngas fermentations also led to higher production of acetate and ethanol.

Introduction

Synthesis gas fermentation, which uses the combined process of gasification and fermentation, offers an alternate method for converting lignocellulosic biomass into biofuels to that of just biochemical processing (Slivka et al., 2011). Within this route, gasification is used to create single carbon gases [carbon monoxide (CO), carbon dioxide (CO_2)] and hydrogen (H_2), often referred to as synthesis gas (syngas) through the incomplete combustion of biomass. Autotrophic bacteria, such as *Clostridium autoethanogenum*, *Clostridium ljungdahlii, Clostridium carboxidivorans, Moorella thermoacetica, and Butyribacterium methylotrophicum* (Abrini et al., 1994; Datar et al., 2004; Heiskanen et al., 2007; Liou et al., 2005; Pierce et al., 2008; Tanner et al., 1993; Vega et al., 1989), possess the capacity to metabolize synthesis gas streams into useful alcohols and acids. *C. autoethanogenum*, which is gaining interest as an organism for study, can utilize not only synthesis gas but also xylose for ethanol production. The capacity for xylose metabolism is a unique characteristic among autotrophs that can be exploited for the purpose of using pentose sugar byproduct streams from biomass processed through conventional pretreatment and enzymatic hydrolysis operations for fuels and chemicals. Often organisms, such as *Zymomonas mobilis* and *Saccharomyces cerevisiae* (Hahn-Hägerdal et al., 2007; Jeffries, 2006; Zhang et al., 1995), must be genetically modified to enable xylose metabolism, so the capability of natural xylose metabolism in combination with use of gaseous carbon streams by *C. autoethanogenum* is highly advantageous.

During syngas fermentation, *C. autoethanogenum* utilizes the acetyl-CoA pathway (also known as the Wood-Ljungdahl pathway) to yield metabolic products from CO and CO_2+H_2. The downside to the use of this pathway is that the reductant demand is high, and it requires an initial ATP input (Drake et al., 2008; Ragsdale and Pierce, 2008). Although the subsequent production

of acetate by the pathway may provide enough ATP for this mechanism of metabolism to continue, this does not negate the fact that the initial bioenergetics is inferior. In addition, if this organism is to be a viable candidate for alcohol production on a larger scale with syngas, then ideally its energetics need to be optimized in a manner which not only facilitates C1 gas utilization but also shifts metabolism towards solventogenesis. Prior work with a genetically similar autotroph, *Clostridium ljungdahlii*, has found that preadaptation of the inoculum to sugar could increase the cellular metabolites and end products during fermentations using only syngas as the carbon source (Bruno-Barcena et al., 2013; Tirado-Acevedo et al., 2011). Preadaptation has the potential to influence the expression of particular proteins used for substrate transport and within the metabolic pathways, thereby altering the organism's specificity for and/or ability to metabolize a given substrate.

Although other studies featuring *C. autoethanogenum* have shown success with metabolism on solely CO (Abubackar et al., 2015a; Guo et al., 2010), gasification of agricultural residues yields more compounds than just CO. Besides the gases mentioned previously (CO, CO_2, and H_2), lignocellulosic biomass gasification also yields methane, nitrogen, tars, and ash (Godfrey, 2012; Slivka et al., 2011). Once the product gas has been refined to remove the toxic impurities, the remaining CO and CO_2+H_2 can then be used as substrates in biomass-derived syngas fermentations to drive the Wood-Ljungdahl pathway toward the creation of cellular biomass and desired end products. Additionally, Heiskanen et al. (2007) has shown during work with *Butyribacterium methylotrophicum* that the presence of CO, CO_2, and H_2 together in the culture headspace during growth on these three gases as the primary substrate achieved a higher reactant to product conversion than growth on solely CO. The point here being that more work should be done on *C. autoethanogenum*'s usage of the gas-mix combination of CO, CO_2, and H_2

as a substrate, as it is more similar to the actual syngas combination produced by lignocellulosic biomass gasification, and it may yield more practical product ratios and metabolic conditions than the use of CO alone.

This study sought to utilize *C. autoethanogenum*'s ability to metabolize xylose in hopes that it would provide energy intermediates necessary to enhance the organism's metabolism of syngas. Specifically, the cells were preadapted to conditions containing xylose, syngas, and a combination of xylose-syngas as the carbon source to determine if the physiology and bioenergetics of these cultures would be suitable to support the cells when used as inoculum in subsequent reactors containing syngas or a xylose-syngas mixture. In addition, it was hypothesized that if xylose could indeed provide favorable energetics for fermentations metabolizing syngas at the outset, then more metabolically active cells as well as the provision of excess reducing equivalents to enhance ethanol production could ultimately result during the fermentations. Agitation was also introduced as a variable during preadaptation because of its impact on mass transfer and hydrogen saturation in bacterial cultures in general. In short, the objective of this study was to explore the effects of inoculum carbon source pre-adaptation (xylose, stationary-xylose-syngas, agitated- xylose-syngas, and syngas) on biomass and product formation by *C. autoethanogenum* during growth in two different types of fermentations (xylose-syngas and syngas).

Materials and Methods

Organism, medium, and inoculum preparation

C. autoethanogenum (DSM 10061) was grown on DSMZ 640 basal medium under a batch, anaerobic atmosphere. The components of DSMZ 640 medium (pH 6.0) were described previously (Cotter et al., 2008, 2009). Briefly, it contains: trypticase peptone, yeast extract,

cysteine hydrochloride, 640 salt solution, SL-10 trace element solution, 0.1% w/v resazurin, and is brought to volume with distilled water. Medium was dispensed anaerobically under a nitrogen (Airgas National Welders) or pure synthesis gas (20% CO, 20% CO_2, 10% H_2, 50% N_2; Arc3 Gases [formerly known as Machine & Welding Supply Company]) atmosphere depending on fermentation treatment into either Balch tubes (10 ml) or serum bottles (50 ml) and autoclaved for 30 min (121°C, 17-18 psig). Seed cultures of *C. autoethanogenum* were revitalized from frozen stock cultures (-80°C) by aseptically inoculating 10 mL Balch tubes containing 5 g/L xylose and a nitrogen headspace with a 5% v/v inoculum followed by incubation for 72 hours at 37°C (no agitation). With successive transfers to fresh medium, incubation was repeated for a 48 hour, and then a 24 hour incubation period.

Xylose pre-adapted inoculum for experimental growth was prepared by transferring *C. autoethanogenum* cultures (5% v/v inoculum) to 10 mL Balch tubes with 2.5 g/L xylose and an N_2 headspace, and then incubating at 37°C with 100 rpm orbital shaking until appropriate cell density was reached (~24 hours, 270 mg dry cells/L). In order to generate enough inoculum for all treatments inoculated with these cells, pre-adapted cultures were subsequently scaled up to 50 mL serum bottles with the same growth conditions. Xylose-syngas (mixed-carbon) pre-adapted inoculum was prepared by transferring *C. autoethanogenum* cultures (5% v/v inoculum) to 50 mL serum bottles with 2.5 g/L xylose and a syngas headspace, and then incubating at 37°C with 100 rpm orbital shaking until appropriate cell density was reached (~36 hours once cultures were fully adapted, 280 mg dry cells/L). Syngas pre-adapted inoculum was created in a similar fashion to the mixed-carbon pre-adapted inoculum (i.e. 50 mL bottle with a syngas headspace and incubation at 37°C with 100 rpm orbital shaking) except that the liquid volume occupied by xylose solution was replaced with sterile, deionized, distilled water prepared under a nitrogen

headspace. The syngas pre-adapted inoculum was also subjected to densification by allowing the culture to grow for 24-26 hours, refreshing the batch syngas headspace by aseptically vacuuming out a portion of the used gas and then adding fresh, filter-sterilized syngas with final pressure adjustment to 1 atm to supply additional substrate, and then allowing the cells to grow for an additional 24-26 hours until they reached 110 mg dry cells/L. Variants of the xylose and xylose-syngas pre-adapted inocula were created by incubating the cultures under stationary conditions (i.e. no agitation) as well. Based on initial work, xylose inoculum grew identically during both agitated pre-adaptation and stationary pre-adaptation conditions; however, the xylose-syngas inoculum behaved differently under these two parameters. Specifically, the xylose-syngas preadapted inoculum incubated with stationary conditions grew similarly to the xylose preadapted cells while the xylose-syngas preadapted inoculum incubated under agitated conditions displayed a defined lag during its preadaptation period. As a result, two pre-adaptation inoculum levels (agitated and stationary incubation) were used for the xylose-syngas inoculum, and xylose pre-adapted inoculum were collectively termed "xylose" regardless of the use of agitation. Since agitation was required to attain viable quantities of syngas pre-adapted inoculum and adequate substrate mass transfer to the cells, there was no variant of this substrate pre-adaptation.

Experimental design and statistical analysis

Two experimental factors, carbon source preadaptation inoculum type (xylose, stationary-xylose-syngas, agitated-xylose-syngas, and syngas) and fermentation type (xylose-syngas and syngas), were investigated over time to determine their effect on the growth and metabolism of *C. autoethanogenum*. A xylose fermentation with xylose pre-adapted inoculum was used as a baseline control for *C. autoethanogenum* growth. Figure 2.1 presents a schematic

of the experimental set-up. The reactors were 160 mL serum bottles (Wheaton) plugged with butyl rubber stoppers (Bellco Glass) and contained 50 mL batch-liquid DSMZ 640 growth medium as detailed above plus batch-gas headspace at atmospheric pressure. The xylose-syngas and syngas fermentations contained syngas (20% CO, 20% CO_2, 10% H_2, 50% N_2; Arc3 Gases) in the headspace while the xylose only fermentations contained N_2 gas (Airgas National Welders). Those reactors which had xylose (xylose-syngas and xylose fermentations) were supplied with sugar at an initial concentration of 2.5 g/L. This starting concentration of xylose was chosen to minimize excess xylose present and to ensure full sugar consumption during the xylose-syngas fermentation if the cells showed diauxic growth with xylose as the primary substrate and syngas as the secondary substrate as observed in preliminary experiments (data not shown). Earlier work with this organism using xylose as the sole carbon source also proved the maximum amount of xylose consumed before cell growth ceases is ~3 g/L (Cotter et al., 2008). In order to ensure that all treatments received the same initial density of *C. autoethanogenum* cells, reactors were inoculated with 5% v/v aliquots of designated pre-adapted cultures normalized to a stock optical density of 0.4 (~127 mg dry cells/L per aliquot). The experimental treatment cultures were incubated in a 37°C water bath with 100 rpm orbital shaking for 64-96 hrs. Liquid (3 mL) and gas (1 mL) samples were collected from the reactors every 8 hours over the growth period beginning at time zero. The response variables were CO, CO_2, and H_2 composition within the headspace, cell concentration, soluble xylose concentration, and primary end products (ethanol and acetate) as a function of time. Treatment combinations (preadaptation type x fermentation type) were replicated with three biological repeats, and within each repeat all treatments were tested in duplicate. This experimental plan was chosen to complement the work done in our lab with a related strain, *C. ljungdahlii*, (Bruno-Barcena et al., 2013; Tirado-Acevedo

et al., 2011) and assess the performance of *C. autoethanogenum* under a batch syngas headspace as prior work used continuous syngas flow to the reactors (Cotter et al., 2009).

The main and interaction effects of carbon source preadapted inoculum type and fermentation type on maximum cell growth and end product (ethanol and acetate) values in *C. autoethanogenum* cultures were evaluated using the General Linear Model (GLM) in SAS® Version 9.4 (SAS Inc., Cary, NC). Assessment of statistical differences between treatments was made at an α level of 0.05.

Biomass, substrate, and end product analyses

Culture concentration was measured using a UV-visible spectrophotometer (Shimadzu UV-1700) at a wavelength of 600 nm and a dry cell weight to optical density (OD) conversion factor of 317 mg dry cells/OD (determined experimentally through previous experiments). Culture purity and pH were checked at the end of the experimental period to determine whether foreign cells were present and to assess if the culture was still within the optimum pH range for growth, respectively.

Headspace gas composition was analyzed via gas chromatography using a thermal conductivity detector (TCD, Shimadzu GC-2014). Samples were collected in sample lock, gas-tight syringes (Hamilton Company, Reno, NV, part no. 81556), held at room temperature prior to analysis, and injected into a gas actuating valve (Valco Instruments Co. Inc, Houston, TX) to ensure precise injection (125 μL) into the gas chromatograph. The concentrations of CO, CO_2, and H_2 were quantified with a Carbosieve SII, 100/120 mesh stainless steel column. The column temperature was held isothermally at 50°C for 9 min, ramped to 200°C at a rate of 32°C/min and held for 3 min, and then ramped to 225°C at 32°C/min and held for 7 minutes. The injector

temperature was 200°C while the detector (TCD) temperature was 250°C. Helium was used as the carrier gas at a flowrate of 30 mL/min.

Water-soluble analytes present in the culture broth, specifically xylose, acetate (in the form of acetic acid), and ethanol, were analyzed by HPLC (Shimadzu LC-20AD). Prior to quantification, liquid samples were centrifuged (10 min, 20,800 *x g*, 25°C), and the supernatant (800 µL) was filtered through a 0.2 µm syringe filter (Whatman, cat no. 6768-1302). Clarified samples were then analyzed on a Phenomenex Regex ROA column (300 x 7.8 mm, part no. 00H-0138-K0) at 65°C using a refractive index detector with the cell set at 40°C and 5 mM sulfuric acid as the eluent (0.6 mL/min).

Results and discussion

Performance of the xylose fermentation

The control fermentation with xylose pre-adapted inoculum grown in a reactor with 2.5 g/L xylose as the sole carbon source reached a peak cell density of 447 mg dry cells/L after 40 hours growth (Fig. 2.2a) with no lag phase observed when the data was linearized (linearized data not shown). These cultures made use of all the available carbon from xylose (Fig. 2.2b) as the soluble xylose concentration had dropped to 0.08 g/L after 40 hours and all xylose was consumed by hour 48 when the culture showed signs of cell lysis. Both acetate and ethanol (Fig. 2.2c, 2.2d) were growth associated end products with acetate production correlating directly with initial cell growth and ethanol formation commencing around hour 16 and continuing to increase exponentially until cell growth ceased. A reasonable cause for the later start of ethanol production is related to the changing pH conditions (data not shown) associated with acetate production and the cell's need to remove electrons by production of an alcohol to prevent harmful acetic acid creation. The cells generated maximum acetate and ethanol levels of 2.36

and 0.19 g/L, respectively, from growth on solely xylose as the carbon source. These baseline conditions are similar to the end product values observed by Cotter et al. (2008) for *C. autoethanogenum* growth on xylose.

Assessment of xylose-syngas (mixed) fermentations

During xylose-syngas fermentations, proper acclimation of *C. autoethanogenum* to both substrates was crucial. The intent of preadapting some of the inocula to the presence of syngas was to minimize any metabolic perturbation caused by this substrate in a mixed substrate fermentation. However, not all of the inocula with supposed syngas pre-exposure showed this predicted performance in the xylose-syngas reactors (Fig. 2.2) and a limitation of the preadaptation process itself was exposed. Meanwhile, since xylose is a rich energy source any impact to the performance of the inocula not acclimated to sugar as a substrate was brief. This effect was observed in syngas pre-adapted and agitated-xylose-syngas pre-adapted inocula where only a minor lag time occurred, while the xylose and the stationary-xylose-syngas pre-adapted inocula showed a drastic 40-48 hour lag (Fig. 2.2a). Both cultures with inocula pre-adapted to xylose-syngas showed the greatest production of biomass (450-455 mg dry cells/L); however, these maxima were only slightly higher than the cell growth witnessed in a xylose-only fermentation. This indicates that the majority of the biomass carbon in these two xylose-syngas fermentations was derived from xylose. There were differences within the cultures with xylose-syngas pre-adapted inoculum, namely that the stationary-xylose-syngas inoculum took much longer to achieve exponential growth than the agitated-xylose-syngas inoculum (Fig. 2.2a). The effect with the stationary-xylose-syngas inoculum was unexpected as the cells were grown in a reactor with the same carbon sources to which it was supposedly adapted. Growth in the agitated-xylose-syngas inoculum sourced culture was similar at each time point to the xylose-

only fermentation which implies that the utilization of agitation during the preadaptation process played a part in overcoming any carbon source acclimation obstacles, specifically those imposed by syngas. In order to avoid metabolic delays, *C. autoethanogenum* cells must be acclimated to syngas when this gaseous substrate is available. As a result, it is apparent that mass transfer across the gas-liquid interface plays a significant role during adaptation of *C. autoethanogenum*. The increased gaseous mass transfer imposed by non-static conditions allows more syngas to be solubilized within the liquid phase and thus available for interaction with the cells. The capability of this organism to effectively adapt to syngas and respond to its presence in the liquid phase was further demonstrated by the growth performance of the xylose pre-adapted and syngas pre-adapted inocula. Although neither treatment produced significantly different levels of cell density, they did show significant differences in their growth patterns. Since the xylose pre-adapted inoculum was without syngas during its preadaptation stage, the cells responded to the sudden presence of the syngas during the agitated, xylose-syngas fermentation condition by taking 48 hours to acclimate to the new carbon source before using either carbon source to generate any substantial cell mass or end products (Fig. 2.2a). The syngas pre-adapted inoculum, on the other hand, did not appear to experience detrimental metabolic perturbation when cultured with xylose; and since the cells were already conditioned for growth on syngas due to their pre-adaptation conditions, the *C. autoethanogenum* grew without much delay in the xylose-syngas reactors (Fig. 2.2a). Although the syngas pre-adapted inoculum did not grow identically to the agitated, xylose-syngas inoculum during the experimental run, its overall growth was comparable to that treatment (Fig. 2.2a). In fact, all four of the inoculum treatments examined during the xylose-syngas fermentation condition had maximum cell concentrations that were

statistically similar (no significant difference, p-value > 0.05) to each other and the xylose-only fermentation.

All inoculum types showed complete or near complete xylose consumption in xylose-syngas, mixed carbon reactors by the end of the experimental period (either 64 or 96 hours depending on the treatment). However, the observed trend of xylose consumption during the mixed fermentations was not as fast as that observed during the xylose-only fermentation (Fig. 2.2b). As mentioned above, the xylose pre-adapted inoculum grown on 2.5 g/L xylose as the sole carbon source exhausted nearly all of the xylose within 40 hours. The reduced xylose uptake in the xylose-syngas reactors may be related to the cells simultaneously consuming syngas. In other words, either the substrate transporters and/or carbon metabolism were at a point of limitation with dual substrate utilization or the added carbon from syngas allowed the cells to be less dependent on xylose.

All of the xylose-syngas fermentation treatments produced roughly the same maximum amount of acetate (~2.6-2.8 g/L) regardless of pre-adaptation type (Fig. 2.2c), and this level was higher than the concentration of acetate created by the xylose-only fermentation (2.36 g/L). Thus, the carbon from syngas contributed to acid production. Agitated-xylose-syngas and syngas pre-adapted inocula yielded slightly higher maximum acetate levels (2.72-2.76 g/L) than the xylose and stationary-xylose-syngas inocula (2.57-2.66 g/L) during mixed carbon fermentation conditions. Yet, the latter two inoculum types, which displayed a lag, may have achieved slightly higher acetate levels if there had been adequate liquid volume in the reactors after 96 hours growth to allow sample collection at later time points. In support of the concept that acetate is a growth-associated, ATP generating product with *C. autoethanogenum* (Cotter et

al., 2008), the differences in acetate formation mirrored those observed in the extent of biomass production.

The solvent production trend during the xylose-only fermentation showed that *C. autoethanogenum* makes ethanol as a growth-associated product, but when this result was compared to ethanol production during the xylose-syngas fermentations, it revealed that the added presence of syngas severely limited ethanol formation (Fig. 2.2d). Logically this observation makes sense as the metabolism of syngas via the Wood-Ljungdahl pathway (Ragsdale and Pierce, 2008) requires the use of reducing equivalents that would otherwise be sent towards ethanol production in a soluble sugar fermentation. However, the limited ethanol formation was possibly linked to differences in solvent producing proteins expressed in the presence of xylose and not syngas (data not shown). All inoculum pre-adaptation levels, except for the stationary-pre-adapted-xylose-syngas inoculum, exhibited detectable production of ethanol in the xylose-syngas fermentation. In terms of amount, the xylose pre-adapted cells generated 1.6 times more ethanol (0.08 g/L) than the agitated-xylose-syngas and syngas pre-adapted inocula treatments (~0.05 g/L). This proves that despite exposure to syngas in the culture that the xylose pre-adapted cells were still prone to send reducing equivalents directly to an ethanol electron sink to maintain cell homeostasis as opposed to channeling more reducing equivalents into the operation of the Wood-Ljungdahl pathway to fix the gaseous carbon. It is not clear why the stationary-pre-adapted-xylose-syngas inoculum did not produce any ethanol. Perhaps the prolonged exposure to syngas without consuming it (both during preadaptation and the fermentation lag period) affected regulation of the genes necessary for solvent production under sugar-syngas metabolism. Nonetheless, the maximum concentration of ethanol in the xylose-syngas reactors (0.08 g/L) was significantly lower than the 0.19 g/L produced by the

xylose-only fermentation (Fig. 2.2d). When comparing the product ratios, the xylose-only fermentation resulted in 11 g acetate for every 1 g of ethanol produced ($E:A_{molar}$ = 1:9), which is in line with prior work (Cotter et al., 2008), but the xylose-syngas fermentations resulted in E:A mass ratio values ranging from 1:24 to 1:53 ($E:A_{molar}$ = 1:18 to 1:40) for all inoculum sources. Thus, this revealed that addition of syngas to the cultures prompted the cells to produce acetate at a greater rate than they transfer electrons to acetaldehyde forming ethanol in order to reoxidize NADH. Acetate production generates ATP which is required to drive the formation of 10-formyl-tetrahydrofolate and fix CO and CO_2 in the Wood-Ljungdahl pathway (Slivka et al., 2011). This same pathway also requires six electrons which otherwise could have been directed toward ethanol production.

An analysis of the carbon present in the form of soluble compounds (xylose, acetate, and ethanol) within each xylose-syngas fermentation treatment indicated a carbon balance increase of 12-20 mM carbon between the time zero sample and the last experimental sample (i.e. xyl/ace/EtOH carbon rose from 86 mM at hour 0 to 105 mM at hour 88 in the xylose preadapted treatment). This carbon balance increase confirmed that syngas carbon was a substrate for carbon metabolism. As further confirmation of syngas uptake and conversion in the xylose-syngas reactors, the xylose-only fermentation maintained a constant soluble carbon balance in the culture broth for the entirety of the experiment (i.e. xyl/ace/EtOH carbon was 88 mM at hours 0, 32, and 56 with xylose preadapted inoculum).

With the highest ethanol concentrations achieved at or around the same time as the maximum acetate concentrations during the xylose-syngas fermentations, the prior hypothesis that acetogens yield ethanol as a non-growth associated end product did not prove to be correct for *C. autoethanogenum* in these studies. It is typical for acetogenic bacteria to display growth

associated acetate production since creation of this metabolite generates ATP critical for cellular bioenergetics (Klasson et al., 1992). On the other hand, it is uncommon to observe ethanol production during acetogenic growth, as alcohol generation is usually associated with the need to remove excess electrons later in the fermentation when the cell's NAD^+/NADH ratio is too low or the pH is too low (Girbal and Soucaille, 1998; Klasson et al., 1992). Furthermore, most organisms which utilize the Wood-Ljungdahl pathway to metabolize CO and CO_2 need electrons (from H_2 or other sources) to drive this carbon fixation and subsequently yield the precursor acetyl-CoA necessary for either acetate or ethanol production (Slivka et al., 2011; Tirado-Acevedo et al., 2010). However, both this work and other studies (Abubackar et al., 2015b; Cotter et al., 2008, 2009) have shown that *C. autoethanogenum* and its biovar *C. ljungdahlii* generate ethanol in conjunction with biomass production (Bruno-Barcena et al., 2013). This outcome proves that these species are different in their solvent formation behavior.

As mentioned earlier, Tirado-Acevedo et al. (2011) conducted a similar carbon source pre-adaptation study with *C. ljungdahlii*, which is taxonomically the same species as *C. autoethanogenum* but phenotypically a different strain (Bruno-Barcena et al., 2013). The main differences in the *C. ljungdahlii* study were that the organism was pre-adapted to fructose, syngas, or a fructose-syngas mixture before inoculation into reactors containing a fructose-syngas mixture with continuous gas flow and sparging. During these fructose-syngas fermentations, both the syngas pre-adapted and the fructose-syngas pre-adapted *C. ljungdahlii* inocula generated statistically greater ethanol concentrations than the fructose pre-adapted inoculum. Overall, preadaptation to syngas was not deemed a necessary feature for a *C. ljungdahlii* mixed fermentation in that study since there was no variation among biomass and acetate concentrations between the pre-adapted inocula evaluated. In contrast, this study with *C.*

autoethanogenum used agitation instead of sparging. Consequently, this study found that both the enhanced mass transfer imposed by agitation and the presence of syngas during the pre-adaption phase was required to properly adapt the organism to syngas exposure and use when grown on a mixed carbon, xylose-syngas substrate. Another defining feature between the two studies is the bioenergetics difference between pentose metabolism and hexose metabolism (Hahn-Hägerdal et al., 2007; Servinsky et al., 2010; White, 2007):

$3\ \text{xylose} + 5NAD^+ + 5P_i + 5ADP \rightarrow 5\ \text{pyruvate} + 5NADH + 5H^+ + 5ATP + 5H_2O$

while

$3\ \text{fructose} + 6NAD^+ + 6P_i + 6ADP \rightarrow 6\ \text{pyruvate} + 6NADH + 6H^+ + 6ATP + 6H_2O.$

During a fructose-syngas fermentation, the extra pyruvate and reducing equivalents from fructose metabolism allows for a greater flux in downstream metabolic intermediates and electrons which may serve to repair the cells and/or buffer against syngas-induced stress. This bioenergetics boost was not afforded during the xylose-syngas fermentations and hence acclimation to syngas became more important here. Additionally, the extra pyruvate and reducing equivalents available for the fructose based inocula in the previous work afforded more precursors for solventogenesis. This theory may explain why *C. ljungdahlii* grown on fructose-syngas created considerably more ethanol (0.16 g ethanol/g fructose consumed with syngas inoculum) than *C. autoethanogenum* grown on xylose-syngas in this experiment (0.02 g ethanol/g xylose consumed with syngas inoculum).

Assessment of syngas fermentations

Similar to what was observed during the xylose-syngas fermentations, the agitated-xylose-syngas pre-adapted and syngas pre-adapted inocula (Fig. 2.3a) readily grew in reactors with syngas as the only provided carbon source, while the xylose pre-adapted and the stationary-

xylose-syngas pre-adapted inocula (Fig. 2.3b) demonstrated detectible lags during the syngas fermentations (40 hours and 32 hours, respectively). As discussed earlier, this growth delay was likely the result of the cells acclimating to the presence of the syngas in the liquid phase. An interesting observation was that once growth was achieved in the reactors, both types of xylose-syngas pre-adapted inocula showed a brief period of accelerated growth compared to the other syngas fermentation type treatments. For the first 8 hours of active growth, both the stationary-xylose-syngas pre-adapted and the agitated-xylose-syngas pre-adapted inocula grew at a rate of 0.74 mg dry cells/L/hr, while the xylose pre-adapted inoculum grew at 0.25 mg dry cells/L/hr and the syngas pre-adapted inoculum grew at a rate of 0.39 mg dry cells/L/hr. However, only the stationary-xylose-syngas pre-adapted inoculum was able to maintain its culture health and attain a maximum cell density of 101 mg dry cells/L, while the agitated-xylose-syngas pre-adapted inoculum grew to a significantly lower cell density of only 69 mg dry cells/L before beginning to die. It is possible that because the agitated-xylose-syngas pre-adapted cells came from an inoculum environment rich in energy, and they were properly accustomed to growth on syngas, their preexisting bioenergetics allowed them to grow readily in a syngas-only environment. Yet, because the bioenergetics supply of a batch, syngas culture is more limited than that of a xylose-syngas culture, the actively growing cells may not have rationed their energy reserves or needed to divert as much carbon to anabolic pathways (ex. gluconeogenesis) to support accelerated growth. The xylose pre-adapted and syngas pre-adapted inocula also both grew to densities during the syngas fermentation (107 and 105 mg dry cells/L, respectively) that were statistically similar to the cultures with stationary-xylose-syngas pre-adapted inoculum.

The prior *C. ljungdahlii* carbon source pre-adaptation work by Tirado-Acevedo et al. (2011) also had a continuously-fed syngas fermentation treatment set which showed that

preadaptation of the organism to fructose was optimal for both cell growth and end product formation (ethanol and acetate) when syngas was the sole substrate. In this work, preadaptation of *C. autoethanogenum* to only xylose was not deemed sufficient to enable effective and timely metabolism of syngas when it is the sole substrate since the organism still required agitation-based acclimation to syngas in order to utilize it efficiently. Given that sugar pre-adaptation was more energetically beneficial for *C. ljungdahlii* than for *C. autoethanogenum* in these two syngas studies, this proves that the method of sugar uptake into the cell along with sugar pathway regulation can make a difference in creating energetically primed inocula for syngas metabolism. In many cases, pentose uptake in Clostridia is driven by active transport using ATP-binding cassette (ABC) transporters and electrochemical potential-driven transporters (Nölling et al., 2001; Servinsky et al., 2010). In contrast, hexose uptake into the cell is influenced by the phosphoenolpyruvate-dependent phosphotranferase system (PTS) which has an inherent method for regulation through catabolite repression (Servinsky et al., 2010; Wang et al., 2012). In addition, a xylose molecule requires intracellular phosphorylation while fructose is phosphorylated during translocation which is likely more energetically desirable since the molecule will not be brought into the cell unless phosphoenolpyruvate and the phosphate ion it donates for phosphorylation are available. Once inside the cell, fructose-6-phosphate can immediately enter the glycolytic pathway while xylose must wait for the availability of xylose isomerase, xylulose kinase, and an ATP. This difference in the regulation of sugar uptake could be a factor which allows *C. ljungdahlii* cells previously acclimated to fructose to continue to grow well in the presence of only syngas. Genes encoding bacterial transport systems, whether PTS E_{II} domains or non-PTS permeases, are generally contained within operons that also encode enzymes involved in the initial steps of metabolism of the specific substrate. Thus the gene

products should only be required when the substrate is present and represents the best available source of carbon and energy for growth (Mitchell and Tangney, 2005). As mentioned above, the agitated-xylose-syngas pre-adapted inoculum may have experienced growth issues in the syngas fermentation because appropriate gene regulation would be required to transition from xylose utilization to metabolism on syngas alone. The pentose phosphate pathway is not as linear as the entrance to glycolysis, and requires isomerization, transaldolase, and transketolase reactions to generate fructose-6-phosphate and/or phosphoglyceraldehyde, provided, however, that ATP is available for phosphorylation (White, 2007). Since xylose contains 5 carbon units, this means that at least two xylose molecules are required to generate a suitable intermediate for continued carbon metabolism (i.e. 3-carbon phosphoglyceraldehyde or 6-carbon fructose-6-phosphate). A single fructose molecule, on the other hand, can theoretically be processed through the entirely of the glycolytic pathway. Given this information, the agitated-xylose-syngas pre-adapted *C. autoethanogenum* cells grown in syngas were faced with the complication of having not only more enzymes to turn off in the pentose phosphate pathway but also the possibility that the pathway could not be turned off efficiently because an unusable fraction of xylose remained present intracellularly following inoculum transfer.

During the periods of active biomass production in the syngas type reactors, all pre-adaptation types exhibited the same growth-associated trend of acetate generation (Fig. 2.3c, 2.3d). Since the agitated-xylose-syngas pre-adapted inoculum reached a lower maximum cell density than the rest of the syngas fermentation treatments, its associated production of acetate of 0.517 g/L was also, consequently, significantly lower (p-value < 0.05). The other three syngas fermentation treatments created approximately the same level of acetate with maximum production concentrations ranging from 0.759 to 0.828 g/L. In regards to alcohol concentrations

produced during the syngas fermentations, only the xylose pre-adapted inoculum showed a genuine trend of ethanol production, and the maximum amount was less than 0.04 g/L. The syngas pre-adapted inoculum showed signs of producing a minute amount of possibly growth-associated ethanol but the detectible concentration fluxed over time. As a result of the overall lower cell concentrations (< 110 mg dry cells/L) achieved during the syngas fermentations, it is plausible that there were not enough ethanol producing cells to yield detectable levels of alcohol during the experiment. Since the xylose-syngas fermentation type also had lower ethanol productivity, the same root cause could have caused problems in the syngas fermentation type as well. The root cause put forward was that excess reductant was being consumed by the Wood-Ljungdahl pathway in order to metabolize syngas and this was taking away from ethanol production.

Another gas-substrate study with *C. autoethanogenum* demonstrated average ethanol and acetate concentrations of 0.05 g/L and 1.00 g/L, respectively, when continuously-fed syngas with sparging was the sole carbon source for 72 hours (Cotter et al., 2009). Of particular note was the fact that a 36 hour lag in growth was observed during that study which used syngas pre-adapted inoculum and yielded maximum cell concentrations of 150 mg dry cells/L. When comparing the Cotter et al. (2009) study with continuously-fed syngas to this work with batch syngas (both used 20% CO, 20% CO_2, 10% H_2, 50% N_2 from Arc3 Gases), it was discovered that they both had similar ratios for ethanol productivity (g peak ethanol per g dry cell concentration = 0.3). This presents the argument that there is a set rate at which *C. autoethanogenum* metabolizes syngas as the sole carbon source. As a result, if the composition of fed syngas does not change, then the flux towards ethanol also remains constant regardless of whether batch or continuously-fed syngas is used.

For the three inoculum pre-adaptation treatments that showed the best growth during the syngas fermentations (xylose, syngas, and stationary-xylose-syngas inocula), a calculation of the amount of carbon present in the reactors in the form of soluble compounds (acetate, ethanol, and carryover xylose from inoculum transfer) revealed that the carbon balance increased by 26-28 mM carbon between the beginning and end of the experiment. This increase in net carbon present represents the amount of syngas carbon converted to end products as opposed to biomass. Compared to the equivalent inoculum treatments in the xylose-syngas fermentations, the syngas fermentation treatments actually had a greater net increase in soluble carbon in the culture broth over the course of the experiment (ΔC_{syngas} = 26-28 mM versus $\Delta C_{xylose\text{-}syngas}$ = 12-20 mM). This larger rise in the carbon balance indicates that the syngas fermentation type used more syngas carbon as substrate. Since the cells were more dependent on syngas in the syngas fermentations as it was the sole carbon and energy source, it makes sense that the soluble carbon balance would increase to a greater extent from CO and CO_2 uptake in this system. In terms of the amount of xylose that was carried over during inoculation with the pre-adapted inoculum, only 1.3 mM of xylose carbon was present at time zero, for example, in the syngas reactors which received xylose pre-adapted inoculum. On a relative basis, this carbon value is smaller than the standard deviations observed for final end product concentrations so xylose carryover had minimal impact on the actual carbon substrate uptake and product formation.

Utilization of gaseous substrates

During the xylose-syngas fermentations (Fig. 2.4) it was observed that, although CO was also used to provide electrons, the presence of xylose in the system provided a sufficient quantity of additional electrons to the cells so that they did not need to use much H_2. Out of the four inoculum pre-adaptation treatments, the syngas pre-adapted inoculum showed the greatest need

for H_2 as shown by its consumption profile in Figure 2.4d. This outcome was logical given that the syngas inoculum was pre-adapted to a condition that was dependent on H_2 to metabolize some of the carbon. In regards to gaseous carbon use, the syngas pre-adapted inoculum displayed full CO consumption in parallel with a decrease in H_2 and an overall net increase in CO_2 concentration. Changes in headspace composition (Fig. 2.4d) corresponded with the decline in xylose concentration (Fig. 2.2b) showing that *C. autoethanogenum* utilized both substrates simultaneously. Since the cells were consuming xylose in conjunction with the carbon from syngas, the CO_2 levels increased unsurprisingly as a result of sugar metabolism. The other three inoculum pre-adaptation levels (Fig. 2.4a, 2.4b, and 2.4c) demonstrated relatively similar headspace gas trends as the syngas pre-adapted inoculum (Fig. 2.4d) while in the midst of active growth (all inocula consumed CO at a rate of 0.3 %/hr). Gas concentrations remained steady if the cells were in the lag phase (i.e. xylose pre-adapted inoculum in Figure 2.4a and 2.2a), and once the cells began to grow, the CO and H_2 concentrations declined while the CO_2 concentration rose.

Compared to the xylose-syngas fermentations for each inoculum pre-adaptation level, the syngas fermentations (Fig. 2.5) showed similar degrees of CO removal from the headspace (xylose and agitated-xylose-syngas inocula: 0.2 %/hr, stationary-xylose-syngas inoculum: 0.3 %/hr, and syngas inoculum: 0.4 %/hr), but a substantially faster trend of H_2 decline (especially with the syngas pre-adapted inoculum, Fig. 2.5d). The faster H_2 consumption occurred because the cells required the electrons from H_2 to convert CO_2 to a methyl group for acetyl-CoA. Again, changes in headspace composition occurred during active growth in the syngas reactors (Fig. 2.5, 2.3a, and 2.3b), and the lower cell density of the agitated-xylose-syngas pre-adapted inoculum also resulted in reduced headspace gas consumption (Fig. 2.5c). The syngas

fermentations also displayed an increase in CO_2 concentration, but the rise in CO_2 was not as strong as that observed for the xylose-syngas fermentations. Two probable reasons for the CO_2 increase during the syngas fermentations are the water gas shift reaction ($CO + H_2O \leftrightarrow CO_2 + 2H^+ + 2e^-$) (Drake et al., 1980; Newsome, 1980) and natural cellular metabolism (White, 2007).

Conclusion

While *C. autoethanogenum* can metabolize syngas, this substrate does not support cell biomass and metabolite production to the same degree xylose does. In order to improve culture performance, carbon source preadaptation was used to create bioenergetically primed inocula that would minimize growth lag periods during xylose-syngas and syngas fermentations. However, it was discovered that not only substrate adaptation but also the manner in which the cells are acclimated to the specific carbon source can impact *C. autoethanogenum* metabolism. If proper mass transfer of syngas is not imposed during the preadaptation phase, the inoculum will fail to acclimate to syngas and then result in a metabolic lag during the subsequent fermentation. This effect was observed during both xylose-syngas and syngas only fermentations since *C. autoethanogenum* consumes both substrates at the same time. The most noteworthy difference between the xylose-syngas and the syngas fermentations during this study, regardless of preadaptation, was that the cells were less dependent on reducing equivalents from syngas in the presence of xylose due to the additional reduction capacity that sugar provides. Although it was believed that inoculum preadaptation to xylose would contribute more to the bioenergetics of initial syngas metabolism, this result was not observed. Coupling syngas and xylose metabolism in an agitated system resulted in simultaneous consumption once active culture growth commenced. Cultures that had been inoculated with cells with no or inadequate preadaptation to syngas experienced long lag periods when exposed to the substrate in a xylose-

syngas fermentation rather than adopting a single carbon uptake mechanism that could later be evolved into dual substrate consumption. Even though work with the organism, *C. ljungdahlii*, did show that fructose pre-adapted inoculum could enhance a syngas fermentation, it must be acknowledged that there is a difference between pentose and hexose metabolism and the bioenergetics that each process provides to the cell. Since xylose contains less carbon and hydrogen than fructose, it contributes to the central metabolic pathways to a smaller extent and provides less reduction capacity. In addition, xylose is metabolized through the pentose phosphate pathway which is more complex than glycolysis because it requires multiple pentose molecules for reaction. From this study, cellular enhancement of *C. autoethanogenum* in syngas based fermentations was tied more to the effectiveness of gas mass transfer of syngas into the liquid phase than to the potential precursors that could be derived from sugar when xylose was used.

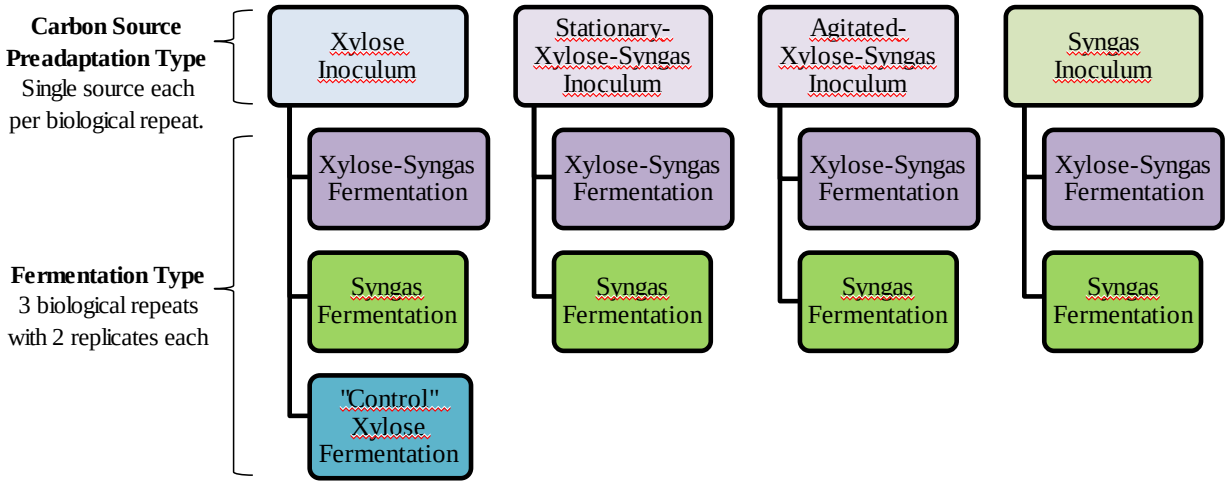

Figure 2.1. Schematic of factors, treatment combinations, and replication for carbon source preadaptation experiments.

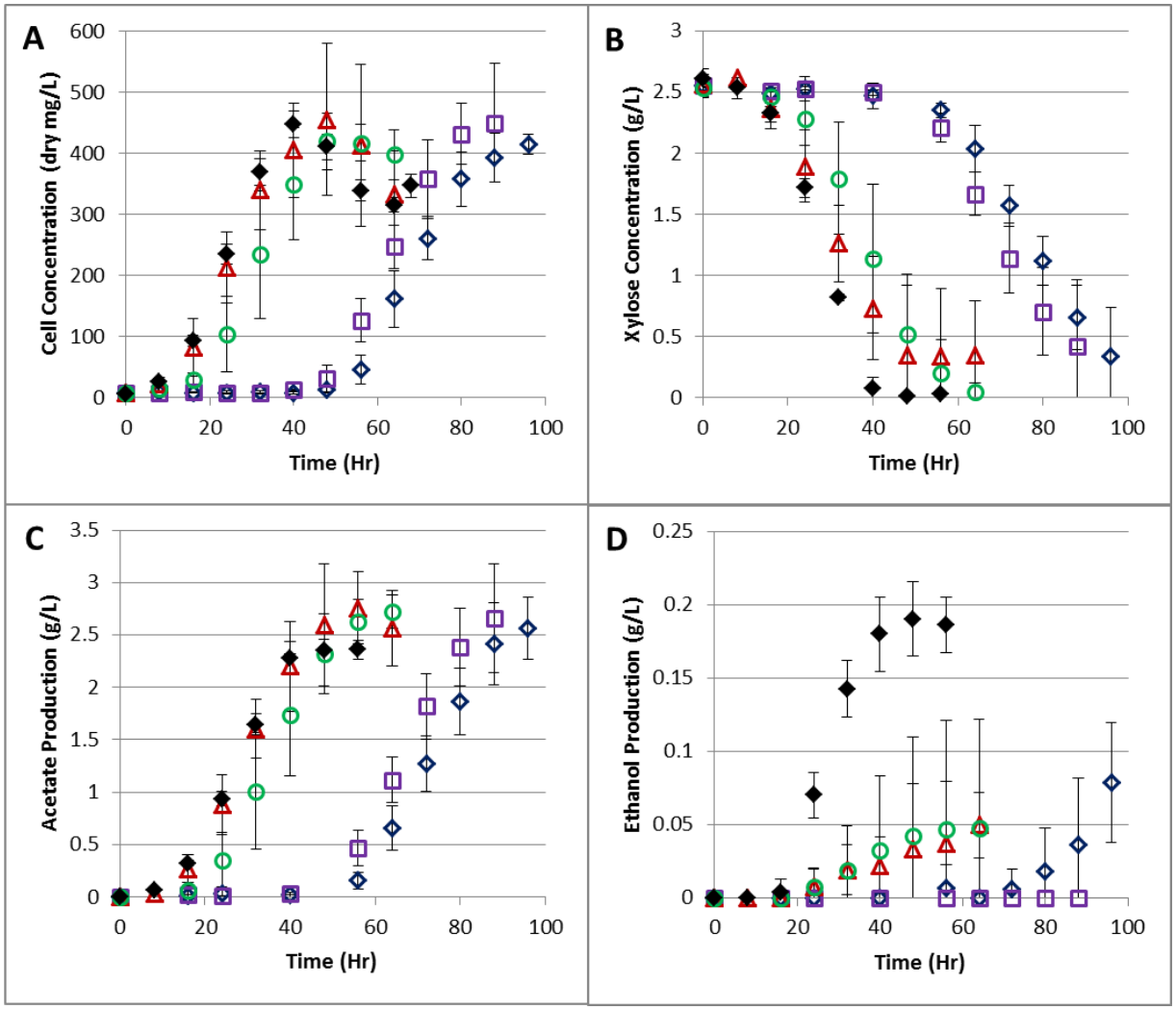

Figure 2.2. *C. autoethanogenum* performance in xylose-syngas (mixed) fermentations (open symbols) and a xylose only fermentation (solid symbols) using different preadaptation sources. A) cell concentration, B) xylose concentration, C) acetate production, and D) ethanol production. Diamond: xylose inoculum, Square: stationary-xylose-syngas inoculum, Triangle: agitated-xylose-syngas inoculum, Circle: syngas inoculum.

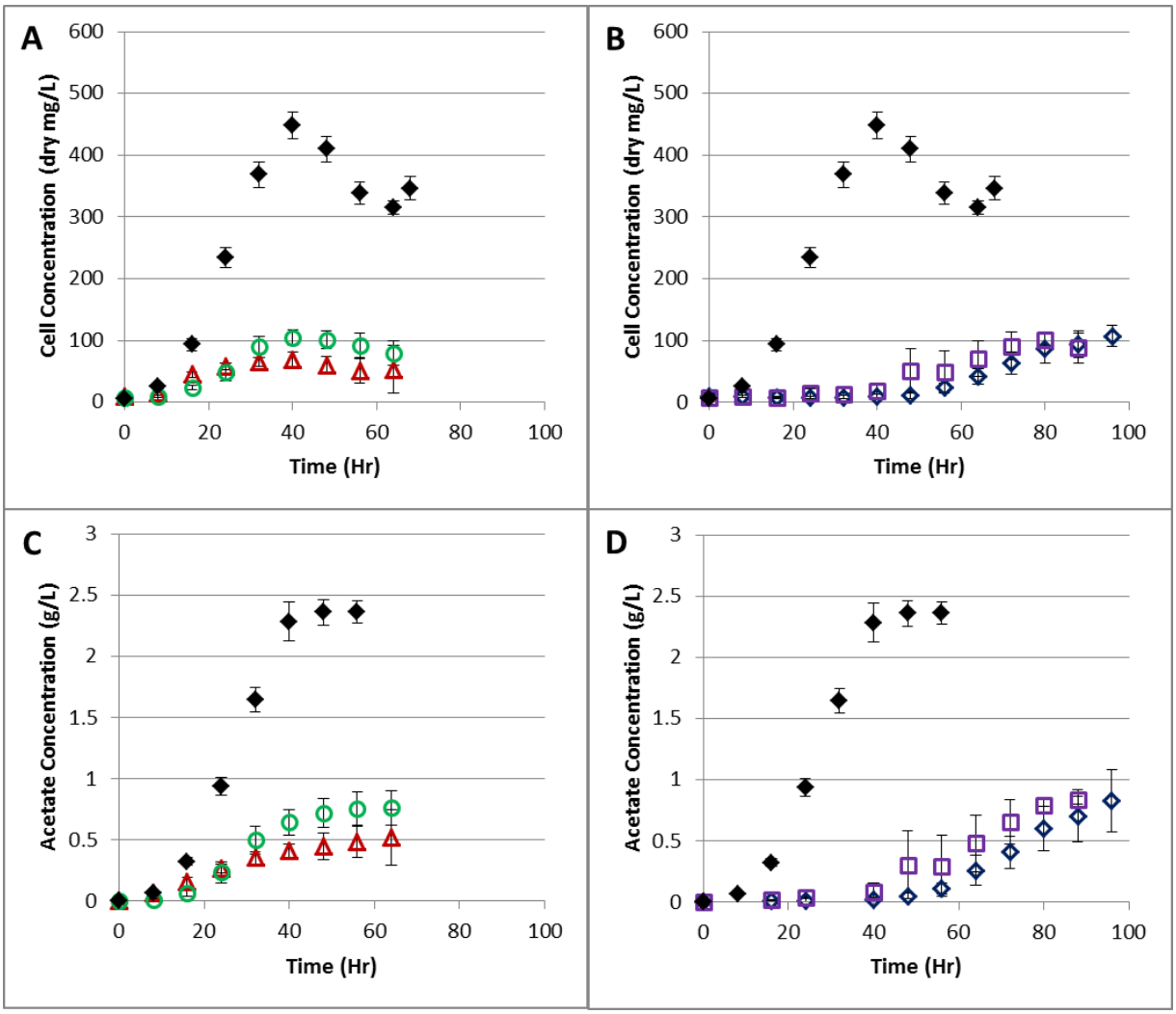

Figure 2.3. *C. autoethanogenum* syngas fermentations (open symbols) compared to a xylose only fermentation (solid symbols). A) cell concentration for agitated-xylose-syngas and syngas inocula and xylose only fermentation, B) cell concentration for xylose and stationary-xylose-syngas inocula and xylose only fermentation, C) acetate concentration for agitated-xylose-syngas and syngas inocula and xylose only fermentation, and D) acetate concentration for xylose and stationary-xylose-syngas inocula and xylose only fermentation. Ethanol trends are not shown due to the low levels produced (<0.04 g/L max). Diamond: xylose inoculum, Square: stationary-xylose-syngas inoculum, Triangle: agitated-xylose-syngas inoculum, Circle: syngas inoculum.

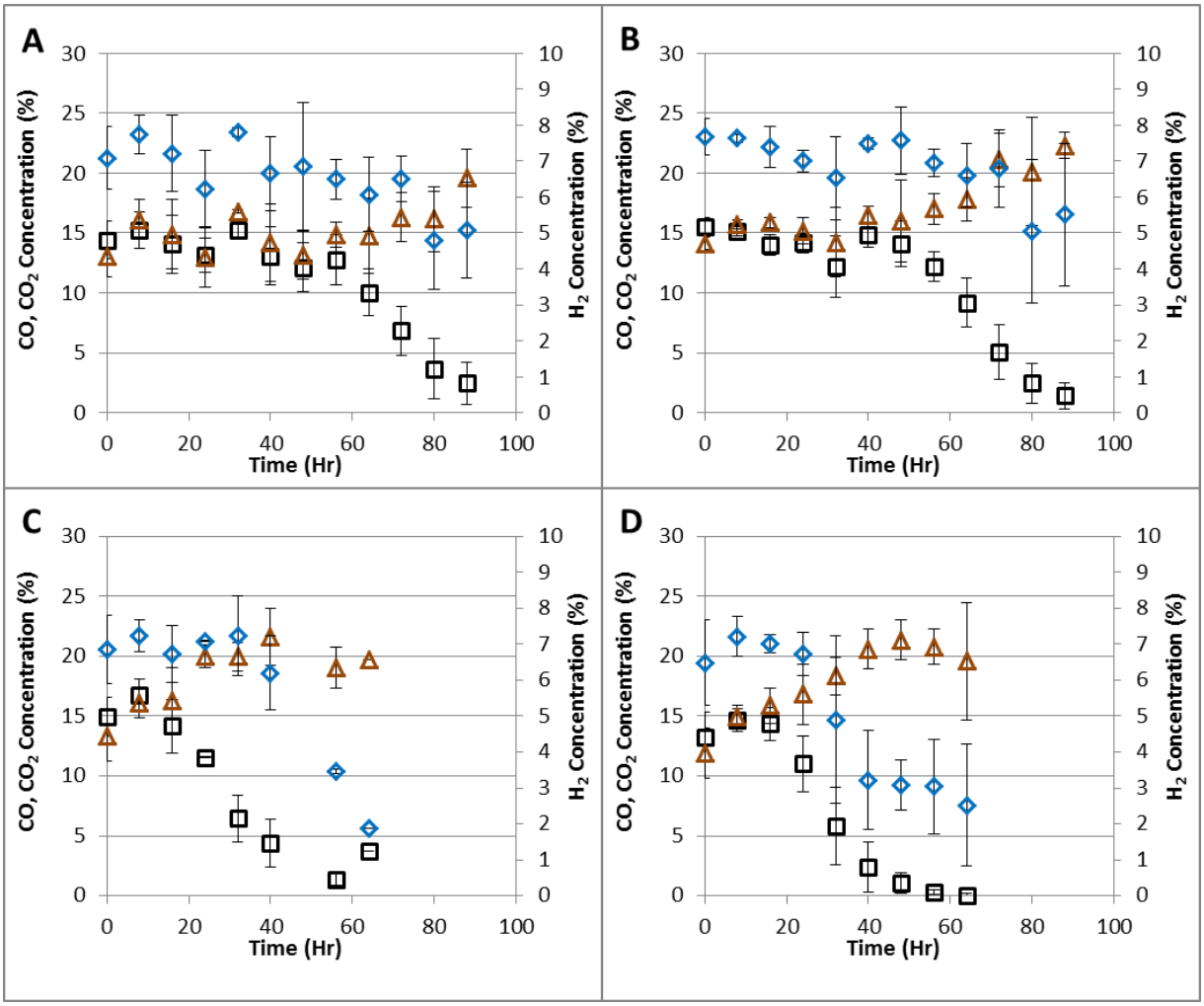

Figure 2.4. Headspace composition during *C. autoethanogenum* xylose-syngas (mixed) fermentations using A) xylose inoculum, B) stationary-xylose-syngas inoculum, C) agitated-xylose-syngas inoculum, and D) syngas inoculum. Square: CO, Triangle: CO_2, Diamond: H_2.

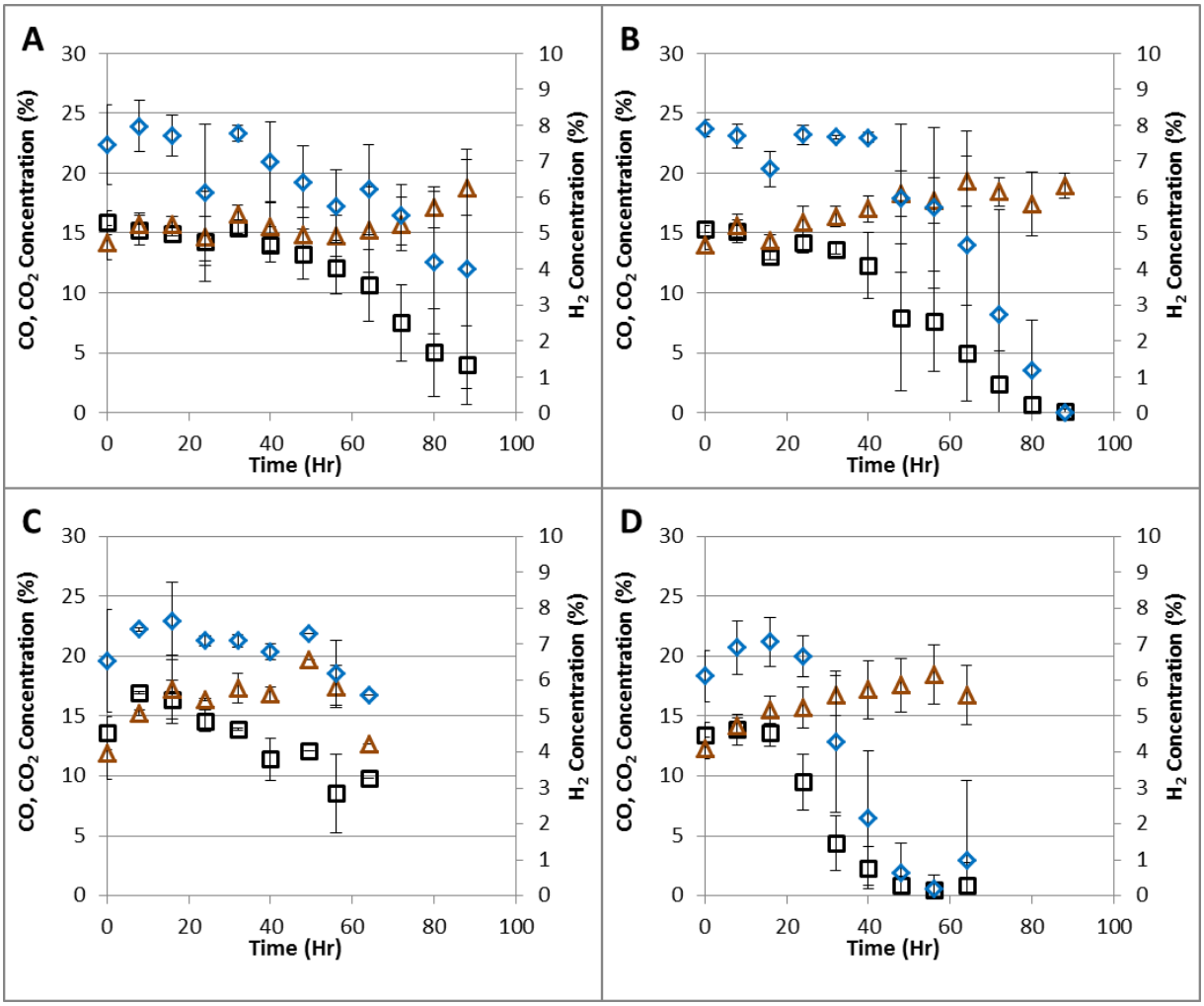

Figure 2.5. Headspace composition during *C. autoethanogenum* syngas fermentations using A) xylose inoculum, B) stationary-xylose-syngas inoculum, C) agitated-xylose-syngas inoculum, and D) syngas inoculum. Square: CO, Triangle: CO_2, Diamond: H_2.

REFERENCES

Abrini, J., Naveau, H., and Nyns, E.J. (1994). *Clostridium autoethanogenum*, sp. nov., an anaerobic bacterium that produces ethanol from carbon monoxide. Arch. Microbiol. *161*, 345–351.

Abubackar, H.N., Veiga, M.C., and Kennes, C. (2015a). Ethanol and Acetic Acid Production from Carbon Monoxide in a *Clostridium* Strain in Batch and Continuous Gas-Fed Bioreactors. Int. J. Environ. Res. Public. Health *12*, 1029–1043.

Abubackar, H.N., Veiga, M.C., and Kennes, C. (2015b). Carbon monoxide fermentation to ethanol by *Clostridium autoethanogenum* in a bioreactor with no accumulation of acetic acid. Bioresour. Technol. *186*, 122–127.

Bruno-Barcena, J.M., Chinn, M.S., and Grunden, A.M. (2013). Genome Sequence of the Autotrophic Acetogen *Clostridium autoethanogenum* JA1-1 Strain DSM 10061, a Producer of Ethanol from Carbon Monoxide. Genome Announc. *1*, e00628-13.

Cotter, J.L., Chinn, M.S., and Grunden, A.M. (2008). Ethanol and acetate production by *Clostridium ljungdahlii* and *Clostridium autoethanogenum* using resting cells. Bioprocess Biosyst. Eng. *32*, 369–380.

Cotter, J.L., Chinn, M.S., and Grunden, A.M. (2009). Influence of process parameters on growth of *Clostridium ljungdahlii* and *Clostridium autoethanogenum* on synthesis gas. Enzyme Microb. Technol. *44*, 281–288.

Datar, R.P., Shenkman, R.M., Cateni, B.G., Huhnke, R.L., and Lewis, R.S. (2004). Fermentation of biomass-generated producer gas to ethanol. Biotechnol. Bioeng. *86*, 587–594.

Drake, H., Hu, S., and Wood, H. (1980). Purification of carbon monoxide dehydrogenase, a nickel enzyme from *Clostridium thermocaceticum*. J. Biol. Chem. *255*, 7174-7180.

Drake, H.L., Gößner, A.S., and Daniel, S.L. (2008). Old acetogens, new light. Ann. N. Y. Acad. Sci. *1125*, 100–128.

Girbal, L., and Soucaille, P. (1998). Regulation of solvent production in *Clostridium acetobutylicum*. Trends Biotechnol. *16*, 11–16.

Godfrey, E.E., III (2012). Gas-Insulated Gasifier for Biomass Derived Producer Gas. North Carolina State University.

Guo, Y., Xu, J., Zhang, Y., Xu, H., Yuan, Z., and Li, D. (2010). Medium optimization for ethanol production with *Clostridium autoethanogenum* with carbon monoxide as sole carbon source. Bioresour. Technol. *101*, 8784-8789.

Hahn-Hägerdal, B., Karhumaa, K., Fonseca, C., Spencer-Martins, I., and Gorwa-Grauslund, M.F. (2007). Towards industrial pentose-fermenting yeast strains. Appl. Microbiol. Biotechnol. *74*, 937–953.

Heiskanen, H., Virkajärvi, I., and Viikari, L. (2007). The effect of syngas composition on the growth and product formation of *Butyribacterium methylotrophicum*. Enzyme Microb. Technol. *41*, 362–367.

Jeffries, T.W. (2006). Engineering yeasts for xylose metabolism. Curr. Opin. Biotechnol. *17*, 320–326.

Klasson, K.T., Ackerson, M.D., Clausen, E.C., and Gaddy, J.L. (1992). Bioconversion of synthesis gas into liquid or gaseous fuels. Enzyme Microb. Technol. *14*, 602–608.

Liou, J.S.C., Balkwill, D.L., Drake, G.R., and Tanner, R.S. (2005). *Clostridium carboxidivorans* sp. nov., a solvent-producing clostridium isolated from an agricultural settling lagoon, and reclassification of the acetogen *Clostridium scatologenes* strain SL1 as *Clostridium drakei* sp. nov. Int. J. Syst. Evol. Microbiol. *55*, 2085-2091.

Mitchell, W.J., and Tangney, M. (2005). Carbohydrate uptake by the phosphotransferase system and other mechanisms. Handb. Clostridia. 155–175.

Newsome, D.S. (1980). The Water-Gas Shift Reaction. Catal. Rev. *21*, 275–318.

Nölling, J., Breton, G., Omelchenko, M.V., Makarova, K.S., Zeng, Q., Gibson, R., Lee, H.M., Dubois, J., Qiu, D., Hitti, J., et al. (2001). Genome Sequence and Comparative Analysis of the Solvent-Producing Bacterium *Clostridium acetobutylicum*. J. Bacteriol. *183*, 4823–4838.

Pierce, E., Xie, G., Barabote, R.D., Saunders, E., Han, C.S., Detter, J.C., Richardson, P., Brettin, T.S., Das, A., and Ljungdahl, L.G. (2008). The complete genome sequence of *Moorella thermoacetica* (f. *Clostridium thermoaceticum*). Environ. Microbiol. *10*, 2550–2573.

Ragsdale, S.W., and Pierce, E. (2008). Acetogenesis and the Wood-Ljungdahl pathway of CO_2 fixation. Biochim. Biophys. Acta BBA-Proteins Proteomics *1784*, 1873–1898.

Servinsky, M.D., Kiel, J.T., Dupuy, N.F., and Sund, C.J. (2010). Transcriptional analysis of differential carbohydrate utilization by *Clostridium acetobutylicum*. Microbiology *156*, 3478–3491.

Slivka, R.M., Chinn, M.S., and Grunden, A.M. (2011). Gasification and synthesis gas fermentation: an alternative route to biofuel production. Biofuels *2*, 405–419.

Tanner, R.S., Miller, L.M., and Yang, D. (1993). *Clostridium ljungdahlii* sp. nov., an acetogenic species in clostridial rRNA homology group I. Int. J. Syst. Evol. Microbiol. *43*, 232-236.

Tirado-Acevedo, O., Chinn, M.S., and Grunden, A.M. (2010). Production of Biofuels from Synthesis Gas Using Microbial Catalysts. In Advances in Applied Microbiology, Allen I. Laskin, Sima Sariaslani, and Geoffrey M. Gadd, eds. (Academic Press), pp. 57–92.

Tirado-Acevedo, O., Cotter, J.L., Chinn, M.S., and Grunden, A.M. (2011). Influence of Carbon Source Pre-Adaptation on *Clostridium ljungdahlii* Growth and Product Formation. J. Bioprocess. Biotech. S2:001 doi:10.4172/2155-9821.S2-001.

Vega, J., Prieto, S., Elmore, B., Clausen, E., and Gaddy, J. (1989). The biological production of ethanol from synthesis gas. Appl. Biochem. Biotechnol. *20*, 781–797.

Wang, Y., Li, X., Mao, Y., and Blaschek, H.P. (2012). Genome-wide dynamic transcriptional profiling in *Clostridium beijerinckii* NCIMB 8052 using single-nucleotide resolution RNA-Seq. BMC Genomics *13*, 102.

White, D. (2007). The Physiology and Biochemistry of Prokaryotes (New York: Oxford University Press).

Zhang, M., Eddy, C., Deanda, K., Finkelstein, M., and Picataggio, S. (1995). Metabolic engineering of a pentose metabolism pathway in ethanologenic *Zymomonas mobilis*. Sci. Wash. *267*, 240-243.

CHAPTER 3

Influence of pH Adjustment on *Clostridium autoethanogenum* Xylose Consumption

Rachel M. Slivka, Mari S. Chinn, Amy M. Grunden, and Jose M. Bruno-Barcena

Abstract

In order to improve conversion of sugars derived from lignocellulosic materials to biofuels, organisms capable of metabolizing the xylose fraction in lignocellulosic hydrolysates are desired. *Clostridium autoethanogenum* is an autotrophic acetogen that also possesses the ability to ferment xylose; however, to date conditions under which it can effectively utilize xylose have not been explored. Four experiments were completed in order to understand the conditions which improve xylose consumption by this organism. The first study sought to challenge the organism with xylose levels ranging from 5 g/L to 45 g/L initial xylose to determine what concentrations, if any, were too high for *C. autoethanogenum* in batch cultures. A second study aimed to determine if nutrients such as vitamins or trace elements were required for efficient substrate consumption. The third study examined the impact of using media buffering versus pH adjustment to either 5.0 or 5.8 with base as a means to provide *C. autoethanogenum* with suitable pH conditions for xylose consumption. This portion of work also used xylose dosing to maintain sugar levels at a minimum concentration. The final study used the optimum pH conditions for xylose consumption and assessed how efficiently initial xylose concentrations ranging from 5 g/L to 30 g/L could be fully utilized. Results of the first study showed that *C. autoethanogenum* has an initial xylose limit of approximately 30 g/L xylose for growth and xylose concentrations as high as 45 g/L delay growth and decrease production of fermentation products. During investigation of the limiting condition affecting xylose utilization, pH rather than select vitamins or trace elements was found to be the critical factor for xylose metabolism. Intermittent pH adjustment of the culture to the growth optimal pH of 5.8 was determined to work best with incrementally-fed xylose. This dosing allowed all fed xylose to be consumed, and the cultures showed a unique biphasic growth phase which

enhanced biomass and end product (ethanol and acetate) output. When the method of intermittent pH adjustment to 5.8 was extended to *C. autoethanogenum* cultures with starting xylose concentrations as high as 30 g/L, the organism was able to fully utilize all available xylose and produce concentrations of 2.4 g/L ethanol and 9.5 g/L acetate from 30 g/L xylose. While these ethanol concentrations are still lower than other xylose fermenting organisms, *C. autoethanogenum* has been proven to be able to survive in and effectively use xylose concentrations typically present in lignocellulosic hydrolysate streams.

Introduction

Lignocellulosic materials are a relatively inexpensive and abundant resource for the production of renewable biochemicals and fuels consisting of feedstocks such as forestry residues (wood), crop residues (corn stover, straw, and grasses), and other solid waste streams (e.g. newspapers) (Balat, 2011). Lignocellulose consists of three main fractions: cellulose (a linear polymer of six-carbon sugar units), hemicellulose (a branched polymer of five- and six-carbon sugars), and lignin. The hemicellulose content of lignocellulose typically ranges from 15-38% dry weight in hardwoods and softwoods to as high as 25-50% dry weight in grasses and herbaceous crop residues (Demirbas, 2005). Furthermore, xylans are the most abundant form of pentose in hemicellulose with the xylose content of softwoods and softwood bark ranging from 9-15% by weight, and the xylose content of hardwoods and hardwood bark being the principal pentose at a weight percentage of 18-39%. The xylose composition of agricultural residues such as straws is 10.6-21%, while stalks (ex. sunflower or corn) are 12.8-19% xylose (Goldstein, 1981). Considering that pentoses, and especially xylose, make up such a large fraction of the available sugar in lignocellulosic process streams, the ability to effectively recover and ferment

pentose sugars into value-added products is vital to make the conversion process economically feasible (Demirbas, 2005).

Typically after an initial pretreatment and enzymatic hydrolysis, the free sugars (6-carbon and 5-carbon) in lignocellulosic hydrolysate are converted to value added products by means of microbial fermentation. Common species, such as *Saccharomyces cerevisiae* and *Zymomonas mobilis*, used to convert glucose to bioethanol are unable to naturally metabolize xylose and other pentoses (Rogers et al., 2007; Talebnia and Taherzadeh, 2006), so alternate microbial catalysts that do not require genetic modification to effectively use xylose should be considered. Prior biomass-derived xylose fermentation studies that used lignocellulosic hydrolysate as the substrate have noted starting xylose concentrations ranging from 7.5 to 11.2 g/L xylose (11-16% of the total sugars present, respectively, in wood chip or corn fiber hydrolysate) (Katahira et al., 2006; Moniruzzaman et al., 1996) with one study even using a concentrated corn stover hydrolysate that contained 71.8 g/L xylose (79% of the total sugars) (Zhao and Xia, 2010). These studies showed that xylose levels were substantial enough to support conversion by fermentation if possible. Additionally, the value gained from the pentose portion of the lignocellulosic streams could help offset some of the cost of producing renewable biofuels from those more complex feedstocks.

Autotrophic bacteria are capable of converting carbon streams derived from plant biomass, with the intended application to capture and convert single carbon gases (CO and CO_2) and hydrogen that are released when lignocellulosic biomass is broken down through the thermochemical process of gasification (material reaction at high temperature without combustion to produce synthesis gas). Several of the acetogenic autotrophs are mixotrophs that utilize both C1 gases and organic substrates like sugars. Two examples are *Clostridium*

autoethanogenum and *Moorella thermoacetica* (formerly *Clostridium thermoaceticum*) which readily ferment xylose and glucose/fructose/xylose, respectively (Abrini et al., 1994; Andreesen et al., 1973; Drake and Daniel, 2004; Fontaine et al., 1942).

Since *C. autoethanogenum* can metabolize xylose it has the potential to make use of the pentose sugar streams derived from lignocellulosic hydrolysates. However, the viability of *C. autoethanogenum* as a comparable candidate for future bio-based product production from xylose warrants further study and an assessment of its ability to metabolize xylose at concentrations found in lignocellulosic hydrolysate (both pre- and post-concentration) is required. It has already been documented that recombinant yeast stains can grow on the xylose content within lignocellulosic hydrolysates (Katahira *et al.*, 2006; Moniruzzaman *et al.*, 1996, 1997), and anaerobes such as *M. thermoacetica* and *Thermoanaerobacter thermosaccharolyticum* HG-8 can subsist on xylose substrate concentrations as high as 30 g/L and 73 g/L (Balasubramanian et al., 2001; Lynd et al., 2001), respectively, so xylose utilization comparable to those concentrations found in biomass hydrolysates have been observed. Meanwhile, studies with *C. autoethanogenum* have been limited to 5 g/L xylose with many reporting less than 60% conversion or consumption when it was the sole carbon source (Abrini et al., 1994; Cotter, 2006; Cotter et al., 2008), and thus the effect of higher xylose concentrations is unknown.

Limited substrate utilization can result if a required nutrient is limiting (Phillips et al., 1993; Sezonov et al., 2007), and nutrient limitation can impact other aspects of cellular performance including growth stage transitions and flux through metabolic pathways. Additional factors that may influence prokaryotic performance with respect to growth and product profiles include: pH, osmolarity, temperature, and pressure (Jansen et al., 1984;

Overmann, 2006). Most acetogens tend to show a growth associated acidogenic phase at more neutral pH followed by the initiation of a solventogenic state once the pH has dropped due to acid production (Durre, 2005; Klasson et al., 1992); however, a few studies have shown that *C. autoethanogenum* may be more sensitive to lower pH levels which could limit its performance (Abubackar et al., 2016a; Martin et al., 2016).

The purpose of this study was to determine the conditions which enable *C. autoethanogenum* to utilize xylose at levels comparable to concentrations obtained from lignocellulosic hydrolysates. The first objective was to challenge the organism with higher xylose levels thereby determining how much xylose *C. autoethanogenum* can withstand before the sugar concentration becomes detrimental to cell health. A second objective was to determine the impact of nutrients on xylose utilization with the goal of discovering if vitamins or certain trace elements were required for maximal substrate consumption. The third objective sought to determine the impact of using buffering versus pH adjustment to either 5.0 or 5.8 to provide the *C. autoethanogenum* cultures with optimal pH conditions for substrate consumption. This portion of work also used xylose dosing to maintain soluble sugar levels at a concentration that the cells were known to be able to metabolize but at the same time gradually boost the total level of xylose consumed. The final objective brought the different parts of the study together and examined the effect of culture pH adjustment to 5.8 while the cells were subjected to different initial xylose levels. Here the final goal was to determine maximum xylose utilization by *C. autoethanogenum* when culture conditions were ideal.

Materials and Methods

Organism, medium, and inoculum preparation

C. autoethanogenum (DSM 10061) was grown on DSMZ 640 basal medium under a batch, anaerobic atmosphere. The composition of DSMZ 640 medium (pH 6.0) was described previously (Cotter *et al.*, 2008, 2009). Briefly, it contains: trypticase peptone, yeast extract, cysteine hydrochloride, 640 salt solution, SL-10 trace element solution, 0.1% w/v resazurin, and is brought to volume with distilled water. Medium was dispensed anaerobically under an inert nitrogen (Airgas National Welders) atmosphere to either Balch tubes (18 mm outer diameter x 150 mm long, 9 mL medium) or serum bottles (160 mL, 72 mL medium) and autoclaved for 30 min (121°C, 17-18 psig).

Seed cultures of *C. autoethanogenum* were revitalized from frozen stock cultures (-80°C) by aseptically inoculating 10 mL Balch tubes containing 5 g/L xylose and a nitrogen headspace with a 5% v/v inoculum followed by incubation for 72 hours at 37°C (no agitation). With successive transfers to fresh medium, incubation was repeated for 48 hour, and then 24 hour incubation periods. Inoculum for experimental growth was prepared by transferring *C. autoethanogenum* cultures (5% v/v inoculum) to 640 medium with 5 g/L xylose and N_2 headspace (serum bottles, 80 mL), and then incubating at 37°C (no agitation) until appropriate cell density was reached (~24 hours, 0.8 OD target ≈ 254 mg dry cells/L).

Experimental design

Four different experiments were conducted to examine *C. autoethanogenum*'s ability to grow in xylose and ultimately improve its xylose utilization. In short, these experiments tested the effects of initial xylose concentration (*Initial Xylose Levels*), supplemental and/or altered nutrients (*Supplemental and Altered Nutrients*), media buffering and media pH adjustment mid-

fermentation (*Xylose Dosing with Buffering or pH Adjustment; Variable Xylose with pH Adjustment*) with the desire of improving growth, substrate consumption, and product formation over time.

General preparation of experimental cultures

The reactors were 160 mL serum bottles (Wheaton) plugged with butyl rubber stoppers (Bellco Glass) and contained 80 mL batch or fed-batch liquid growth medium as detailed below plus batch-N_2 gas at atmospheric pressure. In order to ensure that all treatments received the same initial density of *C. autoethanogenum* cells, reactors were inoculated with 5% v/v aliquots of 5 g/L xylose-adapted culture normalized to a seed culture optical density of 0.8 (~254 mg dry cells/L per aliquot). The experimental cultures were incubated in a 37°C water bath with 100 rpm orbital shaking for 66-336 hours depending on when stationary phase was reached and/or cell death occurred. Liquid (3 or 4 mL) samples were collected from the reactors every 6-16 hours over the growth period beginning at time zero. For those experiments with manual pH adjustment, additional 1 mL liquid samples for pH measurement were collected every 8 hours if no other sample was pulled at that time. The response variables for each experiment (unless noted otherwise) were cell concentration, pH, soluble xylose concentration, and primary end products (ethanol and acetate) as a function of time. Sample material for cell concentration (1mL) and pH (1mL) measurement was immediately analyzed, while material for substrate and product concentrations (2 ml) was frozen at -80°C in microcentrifuge tubes prior to analysis. Culture concentration was measured using a UV-visible spectrophotometer (Shimadzu UV-1700) at a wavelength of 600 nm and a dry cell weight to optical density (OD) conversion factor of 317 mg dry cells/OD (as determined experimentally by separate experiments). Intermittent culture pH was determined with a benchtop pH meter (Fisher Scientific accumet Excel XL15) by

submerging the pH electrode in a culture sample. Culture purity was checked at the end of the experimental period to determine whether foreign cells were present.

Experiment 1: Initial xylose levels.

The first experiment examined the impact of varying xylose concentrations in the growth media at five different levels: 5, 10, 15, 30, and 45 g/L initial xylose. Treatments were studied in triplicate and all experimental parameters (except pH) were measured. Sugar was added to the 640 media post-sterilization using sterile xylose solutions of 1.1%, 2.2%, 3.3%, 6.7%, and 10% w/v to achieve the desired initial xylose concentration in the reactors (36 mL xylose solution per 80 mL liquid volume). Culture pH was allowed to change naturally, and the batch liquid reactors remained untouched except to collect samples every 6 hours. pH data was not collected for this study.

Experiment 2: Supplemented and altered nutrients.

The second experiment modified the components used in the growth media at three different levels: DSMZ 640 medium with no modifications, DSMZ 640 medium with *C. ljungdahlii*'s PETC Modified Trace Elements substituted in place of Trace Element Solution SL-10, and DSMZ 640 medium with Modified Wolfe's vitamin solution added. Each of these trace element and vitamin solutions are described in detail in the studies by Cotter (2006) and Cotter *et al.* (2008, 2009). The purpose of replacing the trace element solution was to elucidate whether components found in PETC Modified Trace Elements but not in Trace Element Solution SL-10, i.e. selenium and tungsten, could improve *C. autoethanogenum*'s long term growth profile and allow it to better utilize xylose. Similarly, the growth media was supplemented with vitamin solution to add growth factors that were otherwise missing from the nutrient composition of DSMZ 640. In addition to trace element and vitamin factors, this study was conducted at initial

xylose concentrations of 5 and 15 g/L xylose for a total of six unique experimental conditions. Sugar levels in the culture media were prepared using 10% and 30% w/v xylose solutions (4 mL added post-sterilization) to achieve the target starting concentrations. More concentrated xylose stock solutions were used during this experiment compared to the initial xylose levels experiment to minimize the amount of water added to the reactors post-sterilization. This experiment was also performed over two growth periods using two sets of inoculum culture with the 5 g/L xylose cultures completed in triplicate during the first growth run and followed immediately by the 15 g/L xylose cultures which were completed in triplicate during the second run set. Culture volume was only altered to allow liquid sample collection every 6 hours, during which time the pH was allowed to change naturally. Samples for pH (5 mL) were only collected prior to inoculation and at the end of cell growth to assess the extent to which the culture pH dropped under each condition tested.

Experiment 3: Xylose dosing with buffering or pH adjustment.

The third experiment involved dosing *C. autoethanogenum* cultures with xylose in 2.5 g/L or 5 g/L increments to achieve a cumulative amount equivalent to 20 g/L xylose concentration (total mass added = 1.6 g xylose). In addition to xylose dosing, two pH related factors 1) media buffering with potassium phosphate or 2) intermittent pH adjustment with 3.0M KOH to pH 5.0 or pH 5.8 were implemented to affect xylose consumption by the cultures. All treatments were evaluated with six culture replicates. In order to confirm that the inoculum used for the experiment was healthy, growth controls were inoculated and grown up alongside the experimental cultures. The growth controls contained 2.5 g/L initial xylose with no media modifications, and the only parameter evaluated was their growth profile which agreed with other cultures grown under these conditions (e.g. initial xylose levels experiment).

For the cultures that were treated with potassium phosphate buffer to maintain pH (pH 5.8), concentrations of 0.05M, 0.1M, or 0.15 M were used. Potassium phosphate buffer was selected for three primary reasons: a) 640 medium has an initial pH of 6.0 prior to inoculation and a pH 5.8 once inoculum has been introduced, b) potassium phosphate salts are already present within the formulation for 640 medium, and c) it is one of the few buffers that maintains pH at 5.8 without adding citric or acetic sodium salts to the system. A typical formulation for a potassium phosphate buffer that maintains a pH of 5.8 is Gomori's recipe for 0.1M potassium phosphate buffer (Cold Spring Harbor Laboratory Press, 2006; Gomori, 1955). Assuming that 0.1M was the recommended strength, that concentration was multiplied by 0.5x and 1.5x in the treatments to help identify a reasonable buffer strength for *C. autoethanogenum* cultures. Buffering was accomplished by adding the appropriate volumes of 1M K_2HPO_4 and 1M KH_2PO_4 solutions to the growth media to achieve the desired buffer treatment concentration. The ratio of 1M K_2HPO_4 to 1M KH_2PO_4 was set based on the Henderson-Hasselbalch equation for a pH target of 5.8. As an example, the media with 0.1M potassium phosphate buffer contained 8.5 mL of 1M K_2HPO_4 and 91.5 mL of 1M KH_2PO_4 per liter of media. Since the salt solution used in DSMZ 640 media contains both K_2HPO_4 and KH_2PO_4, a modified 640 salt solution without potassium phosphate was used for media compounding to facilitate attainment of the desired potassium phosphate buffer concentrations.

As for the cultures treated intermittently with 3.0M KOH (sterile solution under an anaerobic, N_2 atmosphere) to raise the culture pH, target pH adjustment levels were set at 5.8, to match the buffer target, and 5.0, to match the mid-point of *C. autoethanogenum*'s ideal pH range of 4.0-6.0. KOH was selected as the base used for this experiment to have potassium ions rather than excess sodium (for example, from NaOH) added to the growth medium. Cultures with a pH

target of 5.0 were pH adjusted every 16 hours, while cultures with a target of pH 5.8 were pH adjusted every 8 hours for the length of the experiment. The amount of 3.0M KOH required to adjust the respective treatment reactors to the target pH was determined by measuring and then altering the pH of 1 mL culture samples with enough 3.0M KOH to raise the pH to either 5.0 or 5.8, respectively. The base aliquots per 1 ml sample were then scaled up for the volumes present in the reactors at the time of sampling. Losses of volumes as a result of sampling were accounted for.

Post inoculation, all experimental reactors were at an average pH of 5.8 and contained an initial xylose concentration of 2.5 g/L which was achieved by aseptically adding 5% (w/v) xylose solution (sterile, 4 mL) to the media post-sterilization. Then, after every 32 hours of growth, xylose was dosed to the reactors in 1 mL aliquots of 20% (w/v) xylose solution which provided 2.5 g/L sugar to the liquid volume on an 80 mL basis. At the same time as the dosing, reactor volume was brought back up to 80 mL by adding the appropriate volume of replacement media (either buffered or non-buffered DSMZ 640 media, pH 6.0). Upon reaching the 128 hour time point, the size of the xylose dose was increased to 5 g/L (2 mL xylose solution per 80 mL liquid volume) for this and all subsequent doses until the equivalent of 20 g/L initial xylose was attained (160 hours into the experiment), as it was presumed that some treatments were low in available sugar due to an observed drop in cell concentration. Since the reactors with 0.15M buffer were initially slow to grow, their 2.5 g/L xylose dose at hour 32 was withheld and subsequently added to the cultures at hour 192, and all remaining dose times and amounts were the same as for the other treatments (5 g/L). Samples for analysis of cell concentration, pH, substrate, and end products were collected every 16 hours (4 mL), with additional 3 mL samples collected after xylose dosing to establish the new concentrations of cells, xylose, and end

products as a result of the volume addition. Treatment cultures with pH adjustment to 5.8 also had additional 1mL samples collected every 8 hours for the purpose of determining the current pH. A representaion of the changes in culture volume due to additions and losses for the first 32 hours of the experiment is shown in Table 3.1. The volume changes then repeated on this same 32-hour basis hereafter until xylose dosing ceased at which point only the 1mL and 4 mL samples and base addition continued.

Experiment 4: Variable xylose with pH adjustment.

The final experiment evaluated xylose utilization with starting concentrations of 5, 10, 20, and 30 g/L xylose while intermittently adjusting the pH to 5.8 with 3.0M KOH. In addition to the xylose conditions with pH adjustment, a control treatment with 5 g/L initial xylose and no pH adjustment was also grown for evaluation. All treatments including the control were evaluated with four culture replicates. Initial xylose concentrations were achieved in the reactors by adding the appropriate volumes of sterile, 20% w/v xylose solution and sterile, anaerobic water (N_2 atmosphere). Liquid samples (4 mL) were collected from each reactor every 16 hours to measure pH, cell concentration, and soluble components in the broth with additional samples (1 mL) collected when needed to determine the culture pH at 8 hour intervals. Following measurement, the pH samples were adjusted to pH 5.8 with 3.0M KOH and then the volume ratio of base added per 1 mL sample was used to calculate the scaled volume of 3.0M KOH (sterile solution under an anaerobic, N_2 atmosphere) required to adjust the cultures in each reactor to pH 5.8. After every 32 hours of growth, the volume in each reactor, except for the control treatment reactors, was brought back to 80 mL by adding the appropriate volume of replacement media (DSMZ 640, pH 6.0) and xylose solution. In order to ensure that the replacement volume had the same xylose concentration as the reactors, the xylose concentration

of samples was measured at these time points using a YSI biochemical analyzer (YSI 2950) for more immediate feedback and xylose solutions with different weight percentages (5, 10, or 20% w/v) were utilized. Following volume replacement, 3 ml liquid samples were collected from each reactor to establish a new reference point for the concentration of cells, substrate, and products. In order to mimic the volume change of the earlier experiment with dosed xylose and pH adjustment to 5.8, volume replacement for this experiment was discontinued after 160 hours culture growth.

Statistical analysis

The main and interaction effects of factors for the described experiments on cell growth, xylose utilization, and end product formation (ethanol and acetate) in *C. autoethanogenum* cultures were evaluated using the General Linear Model (GLM) in SAS® Version 9.4 (SAS Inc., Cary, NC). Assessment of statistical differences between treatments was made at an α level of 0.05. The impact of added and/or altered components in the trace element or vitamin solution were statistically analyzed over time, while the impact of buffer concentration, degree of pH adjustment, and initial xylose concentration with pH adjustment to 5.8 were statistically evaluated at the maximum value for the response variables.

End product analyses

Water-soluble analytes present in the culture broth samples, specifically xylose, acetate (in the form of acetic acid), and ethanol, were analyzed by HPLC (Shimadzu LC-20AD). Prior to quantification, thawed liquid samples were centrifuged (10 min, 20,800 *x g*, 25°C) and the supernatant (800 µL) was filtered through a 0.2 µm syringe filter (Whatman, cat no. 6768-1302). Clarified samples were then analyzed on a Phenomenex Regex ROA column (300 x 7.8 mm, part no. 00H-0138-K0) at 55°C using a refractive index detector set at 40°C and 5 mM sulfuric acid

as the eluent (0.6 mL/min). Xylose concentration in the culture broth was also analyzed mid-experiment using an YSI biochemistry analyzer (YSI 2950) setup to run xylose chemistry (YSI 2761 xylose membrane, YSI 2767 xylose standard solution, and YSI 2357 buffer). Sugar analysis mid-experiment via YSI was performed because it allowed more immediate estimates (i.e. 2-3 minutes vs. hours) of the xylose concentrations within all the replicates for xylose solution and media adjustment additions.

Results and Discussion

Initial xylose levels

The assessment of *C. autoethanogenum* performance under different initial xylose concentrations elucidated that there is an upper threshold where sugar can no longer be consumed by the cells and also a sugar concentration where cell growth is limited. Under conditions during which the pH was allowed to change naturally with cellular metabolism, *C. autoethanogenum* tolerated up to 30 g/L xylose with minimal detriment to cell function. Between 5 to 15 g/L initial xylose, the cells exhibited similar growth patterns with the cultures reaching stationary phase after approximately 48 hours (Fig. 3.1a). At the 30 g/L level, cellular performance was slightly depressed compared to the lower treatments, but not enough to indicate that cells cannot tolerate exposure to this sugar load. Similar results were observed for the creation of end products (Fig. 3.1b, 3.1d) with maximum concentrations of 3.1-3.3 g/L acetate and 0.19-0.46 g/L ethanol achieved across all levels at and below 15 g/L initial xylose. The extent of end product variability, especially for ethanol, as displayed in Figures 3.1b and 3.1d was attributed to the commonly observed sensitivities of the organism. At the highest concentration tested, 45 g/L initial xylose, there was a pronounced 24 hour lag in cell growth accompanied by a related lag in growth-associated acetate production. Besides attaining lower

biomass and acetate maxima compared to the other treatments, the 45 g/L xylose treatment also failed to produce detectable concentrations of ethanol. The inferior performance combined with the growth delay indicated that this sugar concentration was too high and caused the cells to enter a state of osmotic shock. Although *C. autoethanogenum* may not be able to withstand xylose streams more concentrated than 30 g/L xylose, this experiment demonstrated, nonetheless, that it can tolerate and remain viable within the range of xylose concentrations in streams derived from lignocellulosic hydrolysate prior to concentration.

The impact of higher initial substrate loading on microorganism performance has been well documented in prior literature. For example, evaluation of *Pichia stipitis* and *Candida shehatae* performance on different initial xylose concentrations found that maximum ethanol production could not be attained above 50 g/L xylose, growth rates began to decline above 20 g/L and 50 g/L, respectively, and at initial xylose levels higher than 90 g/L *P. stipitis* had trouble utilizing all of the available sugar (du Preez et al., 1986). Another study with *Klebsiella oxytoca* showed that the maximum specific growth rate decreased at xylose concentrations greater than 20 g/L and the cells could not grow in conditions more concentrated than 160 g/L xylose (Jansen et al., 1984) These instances of substrate inhibition at higher xylose concentrations were the result of decreases in water activity as the solute level increased (Hahn-Hägerdal, 1986; White, 2007). An option to attain higher product concentrations in the fermentation broth while avoiding inhibitory solute levels is to introduce a slow-feed of xylose at an optimal concentration for the cells (Jansen et al., 1984; Olson and Johnson, 1948).

Higher initial xylose concentrations did not improve xylose utilization during the course of the experiment (Fig. 3.1c) since the 5 g/L reactors consumed the highest xylose load at 3.12 g/L. Cotter *et al*. (2008) also saw a maximum xylose consumption of ~3 g/L under similar

conditions with 5 g/L initial xylose. The cap in xylose utilization brought two points to light: the cells were likely not using affinity based xylose transporters under these experimental conditions, and more importantly, there was a limiting nutrient or condition that was preventing further xylose uptake by the cells.

Determination of the limiting factor impacting cell function

Overmann (2006) states that there are 12 macroelements (C, O, H, N, S, P, K, Mg, Ca, Na, Cl, and Fe) that make up 98% of the total dry weight of prokaryotes. There are also 10 microelements (Mn, Co, Cu, Mo, Zn, Ni, V, Se, W, and B) that should be supplied in the growth media of prokaryotes at concentrations of 0.01-1 μM with selenium (Se) and tungsten (W) being of importance to strict anaerobes. Some of these nutrients are supplied to the cell in the form organic substrates such as sugars, while others are provided to the growth media in the form of stock solutions of trace elements and salts (DSMZ, 2018). Growth factors may also be added to the growth media in small concentration to reduce the need for de novo biosynthesis of compounds within the cell. The three categories of growth factors are vitamins (ex. biotin, *p*-aminobenzoic acid, folic acid, riboflavin, pantothenic acid, and nicotinic acid), amino acids, and nitrogenous bases (purines and pyrimidines) (Overmann, 2006). Phillips et al. (1993) conducted a medium development study with *C. ljungdahlii* (which is closely related to *C. autoethanogenum*) and found that the B-vitamins biotin, thiamine-HCl, and Ca-D-pantothenate are required for growth and that suboptimal concentrations of certain elements (iron in particular) within the trace metals solution could cause growth limitation. Once the medium used with *C. ljungdahlii* was reformulated, total product concentrations (ethanol and acetate) shifted remarkably upward. In another study, Saxena and Tanner (2011) discovered that separately increasing the ion concentrations of Ni^{2+}, Zn^{2+}, SeO^{4-}, and WO^{4-} with *Clostridium*

ragsdalei improved ethanol production and in some cases increased growth and enzyme activities.

Further study into factors limiting *C. autoethanogenum* function and preventing greater xylose utilization, led our research team to question whether nutrients such as growth factors (i.e. vitamins) or certain trace elements were missing from the DSMZ 640 basal medium used to grow the cells. In order to answer this query, the DSMZ 640 basal medium was supplemented with modified Wolfe's vitamin solution to provide additional growth factors (e.g. folic acid, thiamine, nicotinic acid, para-aminobenzoic acid, etc.). Additional treatments replaced the SL-10 trace element solution used in DSMZ 640 medium with PETC modified trace elements as the latter had the added presence of selenium and tungsten. Both modified Wolfe's vitamin solution and PETC modified trace element solution have been used in the successful culture of the related species *Clostridium ljungdahlii* (Bruno-Barcena et al., 2013; Cotter et al., 2008; Tirado-Acevedo et al., 2011).

As Figure 3.2 shows, there were both significant and insignificant statistical differences between the treatments when testing for increased carbon use with either altered trace elements or the addition of vitamin solution. Overall, the control conditions (no change in medium formulation) showed the greatest utilization of xylose for this experiment (Fig. 3.2c). For xylose consumption at 5 g/L initial xylose, the control treatment had statistically higher consumption than the vitamin treatment but not statistically higher consumption than the trace element treatment. In terms of xylose consumption at 15 g/L initial xylose, the control treatment had statistically higher consumption than the trace element treatment but not statistically higher consumption than the vitamin treatment. Between the two sugar treatment levels, the 15 g/L xylose cultures had consistently higher cell concentrations, xylose consumption, and end product

generation than the 5 g/L xylose cultures. Since the two sugar treatments were grown up a few days apart, they were inoculated with different inoculum sets (inoculum density - 5 g/L: 266 mg dry cells/L, 15 g/L: 273 mg dry cells/L) that were derived from the same aliquot of frozen stock culture, and as a result some of the sugar effect observed may be attributed to the fastidious nature of the cells. However, the sugar effect may also indicate that the cells are capable of transporting more xylose substrate across the cell membrane at higher sugar concentrations during mid- to late-exponential growth (Fig. 3.2a, 3.2c). At the end of the experiment (elapsed fermentation time of 67 hours) when xylose utilization and biomass production had ceased, all reactors had an average pH of 3.97 or 3.91, for the 5 g/L and 15 g/L initial xylose treatments respectively, regardless of the supplemental nutrient conditions applied. Given that the lower pH limit for ideal *C. autoethanogenum* growth is 4.0, the cultures had obviously reached the point where environmental acidity became the limiting factor. At an initial xylose concentration of 5 g/L, the use of PETC modified trace elements positively enhanced final ethanol production and lowered the maximum acetate concentration (Fig. 3.2b, 3.2d). This treatment also resulted in a lower maximum concentration of cells capable of metabolizing xylose into value added end products (Fig. 3.2a). There was little biomass or end product difference between the control and the treatment supplemented with modified Wolfe's vitamins over the course of active cell metabolism at this xylose concentration. When the initial xylose concentration was raised to 15 g/L, the results observed were similar to the 5 g/L concentration treatments however, in combination with the use of vitamin solution yielded a higher biomass concentration. The presence of trace elements (i.e. selenium and tungsten) found in PETC modified trace elements may have had some minimal impact (3-6% increase in ethanol production and 3-4% decrease in

acetate production compared to the control medium), but they did not significantly enhance xylose consumption (4-9% lower xylose consumption compared to the control medium).

Abubackar et al. (2015a) studied trace elements and vitamins in batch *C. autoethanogenum* cultures but with CO as the carbon source and a culture incubation temperature of 30°C instead of the optimal 37°C (Abrini et al., 1994). The concentrations of selenium and tungsten used in the PETC modified trace element solution for this work were 0.25 μM and 0.136 μM, respectively, and approximately double the concentrations tested by Abubackar et al. (0.144 μM Se and 0.075 μM W) when supplementing SL-10 trace elements solution. Contrary to the Abubackar et al. (2015a) study reporting little change from selenium addition and a large improvement in ethanol to acetate ratio from tungsten addition, the impact of using both components at the same time in this study may have been counterproductive because the ethanol to acetate ratio only slightly improved compared to the control medium. Similar to this work, Abubackar et al. (2015a) also saw no improvement from the use of vitamin solution.

Ultimately, the use of a trace element solution containing selenium and tungsten (e.g. PETC modified trace element solution) appears to be more influential on the conversion of downstream metabolites and end products than to the cells' ability to consume and process carbon within the central metabolic pathways. This signifies that the presence of selenium and tungsten are not critical to enhanced xylose metabolism by *C. autoethanogenum* and that the microelement concentrations within SL-10 trace elements solution are sufficient for normal cell function. The addition of modified Wolfe's vitamin solution to the growth media also failed to show a dramatic improvement in *C. autoethanogenum*'s xylose consumption, or cell performance in general, compared to how the organism performed on unaltered DSMZ 640 medium. Complex medium formulations such as DSMZ 640 commonly use yeast extract to

provide a source of vitamins for bacterial growth with the downside that exact vitamin concentrations are undefined. However, based on the evidence here, it can be deduced that the concentration of yeast extract (1 g/L) used in DSMZ 640 medium is sufficient enough to provide necessary levels of vitamins such as biotin, thiamine-HCl, and Ca-D-pantothenate for peak *C. autoethanogenum* growth and carbon utilization.

The stability of the cell membrane and its potential deficiencies were also briefly evaluated as a limiting factor to xylose consumption. The cell membrane not only contains the sugar transporters used to bring xylose into the cell, but also provides a protective barrier against environmental conditions so that the cell can maintain the internal homeostasis necessary for carbon metabolism to occur. Since the availability of divalent cations, specifically Ca^{2+}, is critical to proper proton transfer and membrane maintenance this nutrient was added to the basal medium, but its presence did not appear to have a significant effect on cellular metabolism or xylose consumption (data not shown). However, preliminary work leading to the third experimental objective where the pH of the culture broth was adjusted mid-growth showed that the eventual decay of culture pH to toxic levels ($pH \leq 4.0$) could be circumvented for a brief period and this allowed the cells to display enhanced metabolism, a 55% improvement in xylose consumption, and a delay in cell death (data not shown).

Impact of buffering versus pH adjustment

Building upon prior observations that *C. autoethanogenum* cultures prematurely cease metabolic activity as a result of natural pH change to a point of acid toxicity (~ pH 4.0), continued work sought to determine whether additional potassium phosphate buffering capacity in the growth media or pH adjustment with base could be used to attain effective pH conditions for this organism and allow continued substrate utilization. This experiment also exposed the

cells to a lower initial xylose load of 2.5 g/L followed by additional 2.5 g/L or 5 g/L xylose doses every 32 hours at which point the cells should have been in need of more substrate. The justification for providing small, recurring aliquots of xylose to *C. autoethanogenum* was that hopefully the cells would never be presented with more sugar at one time than they were known to metabolize effectively, creating additional osmolality challenges. Among the five conditions tested, there was a noted difference between the performances of those cultures treated with potassium phosphate buffer versus those treated with 3.0M KOH to adjust pH. As Figure 3.3 shows, the pH adjusted treatments had better culture productivity across all parameters measured than buffered treatments.

In terms of culture growth, buffer concentrations above 0.05M potassium phosphate appeared to have an initial inhibitory effect on biomass production (Fig. 3.3a). This inhibition was quite pronounced at the 0.15M buffer concentration with the growth lag also resulting in delays in xylose consumption and end product formation (Fig. 3.3b, 3.3d). A slight growth offset was seen with 0.1 M buffer, and as a second negative effect, this buffer concentration treatment failed to effectively maintain pH at the 5.8 target for the full length of the experiment. The 0.1M buffer only appeared to have kept the growth media buffered for a little over 16 hours (Fig. 3c) with the sample pH dropping to 5.4 at hour 32 and pH 4.4 by hour 65 when the culture reached its peak cell concentration of 428 mg dry cells/L. As for the 0.05M buffer, it did nothing to slow down the pH decline in the reactors and the cultures reached pH 4.25 and a maximum density of 456 mg dry cells/L by hour 48 which is when a *C. autoethanogenum* culture grown on xylose without pH maintenance typically reaches its peak biomass (Figure 3.2a and Cotter *et al.*, 2008). The xylose consumption trends (Fig. 3.3e, 3.3f) for the buffered treatments mirrored the observations for cell growth and pH change. Delays in cell growth matched delays in xylose

consumption for the periods when the buffer prevented drops in culture pH. When the cultures were increasing in cell concentration, the total quantity of xylose consumed also increased. Then, when cell growth slowed and decayed in parallel with the accumulation of undissociated acid in the environment at lower pH's (pH 4.0-4.76), xylose consumption also slowed or came to a halt. It should be noted, however, that as the experiment progressed xylose dosing began to affect the fraction of net xylose consumed per the cumulative amount of xylose fed (Fig. 3.3e). The buffered treatments consumed xylose slower than the expected rate and as a result additional sugar was dosed to the cultures before the prior aliquot could be fully utilized and the xylose concentration built up in a manner inversely proportional to the cell concentration. This effect was further exacerbated at hour 128 when the xylose dose increased from 2.5 g/L to 5 g/L because of the incorrect assumption that biomass concentration was decreasing as a result of low available xylose (see Materials and Methods). Yet, on the positive side, all of the buffer treatments consumed a progressively higher total xylose load as the buffer concentration increased with consumption values of 4.07, 5.07, and 7.21 g/L, respectively for 0.05M, 0.1M, and 0.15M buffer. Media buffering did have a somewhat helpful effect on the level of xylose consumed compared to cultures with unaltered, naturally changing pH (~3 g/L xylose consumed, Fig. 3.1c). Similarly, the end products generated by the buffer treatments ranged from total production of 3.11 g/L acetate and 0.15 g/L ethanol with the 0.05M buffer to 5.31 g/L acetate and 0.49 g/L ethanol with the 0.15M buffer (Fig. 3.3b, 3.3d). Only the 0.15M buffer treatment produced more acetate than cultures in the initial xylose concentration experiment with unaltered, naturally changing pH (Fig. 3.1b) and there was not a large difference between the produced ethanol values (Fig. 3.1d and 3.3d). The 0.15M buffer treatment also showed a period of biphasic growth. Two contributing factors to that observation may have been the delay in

active growth and the timing of xylose additions. Overall, it was observed that, for as long as the potassium phosphate buffer treatments provided buffering to the media, they seemed to stunt cellular metabolism. Two setbacks to phosphate buffer use which could have occurred here during the period of pH buffering are that they inhibit enzymatic reactions (possibly impacting membrane complexes) and that they sequester divalent cations (ex. Mg^{2+}) in the media which are required to maintain a robust cell membrane and proton transfer (Cold Spring Harbor Laboratory Press, 2006). Although potassium phosphate buffer was unable to maintain the extracellular pH, it is quite possible that the extra potassium ions released by dipotassium phosphate during the buffering reaction were able to prolong maintenance of the intracellular pH by dissipating the membrane potential and allowing more protons to be pumped out of the cell (White, 2007). The longer the intracellular pH of *C. autoethanogenum* was maintained and extracellular pH remained unbuffered, the more capable the cells were to metabolize xylose and consequently produce more biomass and end products.

Kundiyana et al. (2011) found that for *Clostridium ragsdalei*, grown at a favorable temperature (32°C or 37°C) on syngas, the occurrence of the switch from acidogenesis to solventogenesis was delayed with increasing buffer concentrations. In this same study, treatments with no buffer and grown at 32°C showed higher biomass concentrations than treatments that used buffer in the medium. An earlier study by this same group (Kundiyana et al., 2010), also showed that while buffering may initially keep the pH elevated (and hence delay the acid to solvent production switch), the culture pH still drops and after a certain point in time there is no difference between the pH of a buffered versus an unbuffered culture. Both of these studies reaffirm the observations seen here related to growth rate and media buffer capacity

where buffering slows the metabolism of similar autotrophic acetogens and only has limited capacity for maintaining external and internal pH.

The two treatments subjected to pH adjustment with 3.0M KOH reached initial growth maxima of 406 and 431 mg dry cells/L at 48 hours, for pH adjustment treatments to 5.0 and 5.8 respectively, and then the cells switched their physiological state to allow continued growth and metabolism (Fig. 3.3a). The initial growth peak agreed with what was observed with the buffer treatments and the earlier *C. autoethanogenum* studies (Fig. 3.1a) after 48 hours of active growth; however, the appearance of biphasic growth was a novel and desirable feature that served to greatly improve culture productivity. In association with the second exponential growth segment for the pH adjusted cultures, both xylose consumption and end product formation increased strongly and the pH shifts observed between pH adjustments became more drastic (Fig. 3.3b, 3.3c, 3.3d, and 3.3f). After the second growth period, the cultures with pH adjustment to 5.8 achieved a maximum cell concentration of 1,116 mg dry cells/L, however, the cell concentration could have been higher had the cells not begun to die from increased rate of xylose consumption and lack of available xylose beyond the final dosing time. Sugar dosing for this treatment ceased after 162 hours when the total added sugar mass reached the point where it was deemed equivalent to an initial sugar concentration of 20 g/L, and over 99% of fed xylose was consumed by hour 210 for pH 5.8 treatments (Fig. 3.3e). Before ethanol and acetate levels in the cultures leveled off following sugar exhaustion, the treatment with pH adjustment to 5.8 had produced 13.04 g/L total acetate and 1.53 g/L total ethanol from a net total of 18.5 g/L xylose. Although the cultures with pH adjustment to 5.0 did not consume all of the available xylose, they had generated 9.03 g/L total acetate and 1.31 g/L total ethanol from a net total of 12.53 g/L xylose by the end of the experimental period. These cultures also appeared to enter a

stable stationary phase as opposed to outright dying which indicates that cellular regulation as opposed to extremely adverse conditions (ex. pH ≤ 4.0 or no available substrate) caused the cells to limit further growth. All of the results for both of the pH adjustment treatments were a definite improvement compared to the initial xylose concentration experiment with unaltered, naturally changing pH (Fig. 3.2, 3.3). The difference in pH adjustment to 5.0 versus 5.8 did have an impact on cellular performance and cultures with a higher pH adjustment target maintained a higher ratio of xylose consumption and demonstrated biphasic growth sooner than the lower pH target. Although the 5.0 pH target was centered in the ideal pH range for *C. autoethanogenum*, this target was also closer to the dissociation point for acetic acid/acetate (pKa = 4.76) which means that the cells may have been subjected to more of the harmful acid form of this metabolite. Given the significantly higher biomass production by the 5.8 pH target during the second growth phase, this treatment may be better at maintaining cells in an optimal growth state capable of converting more xylose to end products. Although grown on CO as the substrate, Abubackar et al. showed that *C. autoethanogenum* produced more acetic acid at higher pH (5.75) versus lower pH (4.75) (Abubackar et al., 2015b) and cyclic pH shifts from 5.75 to 4.75 and back allowed enhanced production of ethanol to a concentration of 7.1 g/L after a period of 9.8 weeks (Abubackar et al., 2016a). That earlier study also reported no distinct acidogenic versus solventogenic phase (i.e. ethanol was growth associated) (Abubackar et al., 2015b) which the work here observed as well. In another study, Martin et al. (2016) observed that lowering the culture pH from 5.5 to 4.5 failed to initiate the shift to soventogenesis and resulted in lower substrate consumption, and total and individual product concentrations in *C. autoethanogenum* grown on syngas (60% CO, 35% H_2, and 5% CO_2, molar) in two-stage continuously fed reactors. This was unlike the two *C. ljungdahlii* species (PETC [ATCC 55383] and ERI-2 [ATCC 55380])

also tested during the study which showed a decrease in acetate concentration per cell and a consistent ethanol concentration per cell (cell mass was increasing) when the pH dropped to 4.5 in the second reactor stage. Overall, Martin et al. concluded that *C. autoethanogenum* was sensitive to low pH. The experimental information collected and presented here also supports the theory that *C. autoethanogenum* has poor low pH tolerance on soluble sugar as if the cell membrane is not as resilient to extracellular acidity as other acetogenic species. The cells consumed less sugar when the extracellular pH was allowed to drop lower or was adjusted to a lower pH target, and this indicates that the bacterium has to balance carbon assimilation against the risk of transporting in acid that could lower the intracellular pH. Greater consumption of carbon will lead to higher rates of metabolic flux and hence greater amounts of end products; however, since one of its major end products, acetate, is a pH lowering acid, *C. autoethanogenum* must prevent the pH from becoming too low. The two responses that the organism exhibited in this experiment to prevent acidification were reduced xylose consumption and acetate generation at lower pH and initiated production of growth-associated alcohol to maintain a desirable acetic acid to acetate concentration ratio.

The average end product ratios present within the cultures during this experiment were better for the treatments with pH adjustment via 3.0M KOH compared to those with potassium phosphate buffering. Just as the xylose consumption and end product yields improved as the concentration of buffer increased, the ethanol to acetate mass ratio also shifted more favorably towards ethanol production. The 0.5M, 0.1M, and 0.15M buffer treatments generated respective ethanol to acetate mass ratios of 1:16.2, 1:11.2, and 1:10.1 ($E:A_{molar}$ = 1:12.4, 1:8.6, and 1:7.7, respectively). As a comparison point, *C. autoethanogenum* grown on 5 g/L initial xylose with no pH modification gave an $E:A_{mass}$= 1:10 (initial xylose levels experiment and Cotter et al., 2008),

while cultures grown under similar no pH modification conditions with only 2.5 g/L initial xylose gave an $E:A_{mass}$= 1:11 (unpublished work). The cultures with pH adjustment to 5.0 showed a much improved ethanol to acetate mass ratio of 1:5.1 ($E:A_{molar}$ = 1:3.9) which was observed in the last experimental samples collected for that treatment (hour 320). While not as high, a maximum ethanol to acetate mass ratio of 1:7.7 ($E:A_{molar}$ = 1:5.9) was seen in the cultures with pH adjustment to 5.8 after 258 hours of culture growth, along with greater total concentrations. As the end product ratio is an indicator of the carbon and energy flux within the cells at a point in time, it was also observed that the treatment with pH adjustment to 5.8 showed a shift in its ethanol to acetate mass ratio to 1:5.7 ($E:A_{molar}$ = 1:4.4, hour 288) once the cultures began scavenging the end products (notably acetate) for reincorporation into needed compounds. Abubackar et al. (2015a, 2016a, 2016b) has shown previously that *C. autoethanogenum* is capable of converting acetate into other metabolites such as ethanol. The variation in ethanol to acetate ratio between the two treatments with pH adjustment and also in relation to *C. autoethanogenum* cultures with no pH adjustment is best explained by a two-fold hypothesis. The effect of maintaining the culture pH at a higher level more desirable to the cells (i.e. pH ≥ 5.0) alters the overall product formation because more substrate can be consumed at these conditions; and, as a result of the increased ethanol formation in relation to acetate production at a desirable pH versus a more harmful pH, the product ratios shift. Secondly, a lower but still desirable culture pH (i.e. pH 5.0 versus 5.8) will have lower cell growth compared to a higher pH condition and lower production of grow-associated end products. With the lower pH, the proportional decrease in acetate production from slowed growth will be greater than the proportional decrease in ethanol production. Since ethanol is induced by the presence of reducing equivalents and prevents the conversion of acetate to the more harmful acetic acid

form, a lower pH value will cause higher ethanol production and more promising ethanol to acetate ratios. This is especially important because a lower extracellular culture pH shifts the acetic acid to acetate ratio towards acid and acetic acid can more easily lower the intracellular pH because of its membrane permeability. Both Martin et al. (2016) and Abubackar et al. (2015a) showed greater ethanol to acetate ratios at lower pH (4.5-4.75 versus 5.5-5.75) in *C. autoethanogenum* with production of less acetate at this lower pH value.

Utilization of variable initial xylose concentrations

When pH adjustment every 8 hours to a target of 5.8 (3.0M KOH) was extended to *C. autoethanogenum* cultures with starting xylose concentrations ranging from 5-30 g/L, the results reinforced prior observations and a new level for xylose utilization was achieved. As shown in the Figure 3.4a, biphasic growth occurred again at the higher two sugar levels (20 g/L and 30 g/L initial xylose). Since all treatments which underwent pH adjustment showed complete xylose utilization (Fig. 3.4b), the lack of biphasic growth at the 5 g/L and 10 g/L treatment levels was likely the result of limited sugar availability because both cultures were out of xylose by the time the second exponential growth phase began in the 20 g/L and 30 g/L cultures. The control treatment, with 5 g/L initial xylose and no pH adjustment, had only consumed 3.26 g/L xylose by the time its growth ceased at pH 4.0 from the acidic environment. In addition, the control treatment produced maxima of 393 mg dry cells/L, 1.82 g/L acetate, and 0.09 g/L ethanol (Fig. 3.4a, 3.4d and 3.4f).

Prior to the initiation of the biphasic stage of cellular performance the treatments behaved fairly similarly and in particular similar pH shifts across treatments were observed between pH adjustments (Fig. 3.4c) until the xylose was depleted for each treatment and cell lysis started. There was not a significant difference between the amount of biomass produced by the 5 g/L and

the 10 g/L initial xylose treatments, nor was there significant variability between the concentration of ethanol created by the control, 5 g/L, or 10 g/L treatments (Fig. 3.4f) even though the cultures consumed different amounts of xylose (Fig 3.4b). The 5 g/L and 10 g/L treatments did produce statistically significant different amounts of acetate (Fig. 3.4d) at 2.41 g/L and 3.86 g/L, respectively, which accounts for the sugar difference between the two conditions (additional sugar may have been lost due to dilution if the xylose concentration in the media replacement was not matched precisely). Once the second growth phase started, the two higher sugar treatments both displayed significant increases in the concentrations of growth-associated ethanol and acetate generated (Fig. 3.4d, 3.4f). The 20 g/L xylose cultures yielded 7.16 g/L acetate (nearly double the concentration produced by the 10 g/L xylose cultures), while the 30 g/L treatment produced significantly more acetate at 9.47 g/L. Ethanol production was also significant with the concentration doubling from 1.17 g/L with 20 g/L xylose to 2.43 g/L with 30 g/L initial xylose in the reactors. The ethanol concentration generated by the 30 g/L xylose treatment with pH adjustment was the highest value thus far for this series of studies, and equated to the cultures having an ethanol to acetate mass ratio of 1:3.3 ($E:A_{molar}$ = 1:2.5) at the maximum ethanol value (Fig. 3.4e). It was also the best product ratio observed throughout all four of these experiments. As Table 3.2 shows, it was also observed that as the initial xylose concentration increased from 5 g/L to 30 g/L across the pH 5.8 adjusted treatments, the acetate yield per gram of xylose consumed decreased by 29% from 0.51 g/g to 0.36 g/g, while the ethanol yield per gram of xylose consumed increased by 200% from 0.031 g/g to 0.094 g/g. Although the two cultures consumed distinctly different amounts of xylose, the 20 g/L and 30 g/L xylose treatments reached their maximum cell concentrations, 882 mg dry cells/L and 1238 mg dry cells/L respectively, within 16 hours of each other and exhausted their available xylose at

relatively similar points in time (Fig. 3.4b). The increased rate of xylose utilization by the 30 g/L xylose treatment indicated that the cultures were expressing an altered mechanism for xylose transport which may be related in turn to the simultaneous occurrence of biphasic growth, shifts in the rate of ethanol and acetate production, and greater drops in pH between pH adjustment time points. As further support for this point, the 20 g/L xylose treatment took approximately 136 hours to consume its first 10 g/L of xylose (at the same point in time the 10 g/L treatment had consumed all but 0.5 g/L xylose), but only 104 more hours to consume the majority of the remaining xylose. Likewise, the 30 g/L xylose treatment consumed its first 10 g/L xylose in about 136 hours, and then consumed the remaining ~20 g/L sugar at an even faster rate with near exhaustion just 120 hours later. This also indicated that the cells were experiencing better energetics during the latter half of the experiment in order to be able to sustain a higher rate of xylose transport and utilization.

If enough reductant was available, the change in energetics could be the result of *C. autoethanogenum* metabolizing the CO_2 created during xylose metabolism in the Wood-Ljungdahl pathway for carbon fixation (Drake et al., 2008). Between the gradual increases in CO_2 partial pressure under a batch headspace the longer the experiment runs, which would enhance CO_2 solubility, and the ability of acetogens to metabolize C1 gases at low versus dense culture growth (Vega et al., 1990), the Wood-Ljungdahl pathway may not activate in *C. autoethanogenum* when sugar is the only provided substrate unless the C1 gasses reach a high enough concentration. This higher gas concentration may only be achievable when higher loads of xylose (>10 g/L total xylose) are metabolized. Gas analysis of the culture headspace ($CO_2 \rightarrow$ CO) would be required to test this theory, but additional work by this group has shown that pH adjustment of xylose-grown cultures at a larger scale (250 mL) only results in biphasic growth

and higher cell concentrations when the headspace is batch and not continuous (data shown in Supplemental Appendix B). If the Wood-Ljungdahl pathway was activated during the second half of the experiment, this would have provided more carbon for incorporation into metabolites and the high reductant demand of the pathway would help to maintain intracellular pH. In addition, enzymology studies of *C. autoethanogenum* during autotrophic metabolism have shown that the organism uses an $NADP^+$-dependent enzyme to convert CO_2 to formate in the first step of the Wood-Ljungdahl pathway (Wang et al., 2013), and since NADP(H) tends to be growth associated this may indicate that continued biomass production is ideal during pathway operation. The organism also uses an Rnf complex in conjunction with an F_1F_0-type ATP synthase to provide ATP that makes the Wood-Ljungdahl pathway energetically feasible during autotrophic metabolism (Mock et al., 2015). If this method of ATP synthesis is active during mixotrophic metabolism as well, it may provide further insight into the nature of the increased bioenergetics witnessed here.

The key to success in enabling *C. autoethanogenum* to metabolize higher xylose loads and to yield greater end products appears to be related to pH and H^+ concentration. A pH target of 5.8 is akin to the initial pH of *C. autoethanogenum* cultures following inoculation and is thus a state optimized for cell growth. While ample studies with acetogens indicate that the desired state for ethanol production is within the lower end of the pH range with cells in stationary growth (Durre, 2005; Klasson et al., 1992), *C. autoethanogenum* seems to produce ethanol as a co-product with growth-associated acetate and cannot truly unlock its solvent-producing potential with xylose as the substrate unless it maintains a higher pH conducive to growth. It may be that while traditional acetogens allow the extracellular pH to decrease by shuttling H^+ ions outside the cell as a means to maintain intracellular pH, *C. autoethanogenum* prefers a

higher extracellular pH for optimal performance and in order for it to maintain its intracellular pH it has to get rid of electrons from NADH in an electron sink such as ethanol or convert intracellular acetic acid into acetaldehyde (and subsequently form ethanol) via aldehyde:ferredoxin oxidoreductase (Marcellin et al., 2016; Mock et al., 2015). Just as traditional acetogens eventually begin synthesizing ethanol instead of acetate as a means of slowing the decline of extracellular pH, as a result of high concentrations of extracellular and intracellular acetic acid, *C. autoethanogenum* synthesizes growth-associated ethanol to maintain pH while at the same time making acetate to provide ATP to meet cellular energy requirements. As carbon funnels through to acetyl-CoA, the *C. autoethanogenum* cell will theoretically want to produce ethanol and acetate nearly simultaneously so that there are less free H^+ ions available for the formation of more harmful, membrane permeable acetic acid and as a result the concentration ratio of acetate (higher pH) to acetic acid (lower pH) will be kept in check at a level well above the dissociation constant (pKa 4.76) that is optimal for both intracellular and extracellular pH. However, this theory only works if the enzymatic rate of reactions from acetyl-CoA to acetyl phosphate to acetate matches the rate from acetyl-CoA to acetaldehyde to ethanol or the reaction from acetic acid to acetaldehyde and then to ethanol occurs rapidly. Since *C. autoethanogenum* cultures with unaltered, naturally changing pH demonstrated a drop in pH as shown by the control treatment (Fig. 3.3c) in this experiment, the rate of acetate production is obviously faster than that of ethanol and the cultures are unable to naturally maintain the extracellular pH conditions needed for optimal cell performance and substrate utilization, requiring external base addition. In addition, xylose transport into the cell requires energy input from ATP (White, 2007) and the ATP demand goes up as more xylose is taken up by the cells. Therefore, utilization of higher concentrations of xylose requires production of higher concentrations of

ATP-yielding metabolites such as acetate. This work has shown that xylose utilization increases proportionally with acetate production (Fig. 3.4b and 3.4d) and, when excreted from the cell, acetate raises the potential for the pH to drop thus making it necessary for external methods of pH maintenance to be implemented for culture health and continued sugar metabolism. Based on the enhanced xylose utilization, this experiment has identified the conditions necessary for *C. autoethanogenum* to be able to metabolize xylose at concentrations that are 1) comparable to other xylose-fermenting microorganisms and 2) present in lignocellulosic biomass-derived hydrolysates.

Conclusion

When this study began, *C. autoethanogenum* had been identified as an organism with limited xylose utilization. However, it has now been revealed that *C. autoethanogenum* is actually a pH sensitive organism that requires an environmental pH optimized for growth in order to maximize its utilization of xylose. Unlike other acetogens that can maintain substrate metabolism at extracellular pH values in the lower end of their accepted pH range, *C. autoethanogenum* prefers an extracellular pH in the upper end of its pH range (pH 4.0-6.0), and the higher the pH, the better the organism's capacity to utilize provided sugars such as xylose. Besides the fact that a higher pH is ideal for continued cell growth by the bacteria which in turn provides more biomass for producing end products, the rationale for why *C. autoethanogenum* prefers a higher pH may be tied to when it produces certain end products. Both acetate and ethanol are growth-associated end products for this organism with acetate providing ATP to the organism to sustain metabolic functions including substrate transport, and ethanol preventing the conversion of acetate to acetic acid by accepting electrons from NADH. However, the organism is unable to naturally maintain its pH at an optimal level and this eventually causes xylose

utilization to cease. The implementation of base addition (ex. 3.0M KOH) to the growth media periodically is sufficient to raise the pH to a desirable level for maintenance of xylose uptake and metabolism, and, if the pH adjustment target is high enough (ex. pH 5.8), *C. autoethanogenum* is capable of metabolizing all fed xylose regardless of the amount fed (ex. regular 2.5-5 g/L doses or 30 g/L initial xylose). Since *C. autoethanogenum* is sensitive to pH and acidity, it uses xylose consumption as a method to regulate acetate production at lower versus higher pH levels. The cells also adjust the co-production ratio of ethanol and acetate depending on the pH; however, if the pH becomes too low the stress response of the cells will dictate the product ratio. As the initial concentration of xylose increased in pH adjusted cultures, the production of both acetate and ethanol increased due to greater xylose uptake. Knowing that regulation of environmental pH improves xylose consumption by *C. autoethanogenum*, this feature can now be exploited for future sugar feedstock conversion studies.

Table 3.1. Volume losses due to sampling and gains due to base, xylose, and replacement media addition for the first 32 hours for *C. autoethanogenum* cultures.

Treatment	Time (Hr)				
	0	8	16	24	32
Buffer (0.05, 0.1, 0.15M)	-S4		-S4		-S4, +X, +M, -S3
pH to 5.0	-S4		-S4, +B		-S4, +B, +X, +M, -S3
pH to 5.8	-S4	-S1, +B	-S4, +B	-S1, +B	-S4, +B, +X, +M, -S3

Losses: S4 = 4 mL sample, S1 = 1 mL sample, S3 = 3 mL sample
Additions: B = 0.01-0.60 mL base solution, X = 1 mL xylose solution, M = 9-12 mL media

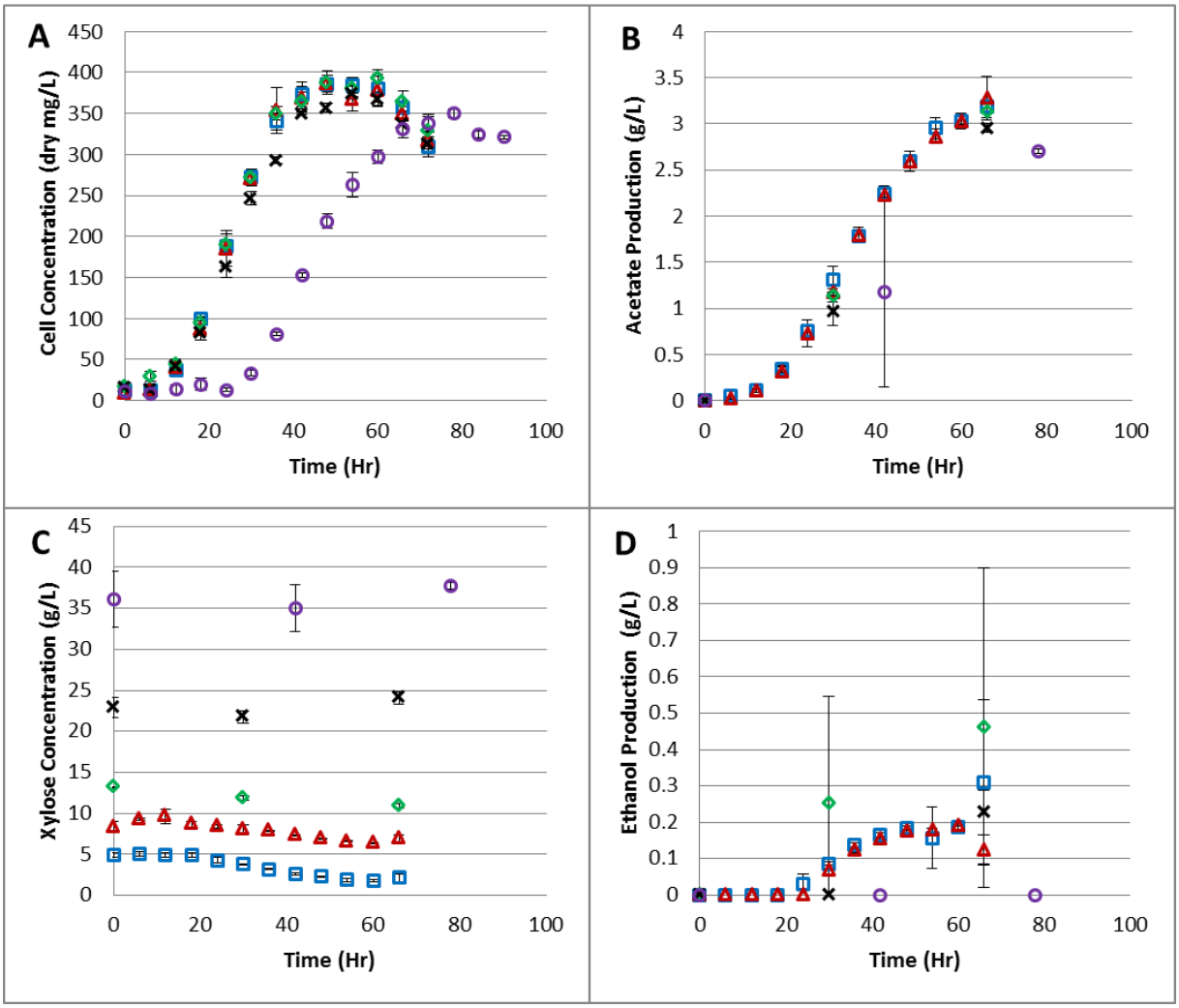

Figure 3.1. Impact of initial xylose concentration on *C. autoethanogenum* performance. Average responses over time: A) cell concentration, B) acetate production, C) xylose concentration, and D) ethanol production. Square: 5 g/L, triangle: 10 g/L, diamond: 15 g/L, X: 30 g/L, circle: 45 g/L initial xylose treatment. Error bars represent standard deviation.

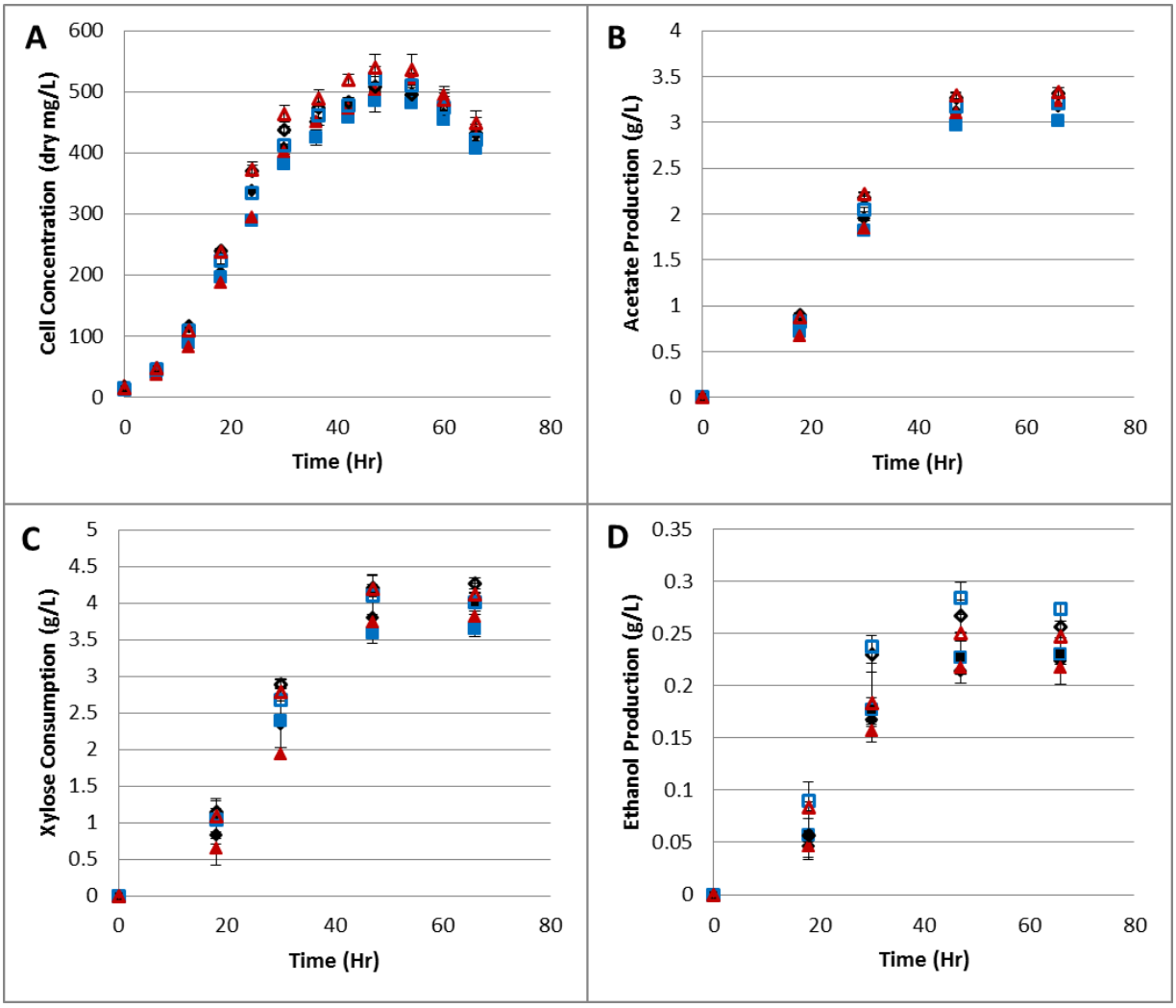

Figure 3.2. Impact of altered trace elements, vitamin solution, and initial xylose concentration on *C. autoethanogenum* performance. Average responses over time: A) cell concentration, B) acetate production, C) xylose consumption, and D) ethanol production. Solid symbols: 5 g/L initial xylose concentration, and open symbols: 15 g/L initial xylose concentration. Diamond: 640 control medium with no change in formulation, square: medium with PETC modified trace elements instead of SL-10 trace elements, and triangle: medium with modified Wolfe's vitamin solution supplemented. Error bars represent standard deviation.

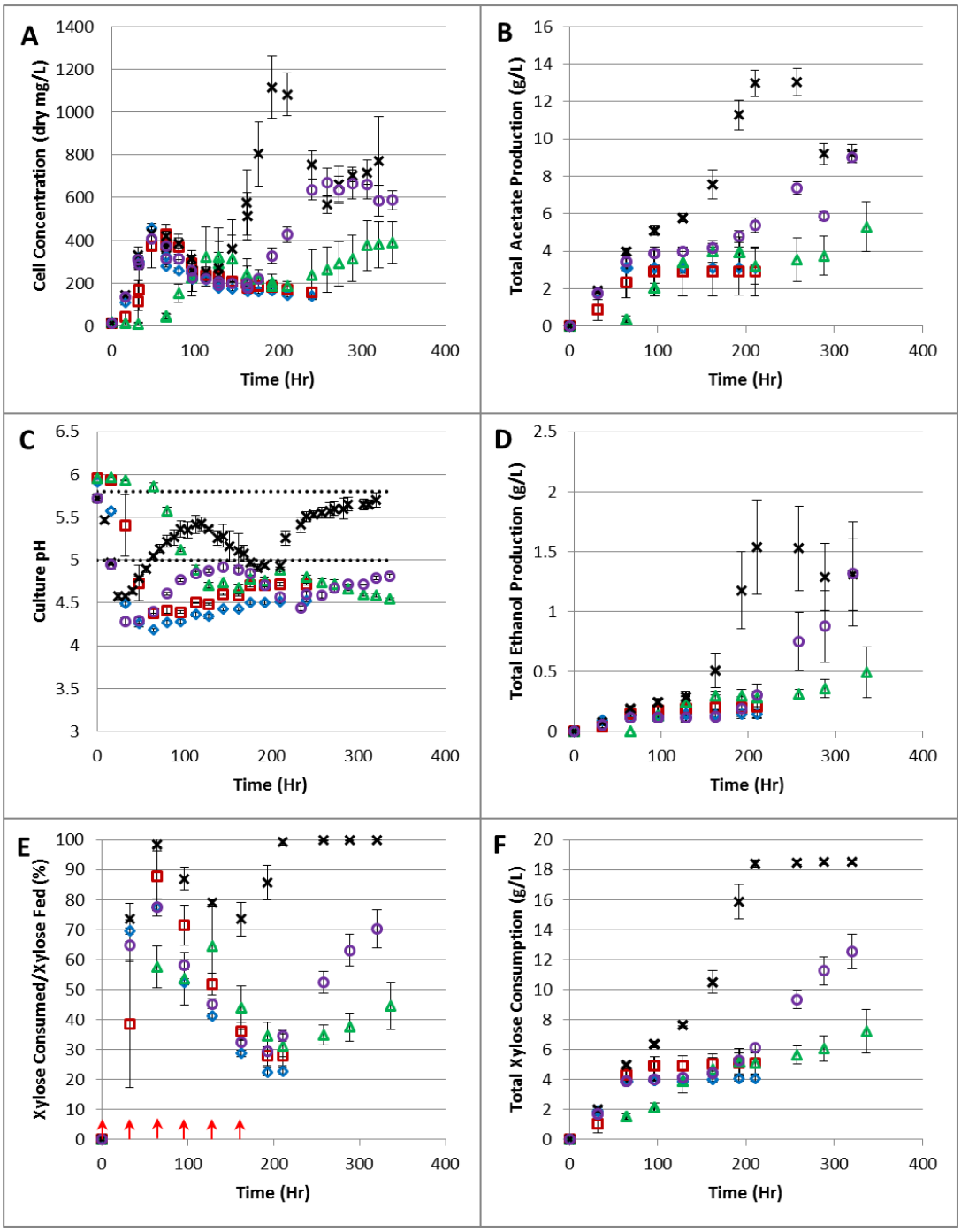

Figure 3.3. Effect of potassium phosphate buffer and pH adjustment via 3M KOH on *C. autoethanogenum* cultures dosed incrementally by 2.5 g/L up to hour 96 and then by 5 g/L to the equivalent of 20 g/L initial xylose. Responses over time: A) cell concentration, B) total acetate production, C) culture pH (dotted horizontal lines indicate pH 5.8 and 5.0 targets), D) total ethanol production, E) percentage ratio of total xylose consumed per cumulative xylose fed with dose times indicated by arrows, and F) total xylose consumption. Diamond: 0.05M buffer, square: 0.1M buffer, triangle: 0.15M buffer, X: pH adjusted to 5.8 every 8 hours, circle: pH adjusted to 5.0 every 16 hours. Error bars represent standard deviation.

Table 3.2. *C. autoethanogenum* product yields from xylose at initial xylose concentrations ranging from 5-30 g/L when cultures were pH adjusted to 5.8 via 3M KOH every 8 hours.

Initial Xylose g/L	pH Adjustment Target	Xylose Consumed %	Avg. Maximum Acetate Yield g/g consumed	Avg. Maximum Ethanol Yield g/g consumed	E:A Mass Ratio
5	None (Control)	62	0.56	0.027	1:21
5	5.8	100	0.51	0.031	1:16
10	5.8	100	0.45	0.034	1:15
20	5.8	100	0.39	0.066	1:5.3
30	5.8	100	0.36	0.094	1:3.3

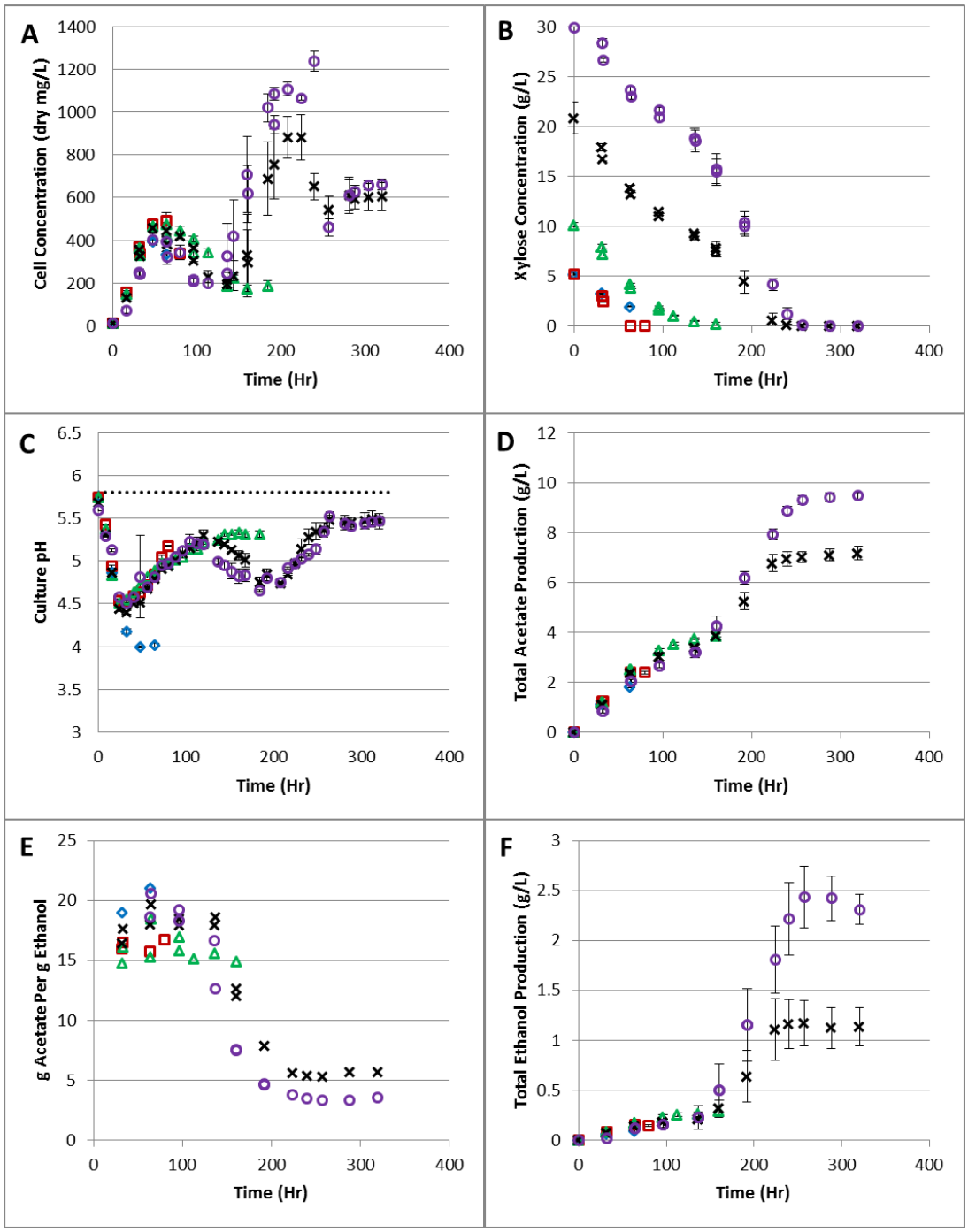

Figure 3.4. *C. autoethanogenum* performance at initial xylose concentrations ranging from 5-30 g/L when cultures were pH adjusted to 5.8 via 3M KOH every 8 hours. Responses over time: A) cell concentration, B) xylose concentration, C) culture pH with pH 5.8 adjustment target indicated with dotted line, D) total acetate production, E) acetate to ethanol production ratio, and F) total ethanol production. Diamond: 5g/L w/ no pH (control), square: 5 g/L with pH, triangle: 10 g/L with pH, X: 20 g/L with pH, circle: 30 g/L with pH. Error bars represent standard deviation.

REFERENCES

Abrini, J., Naveau, H., and Nyns, E.J. (1994). *Clostridium autoethanogenum*, sp. nov., an anaerobic bacterium that produces ethanol from carbon monoxide. Arch. Microbiol. *161*, 345–351.

Abubackar, H.N., Veiga, M.C., and Kennes, C. (2015a). Carbon monoxide fermentation to ethanol by *Clostridium autoethanogenum* in a bioreactor with no accumulation of acetic acid. Bioresour. Technol. *186*, 122–127.

Abubackar, H.N., Veiga, M.C., and Kennes, C. (2015b). Ethanol and Acetic Acid Production from Carbon Monoxide in a *Clostridium* Strain in Batch and Continuous Gas-Fed Bioreactors. Int. J. Environ. Res. Public. Health *12*, 1029–1043.

Abubackar, H.N., Fernández-Naveira, Á., Veiga, M.C., and Kennes, C. (2016a). Impact of cyclic pH shifts on carbon monoxide fermentation to ethanol by *Clostridium autoethanogenum*. Fuel *178*, 56–62.

Abubackar, H.N., Bengelsdorf, F.R., Dürre, P., Veiga, M.C., and Kennes, C. (2016b). Improved operating strategy for continuous fermentation of carbon monoxide to fuel-ethanol by clostridia. Appl. Energy *169*, 210–217.

Andreesen, J.R., Schaupp, A., Neurauter, C., Brown, A., and Ljungdahl, L.G. (1973). Fermentation of Glucose, Fructose, and Xylose by *Clostridium thermoaceticum*: Effect of Metals on Growth Yield, Enzymes, and the Synthesis of Acetate from CO_2. J. Bacteriol. *114*, 743–751.

Balasubramanian, N., Kim, J.S., and Lee, Y.Y. (2001). Fermentation of xylose into acetic acid by *Clostridium thermoaceticum*. Appl. Biochem. Biotechnol. *91*, 367–376.

Balat, M. (2011). Production of bioethanol from lignocellulosic materials via the biochemical pathway: A review. Energy Convers. Manag. *52*, 858–875.

Bruno-Barcena, J.M., Chinn, M.S., and Grunden, A.M. (2013). Genome Sequence of the Autotrophic Acetogen *Clostridium autoethanogenum* JA1-1 Strain DSM 10061, a Producer of Ethanol from Carbon Monoxide. Genome Announc. *1*, e00628-13.

Cold Spring Harbor Laboratory Press (2006). Phosphate buffer. Cold Spring Harb. Protoc. *2006*, pdb.rec8543.

Cotter, J.L. (2006). Ethanol and acetate production from synthesis gas using microbial catalysts. North Carolina State University.

Cotter, J.L., Chinn, M.S., and Grunden, A.M. (2008). Ethanol and acetate production by *Clostridium ljungdahlii* and *Clostridium autoethanogenum* using resting cells. Bioprocess Biosyst. Eng. *32*, 369–380.

Cotter, J.L., Chinn, M.S., and Grunden, A.M. (2009). Influence of process parameters on growth of *Clostridium ljungdahlii* and *Clostridium autoethanogenum* on synthesis gas. Enzyme Microb. Technol. *44*, 281–288.

Demirbas, A. (2005). Bioethanol from Cellulosic Materials: A Renewable Motor Fuel from Biomass. Energy Sources *27*, 327–337.

Drake, H.L., and Daniel, S.L. (2004). Physiology of the thermophilic acetogen *Moorella thermoacetica*. Res. Microbiol. *155*, 869–883.

Drake, H.L., Gößner, A.S., and Daniel, S.L. (2008). Old acetogens, new light. Ann. N. Y. Acad. Sci. *1125*, 100–128.

DSMZ (2018). DSMZ: List of Media for Microorganisms. https://www.dsmz.de/catalogues/catalogue-microorganisms/culture-technology/list-of-media-for-microorganisms.html

Durre, P. (2005). Handbook on Clostridia (CRC Press).

Fontaine, F.E., Peterson, W.H., McCoy, E., Johnson, M.J., and Ritter, G.J. (1942). A New Type of Glucose Fermentation by *Clostridium thermoaceticum*. J. Bacteriol. *43*, 701–715.

Goldstein, I.S. (1981). Organic chemicals from biomass (CRC Press Boca Raton, FL).

Gomori, G. (1955). [16] Preparation of buffers for use in enzyme studies. Methods Enzymol. *1*, 138–146.

Hahn-Hägerdal, B. (1986). Water activity: a possible external regulator in biotechnical processes. Enzyme Microb. Technol. *8*, 322–327.

Jansen, N.B., Flickinger, M.C., and Tsao, G.T. (1984). Production of 2,3-butanediol from D-xylose by *Klebsiella oxytoca* ATCC 8724. Biotechnol. Bioeng. *26*, 362–369.

Katahira, S., Mizuike, A., Fukuda, H., and Kondo, A. (2006). Ethanol fermentation from lignocellulosic hydrolysate by a recombinant xylose- and cellooligosaccharide-assimilating yeast strain. Appl. Microbiol. Biotechnol. *72*, 1136–1143.

Klasson, K.T., Ackerson, M.D., Clausen, E.C., and Gaddy, J.L. (1992). Bioconversion of synthesis gas into liquid or gaseous fuels. Enzyme Microb. Technol. *14*, 602–608.

Kundiyana, D.K., Huhnke, R.L., Maddipati, P., Atiyeh, H.K., and Wilkins, M.R. (2010). Feasibility of Incorporating Cotton Seed Extract in *Clostridium* strain P11 Fermentation Medium During Synthesis Gas Fermentation. Bioresour. Technol. *101*, 9673-9680.

Kundiyana, D.K., Wilkins, M.R., Maddipati, P., and Huhnke, R.L. (2011). Effect of temperature, pH and buffer presence on ethanol production from synthesis gas by "*Clostridium ragsdalei*." Bioresour. Technol. *102*, 5794–5799.

Lynd, L.R., Baskaran, S., and Casten, S. (2001). Salt Accumulation Resulting from Base Added for pH Control, and Not Ethanol, Limits Growth of *Thermoanaerobacterium thermosaccharolyticum* HG-8 at Elevated Feed Xylose Concentrations in Continuous Culture. Biotechnol. Prog. *17*, 118–125.

Marcellin, E., Behrendorff, J.B., Nagaraju, S., DeTissera, S., Segovia, S., Palfreyman, R.W., Daniell, J., Licona-Cassani, C., Quek, L., Speight, R., et al. (2016). Low carbon fuels and commodity chemicals from waste gases – systematic approach to understand energy metabolism in a model acetogen. Green Chem. *18*, 3020-3028.

Martin, M.E., Richter, H., Saha, S., and Angenent, L.T. (2016). Traits of selected *Clostridium* strains for syngas fermentation to ethanol. Biotechnol. Bioeng. *113*, 531–539.

Mock, J., Zheng, Y., Mueller, A.P., Ly, S., Tran, L., Segovia, S., Nagaraju, S., Köpke, M., Dürre, P., and Thauer, R.K. (2015). Energy Conservation Associated with Ethanol Formation from H_2 and CO_2 in *Clostridium autoethanogenum* Involving Electron Bifurcation. J. Bacteriol. *197*, 2965–2980.

Moniruzzaman, M., Dien, B.S., Ferrer, B., Hespell, R.B., Dale, B.E., Ingram, L.O., and Bothast, R.J. (1996). Ethanol production from AFEX pretreated corn fiber by recombinant bacteria. Biotechnol. Lett. *18*, 985–990.

Moniruzzaman, M., Dien, B.S., Skory, C.D., Chen, Z.D., Hespell, R.B., Ho, N.W.Y., Dale, B.E., and Bothast, R.J. (1997). Fermentation of corn fibre sugars by an engineered xylose utilizing *Saccharomyces* yeast strain. World J. Microbiol. Biotechnol. *13*, 341–346.

Olson, B.H., and Johnson, M.J. (1948). The Production of 2,3-Butylene Glycol by *Aerobacter aerogenes* 199 1. J. Bacteriol. *55*, 209–222.

Overmann, J. (2006). Principles of Enrichment, Isolation, Cultivation and Preservation of Prokaryotes. In The Prokaryotes, (Springer, New York, NY), pp. 80–136.

Phillips, J.R., Klasson, K.T., Clausen, E.C., and Gaddy, J.L. (1993). Biological production of ethanol from coal synthesis gas: Medium development studies. Appl. Biochem. Biotechnol. *39/40*, 559–571.

du Preez, J.C., Bosch, M., and Prior, B.A. (1986). Xylose fermentation by *Candida shehatae* and *Pichia stipitis*: effects of pH, temperature and substrate concentration. Enzyme Microb. Technol. *8*, 360–364.

Rogers, P.L., Jeon, Y.J., Lee, K.J., and Lawford, H.G. (2007). *Zymomonas mobilis* for Fuel Ethanol and Higher Value Products. In Biofuels, (Springer, Berlin, Heidelberg), pp. 263–288.

Saxena, J., and Tanner, R.S. (2011). Effect of trace metals on ethanol production from synthesis gas by the ethanologenic acetogen, *Clostridium ragsdalei*. J. Ind. Microbiol. Biotechnol. *38*, 513–521.

Sezonov, G., Joseleau-Petit, D., and D'Ari, R. (2007). *Escherichia coli* Physiology in Luria-Bertani Broth. J. Bacteriol. *189*, 8746–8749.

Talebnia, F., and Taherzadeh, M.J. (2006). In situ detoxification and continuous cultivation of dilute-acid hydrolyzate to ethanol by encapsulated *S. cerevisiae*. J. Biotechnol. *125*, 377–384.

Tirado-Acevedo, O., Cotter, J.L., Chinn, M.S., and Grunden, A.M. (2011). Influence of Carbon Source Pre-Adaptation on Clostridium ljungdahlii Growth and Product Formation. J. Bioprocess. Biotech. S2:001 doi:10.4172/2155-9821.S2-001.

Vega, J., Clausen, E., and Gaddy, J. (1990). Design of bioreactors for coal synthesis gas fermentations. Resour. Conserv. Recycl. *3*, 149–160.

Wang, S., Huang, H., Kahnt, J., Mueller, A.P., Köpke, M., and Thauer, R.K. (2013). NADP-Specific Electron-Bifurcating [FeFe]-Hydrogenase in a Functional Complex with Formate Dehydrogenase in *Clostridium autoethanogenum* Grown on CO. J. Bacteriol. *195*, 4373–4386.

White, D. (2007). The Physiology and Biochemistry of Prokaryotes (New York: Oxford University Press).

Zhao, J., and Xia, L. (2010). Ethanol production from corn stover hemicellulosic hydrolysate using immobilized recombinant yeast cells. Biochem. Eng. J. *49*, 28–32.

CHAPTER 4

Xylose Utilization in the Presence of Synthesis Gas (Syngas): A Proteomic Evaluation of Substrate Transport and Carbon Utilization by *Clostridium autoethanogenum*

Rachel M. Slivka, Mari S. Chinn, Amy M. Grunden, Jose M. Bruno-Barcena, Michael B. Goshe, and Kevin Blackburn

Abstract

C. autoethanogenum is uncommon in that it can metabolize the single carbon gases, CO and CO_2, found in synthesis gas (syngas) which makes it an ideal candidate for the manufacture of value-added products from gasified renewable biomass. It can also utilize xylose as a source of carbon and energy. When xylose, syngas, or the combination of xylose-syngas is used as substrates for *C. autoethanogenum* fermentation, the results produced are drastically different depending on the carbon source(s). This study used proteomics to help understand why the organism's physiology changes and how protein regulation under each of these carbon sources was effected. Metabolic pathways involved in pentose transport and conversion, general sugar metabolism (i.e. glycolysis), mixed-acid fermentation, and energy transfer were determined to have the largest overall change in the up-/down-regulation of protein expression between the heterotrophic (xylose-only), mixotrophic (xylose-syngas), and autotrophic (syngas-only) fermentations. Overall, protein functionality was primarily driven by whether the substrate required the organism to use sugar degradation pathways (xylose and xylose-syngas conditions) versus carbon fixation (syngas-only conditions) to ensure cell survival. Noteworthy findings include the expression of an autoinducer 2 complex during xylose metabolism, the use of an Rnf complex during syngas-only metabolism, and the bifurcated expression of flavoproteins depending on the carbon source available.

Introduction

Given our current energy climate in which there is a need for renewable sources of energy and chemicals, the conversion of lignocellulosic substrates into value-added bioproducts presents a viable option to meet this need. There are two main routes for the biological conversion of lignocellulosic biomass: a biochemical route in which the biomass is pretreated

and then hydrolyzed to produce pentose and hexose sugar streams which feed into fermentations; and a thermochemical route in which the biomass is transformed into one-carbon gases through the gasification process and then the treated synthesis gas (syngas) may be fed into a respective fermentation (Slivka et al., 2011). Each carbon source (pentose, hexose, and syngas) for fermentation requires a microorganism capable of substrate transport and metabolism of the particular sugars or gases in the stream in order for the fermentation to be effective. In addition, each organism creates a different spectrum of end products depending on the metabolic pathways it possesses. For example, *Clostridium beijerinckii* is known to produce butanol (Sandoval-Espinola et al., 2013) while *Clostridium autoethanogenum* produces ethanol and acetate (Abrini et al., 1994) as primary end products. A useful method to discern why an organism behaves under certain conditions is to perform an "omics" evaluation. During a proteomic study, for example, an organism's protein expression patterns are revealed, and by altering a growth condition such as substrate type, changes in protein regulation may be observed.

There has been increased focus on *C. autoethanogenum* as an organism of research interest because of its ability to assimilate one-carbon (C1) molecules such as CO and CO_2+H_2 into acetyl-CoA and its derivatives (Abubackar et al., 2016; Cotter et al., 2009; Guo et al., 2010; Marcellin et al., 2016; Norman et al., 2018). Yet, this organism also metabolizes sugars such as fructose, xylose, and arabinose with xylose being the preferred carbon source (Abrini et al., 1994). Its preference for xylose is unique in that there are fewer organisms capable of natural pentose metabolism than exist for natural hexose utilization. The catabolic sugar pathways (ex. glycolysis and pentose phosphate pathway) provide a considerable source of energy for the cell as well as carbon compounds required for biosynthetic pathways; therefore, it is clear why sugar is a desirable source of carbon for bacteria. However, the Wood-Ljungdahl pathway, which is

used to metabolize C1 molecules in *C. autoethanogenum*, has a high reductant demand and requires the use of anabolism to generate molecules crucial to cell survival. The subsequent creation of carboxylic acids with ATP as a co-product may offset some of the energy demand during flux through the Wood-Ljungdahl pathway, but the pathway's bioenergetics still appear inferior if CO and CO_2 are the only carbon sources available compared to growth on sugars.

Prior information has also been collected which shows that xylose and syngas affect *C. autoethanogenum* in different ways. For instance, the solubility of xylose in the growth media allows easier uptake into the cells versus syngas which must be effectively solubilized in the liquid phase for cell uptake and not simply present in the headspace because of mass transfer effects. However, when the bacteria were presented with a mixture of xylose-syngas and both substrates were solubilized with ideal mass transfer, the bacteria would not consume xylose until they were acclimated to syngas. In another case, *C. autoethanogenum* cells were preadapted to the xylose-syngas mixture, but because syngas was the only substrate fed to the fermentation, the culture died prematurely.

All this information leads one to question how and why does *C. autoethanogenum* exhibit different behaviors when exposed to sugar versus gaseous carbon substrates. What transporters does it possess that make xylose utilization possible, or is xylose metabolism the result of a highly active enzyme for pentose interconversion? If syngas metabolism is inferior to sugar metabolism, how does the cell survive on syngas? Could syngas fermentation be optimized if a secondary source of carbon were available? The purpose of this study was to determine the unique proteins involved in sugar transport, metabolism, and energy transfer in *C. autoethanogenum* during growth on xylose, and to understand how the expression patterns of

these and other proteins change when the organism was exposed to syngas both as a sole carbon source and in a mixed xylose-syngas fermentation.

Materials and Methods

Organism, media, and inocula preparation

C. autoethanogenum (DSM 10061) was grown on DSMZ 640 basal medium under a batch, anaerobic atmosphere. The components of DSMZ 640 medium (pH 6.0) were described previously (Cotter et al., 2008, 2009). The medium was dispensed anaerobically (into either Balch tubes (10 ml) or serum bottles (50 ml)) under a nitrogen (Airgas National Welders) or pure synthesis gas (20% CO, 20% CO_2, 10% H_2, 50% N_2; Arc3 Gases [formerly known as Machine & Welding Supply Company]) atmosphere depending on fermentation treatment and autoclaved for 30 min (121°C, 17-18 psig).

Seed cultures of *C. autoethanogenum* were revitalized from frozen stock cultures (-80°C) by aseptically inoculating 10 mL Balch tubes containing 5 g/L xylose and a nitrogen headspace with a 5% v/v inoculum followed by incubation for 72 hours at 37°C (no agitation). With successive transfers to fresh medium, incubation was repeated for a 48 hour, and then a 24 hour incubation period. Xylose pre-adapted inoculum was prepared by transferring *C. autoethanogenum* cultures (5% v/v inoculum) to 10 mL Balch tubes with 2.5 g/L xylose and an N_2 headspace, and then incubating at 37°C with 100 rpm orbital shaking until appropriate cell density was reached (~24 hours, 300 mg dry cells/L). Xylose-syngas (mixed-carbon) pre-adapted inoculum was prepared by transferring *C. autoethanogenum* cultures (5% v/v inoculum) to 50 mL serum bottles with 2.5 g/L xylose and a syngas headspace, and then incubating at 37°C with 100 rpm orbital shaking until appropriate cell density was reached (~36 hours once cultures were fully adapted, 300 mg dry cells/L). The syngas pre-adapted inoculum was created in a

similar fashion to the mixed-carbon pre-adapted inoculum (i.e. 50 mL bottle with a syngas headspace and incubation at 37°C with 100 rpm orbital shaking) except that the liquid volume occupied by the xylose solution was replaced with sterile, deionized, distilled water kept under a nitrogen headspace. The syngas pre-adapted inoculum was also subjected to densification by allowing the culture to grow for 24-26 hours, refreshing the batch syngas headspace to supply additional substrate, and then allowing the cells to grow for an additional 24-26 hours until they reached 110 mg dry cells/L.

Bacterial culture treatment and harvest conditions

The experimental condition evaluated was *C. autoethanogenum* growth on three different carbon source treatments: xylose as the sole carbon source, syngas as the sole carbon source, and xylose-syngas as a mixed carbon source. Each treatment fermentation was inoculated with cells preadapted to that specific condition, and the replication level was at least triplicate. Treatment cultures were grown in DSMZ 640 medium at 37°C with 100 rpm agitation to late exponential phase to provide the maximum amount of active cells for processing. Xylose fermentation cells were grown for 36 hours on 5 g/L xylose and a nitrogen headspace in nine 50 mL serum bottles to an average culture density of ~350 mg dry cells/L to provide enough material. Three culture replicates (~52.5 mg dry cells total) were processed and used during preliminary runs in order to resolve issues with the methodology used to prepare samples for protein analysis by mass spectrometry. The remaining six xylose culture replicates (~105 mg dry cells total) were processed simultaneously with xylose-syngas and syngas treatments and fed into the treatment mass spectroscopy runs to yield protein expression data. Xylose-syngas fermentation cells were grown for 40 hours on 2.5 g/L xylose and a batch syngas headspace (20% CO, 20% CO_2, 10% H_2, 50% N_2; Arc3 Gases) to an average culture density of ~370 mg dry cells/L in six 50 mL

serum bottles (~110 mg dry cells total). Finally, syngas fermentation cells were grown for 40 hours on a batch syngas headspace in twenty-four 50 mL serum bottles to an average culture density of ~180 mg dry cells/L to yield the necessary material (~132 mg dry cells total).

Cells were harvested by centrifugation (Eppendorf 5810R) at 13,000 × *g* (10 minutes, 4°C). After removing the supernatant, cells were then washed with 50 mM Tris buffer (pH 7.3), and collected again by centrifugation at 13,000 × *g* (10 minutes, 4°C). Each final cell pellet was suspended in 1-3 mL lysis buffer (50 mM Tris buffer, pH 7.3) to create a 1:3 ratio of wet cell weight-to-buffer (g/mL) and to facilitate transfer to a storage tube. The cell slurries for each treatment were pooled so that each storage tube contained 3 xylose pellets, 3 xylose-syngas pellets, or 12 syngas treatment pellets (~15 mL cell slurry per tube). Samples were then preserved at -80°C until further processing was conducted.

Preparation of proteins for mass spectroscopy analysis

The integral membrane and cytoplasmic proteins from *C. autoethanogenum* were enriched, solubilized, and proteolyzed using a modified version of the methodology described in Mitra and Goshe (2009). Upon thawing, the cells were ruptured using a French press (Aminco, Rochester, NY) and intact cells and/or debris were removed using centrifugation at 20,000 × *g* (30 minutes, 4°C). In order to have enough material to fill the pressure chamber, cells for each treatment were combined into two process pools (see above), ruptured, and then each process pool was split in half to facilitate centrifugation and thus produced two technical replicates from this point forward (2 pools x 2 technical replicates = 4 samples per treatment). The lysate was diluted with ice-cold 100 mM sodium carbonate (pH 11) to 0.275 mg/L and agitated gently using a shaker (Labquake, Conroe, TX) for 1.5 hours at 4°C. Next the solution was centrifuged (Beckman L8-55 ultracentrifuge, 11.5 mL tubes) at 140,000 × *g* for 1 h at 4°C to pellet the

bacterial membrane component. This initial ultracentrifuge supernatant was saved for further processing as it contained the cytoplasmic proteins. Following supernatant removal, the membrane pellet was washed with deionized water then lysis buffer (50 mM Tris buffer, pH 7.3), and centrifuged again at 140,000 × *g* for 1 h at 4°C with only the membrane pellet retained afterwards .

The membrane pellet was resuspended in 0.4 mL 50 mM ammonium bicarbonate (pH 8) using a sonicating bath (VWR Aquasonic Model 75T, 35 kHz, Westchester, PA) for 20 minutes alternated with vortexing for 30 seconds every 4 minutes. Next, the membrane fraction was thermally denatured, diluted with 0.6 mL methanol to attain 60% organic solvent (per 1 mL total volume), and solubilized with alternating sonication (VWR Aquasonic Model 75T, 35 kHz, Westchester, PA) and vortexing (20 minute sonication with 30 second vortexing every 4 minutes). The initial ultracentrifuge supernatant containing the cytoplasmic proteins was concentrated and buffer exchanged into 50 mM ammonium bicarbonate (pH 8) using ultrafiltration centrifugal concentrators (Satorius Vivaspin 15R, 2 kDa MWCO) spun at 3000 × *g*, 20°C for 60-80 minute runs. After three buffer exchange cycles, the approximately 0.75 mL cytoplasmic protein samples in ammonium bicarbonate were thermally denatured in a heat block at 90°C for 20 minutes. At this point, the protein concentration was determined through BCA assay, and the cytoplasmic samples were diluted with 50 mM ammonium bicarbonate (pH 8) to a protein concentration of 1.9 mg/mL. After transferring the cytoplasmic samples to siliconized polypropylene Eppendorf tubes (2.0 mL), they were further diluted with methanol to attain 60% organic solvent (0.6 mL methanol : 0.4 mL ammonium bicarbonate) and a protein concentration of 0.5-1.0 mg/mL, and then solubilized in the same manner as the membrane protein samples with alternating sonication and vortexing.

Both the membrane protein and cytoplasmic protein samples were incubated in a boiling water bath for 5 minutes, reduced with a 30-fold molar excess of tributylphosphine to protein, and incubated again for 30 minutes at 37°C. Additional details on this methodology are in Mbeunkui and Goshe (2011). Next, the thiolate groups of the cysteinyl residues in both samples types were alkylated with a 30-fold molar excess of iodoacetamide to protein while the samples were incubated at ambient temperature in the dark with gentle agitation for 90 minutes. The protein samples were then subjected to proteolysis using a 1:50 (w/w) trypsin-to-protein ratio for 2 hours at 37°C, followed by the addition of a second aliquot of 1:50 (w/w) trypsin-to-protein with digestion proceeding for an additional 3 hours at 37°C. Finally, the proteolysis digestion reaction was quenched by placing the samples in ice and then immediately transferring them to a -80°C freezer.

Following thawing and heating for 5 minutes in a boiling water bath to thermally denature the trypsin, all of the samples from both the membrane and the cytoplasmic fractions were found to contain a white, protein concentration-dependent precipitate. In order to remove the precipitate and any residual organic material, the samples were centrifuged (Spectrofuge 16M) at 16,000 × *g* for 10 minutes for the membrane samples and 20 minutes for the cytoplasmic samples. The peptide-containing supernatant was then pipet transferred to new siliconized polypropylene Eppendorf tubes (2.0 mL). Membrane peptide samples were concentrated in a speed vacuum (Labconco CentriVap Concentrator and CentriVap Cold Trap) for 75 minutes to remove the methanol and any excess volume so that the new peptide concentration was 0.213 μg/μL. Over-concentrated samples were brought to volume afterwards with 0.1% formic acid. The cytoplasmic peptide samples were diluted by 1:10 with 0.1% formic acid and then concentrated in a speed vacuum for 90 minutes to a protein concentration of 0.213 μg/μL.

Mass spectroscopy analysis of membrane and cytoplasmic proteins

For each *C. autoethanogenum* carbon source treatment (xylose, xylose-syngas, or syngas grown) and cellular fraction (membrane or cytoplasmic), there were four samples analyzed using mass spectroscopy. Each sample well was loaded with 54 μL of prepared sample to allow 3 sample injections of 18 μL each. Injections were subjected to reverse phase high-performance liquid chromatography with a 120 minute gradient of the organic mobile phase to separate the peptides followed by collision induced dissociation with tandem mass spectrometer measurements (CID with MS/MS; Orbitrap Elite ETD, Thermo Scientific). First, the Proteome Discoverer software package (Thermo Scientific) was used to identify and quantify the peptide spectra produced by the MS instrument; and then, the MaxQuant software package was used to further quantify and correct peptides extracted from the raw data set and perform a database search for protein identification with a 1% false discovery rate (FDR) limit. Proteome UP000017590 for *C. autoethanogenum* DSM 10061 with 4013 protein entries in the UniProtKB database was used for protein identification (The UniProt Consortium, 2017).

Analysis of proteomic data set

MaxQuant data output was loaded into the Perseus software framework in order to assign data labels, filter out possible contaminants, normalize and transform the data, and perform statistical analysis. ANOVA testing was performed on the data with $\alpha = 0.05$, and then the data set were filtered based on statistical significance. Data were then exported to Excel so that index matching could be run against other useful information (ex. protein name, gene name, function, etc.) in the UniProt database for *C. autoethanogenum*'s proteome. Excel was used to calculate the fold difference and run t-test comparisons between each pair of treatments. Proteins with a fold difference (fold difference = $\log_2$ fold change) between treatments greater than two and t-

test p-value less than 0.05 were deemed to have a significant change in protein expression as a result of the treatment carbon source. The data set was then curated through the removal of cytoplasmic proteins that were identified in the membrane data set as well as membrane-bound proteins that were found in the cytoplasmic protein data set. A combination of known protein function, enzyme and protein searches in the KEGG database (Kanehisa et al., 2017), entry searches in the UniProt database, gene searches in the NCBI Gene database (National Center for Biotechnology Information, 2018), and location of the protein in other microorganisms was used to determine the cellular location of each protein. Metabolic pathways listed under the KEGG database genome entry for *C. autoethanogenum* DSM 10061, T02883 (Kanehisa Laboratories, 2018), were then assessed to determine which proteins were expected to be there for *C. autoethanogenum*, and of those identified, which showed up in the experimental data as having a significant expression change between treatments. A similar assessment was also made using the BioCyc Tier 3 Pathway/Genome Database (PGDB) for *C. autoethanogenum* DSM 10061 (caut1341692cyc version 19.0) in the Pathway Tools software program (Caspi et al., 2016; Dale et al., 2010; Karp et al., 2002, 2016; Paley and Karp, 2006). Finally, the experimental protein data was loaded into Pathway Tools and a Differential Pathway Perturbation Score (DPPS) analysis was run to assess which metabolic pathways had the largest overall change in up/down-regulation between the three treatment conditions (Karp et al., 2015). Pictorial representations of metabolic pathways, reactions, and gene operons were created using the Pathway Tools software program (Karp and Paley, 1995).

Results and Discussion

Fermentation performance

When *C. autoethanogenum* growth on xylose was compared to growth on the combination of xylose-syngas or syngas alone as the carbon source, it was evident that sugar confers a different energy dynamic to the cell than gaseous substrates (CO and CO_2) (Fig. 4.1 and 4.2). Some of this variation may be attributed to the solubility of each carbon source in the liquid media in which the treatment cultures were grown, but the root cause of the differentiation may lie in the metabolic pathways used by the cell to process each form of carbon. In terms of substrate conversion to biomass, both the xylose-only and syngas-only treatments readily utilized available xylose or CO and H_2 (CO_2 is both a substrate and metabolic end product) as sources of carbon and reductant to maximize their respective growth potentials (Fig. 4.1a, 4.1c, and 4.2b). The xylose-syngas treatment utilized each substrate source in parallel at a somewhat slower pace but still yielded approximately the same maximum concentration of biomass as the xylose-only treatment (Fig. 4.1a, 4.1c, and 4.2a). Looking specifically at the uptake of xylose, the slower consumption by the xylose-syngas treatment may have been the result of xylose transporter and/or pentose phosphate pathway inhibition by syngas or it may have been that this particular treatment was less dependent on sugar because of the carbon available in syngas. One way to answer this query was to examine the expression data obtained by this study for the applicable proteins to determine if the xylose-only and xylose-syngas treatments exhibited different expression patterns during transport and carbon fixation. This will be discussed further. In terms of metabolite production, the xylose-syngas treatment produced a similar concentration of acetate as the xylose-only treatment (Fig. 4.1b), but an ethanol amount more akin to that produced by the syngas-only treatment (Fig. 4.1d). This may indicate that the energetics and

carbon flow required to produce ethanol were altered when the cells were exposed to syngas. It could also imply that the organism must activate certain syngas-related enzymes that are otherwise down regulated when xylose is the only carbon source available. In short, the physiological differences observed when *C. autoethanogenum* was grown on xylose or syngas as the sole carbon source or a mixture of xylose-syngas were the result of changes in protein expression. Analysis of the effects of these three carbon source treatments on protein expression related to sugar metabolism and product formation pathways are discussed.

Protein differentiation

One feature which made this work unique was that it differentiated between the proteins found in the cell membrane region and those present in the cytoplasm. Membrane proteins can have functions related to transport of chemicals in/out of the cell, cell motility, and cellular protection, while cytoplasmic proteins are responsible for carbon metabolism and biochemical function. Both cell fractions play a part in electron transport and energy conservation. Proteomic analysis revealed that across the three carbon source treatments (xylose, syngas, and mixed xylose-syngas), 48 proteins from the membrane fraction and 165 proteins from the cytoplasmic fraction were both t-test significant (p-value < 0.05) and expressed with a fold difference greater than two (a.k.a. fold change > 4) between two treatments. All other proteins expressed by *C. autoethanogenum* exhibited common regulation between the three treatments (i.e. they fell below the thresholds for statistical significance or fold difference). Figure 4.3 shows the protein distribution among the treatments where the count indicates that a protein was upregulated (expressed more) in the particular treatment(s) versus the remaining treatment(s). Among the membrane proteins (Fig. 4.3a), nine were dominant when the cells were grown with a single, sugar-based carbon source (xylose treatment) and another nine proteins were expressed to

a greater extent when the cells were cultured with a dual carbon source (xylose-syngas treatment). Fourteen proteins showed higher expression amongst both of the treatments containing xylose which indicates that these proteins are likely involved in metabolizing xylose and have to be functional for the organism to process this sugar. Similarly, there were also fourteen proteins dominant when *C. autoethanogenum* metabolizes syngas as a source of carbon (xylose-syngas and syngas treatments). Only one protein had higher expression solely in the syngas-only treatment which implies that its expression was at the base state when syngas was the only carbon substrate provided. Finally, there was one remaining membrane protein that was dominant in the both the xylose and the syngas treatments which indicates that it has higher expression when the organism is consuming a single, non-specific carbon source. These inferences also apply to the counts for the cytoplasmic proteins shown in Figure 4.3b. Out of the proteins which showed higher expression in the cytoplasmic fraction, 56 proteins were common to the metabolism of syngas (xylose-syngas and syngas treatments), while only 33 proteins were seen to be upregulated with growth on xylose (xylose and xylose-syngas treatments).

Xylose transport and conversion

KEGG pathway analysis for xylose transporters showed that *C. autoethanogenum* possesses the proteins for two ATP-binding cassette (ABC) transporters: a D-xylose/ribose complex (RbsABC) and an autoinducer 2 complex (LsrABCD). Both are active transporters which require energy in the form of ATP hydrolysis to import sugar into the cell (Fig 4.4). RbsABC has features of both Type I (ATP hydrolysis is dependent on the presence of substrate) and Type II (ATP hydrolysis is substrate independent) import systems (Clifton et al., 2015). The autoinducer 2 network is a quorum sensing system that consists of the transporter (LsrABCD), a repressor (LsrR), and a cognate signal kinase (LsrK) and uses autoinducer 2 (AI-2) as a signaling

molecule (Li et al., 2007). Interestingly, additional KEGG pathway mapping showed that the complete autoinducer 2 transport complex (LsrABCD) and any other Lsr proteins are missing from the related species, *C. ljungdahlii*, which may provide some insight into why *C. ljungdahlii* metabolizes fructose as opposed to xylose as a preferred sugar substrate (Bruno-Barcena et al., 2013). Experimental protein data only showed significant differential expression of two proteins from these xylose transporters, a monosaccharide-transporting ATPase (CAETHG_4000, LsrA) and a periplasmic binding protein domain-containing protein (CAETHG_4003, LsrB) both from the autoinducer 2 complex. Figure 4.4 and Table 4.1 show the fold differences for CAETHG_4000 and CAETHG_4003. Given that the treatment cultures were harvested at the latter end of the exponential growth phase, the extracellular environment was likely at a point of higher acidity for those cultures (xylose and xylose-syngas grown) which metabolized xylose as a substrate and readily produced acetate. For this reason, these cells were likely sending out a quorum sensing based response to down regulate expression of the monosaccharide-transporting ATPase and the periplasmic binding protein, compared to the syngas grown cells, as a means of not only preventing further xylose conversion to harmful acid but also to redirect the ATP towards more useful biochemical functions such as cell survival. Additional regulation changes of these proteins by the xylose-syngas co-fermentation was the result of CO in syngas providing additional energy to the cells so that they were less dependent on xylose for their energy needs. Figure 4.5a shows the xylose conversion reactions that occur before the sugar molecule enters the pentose phosphate pathway. Up regulation of xylose isomerase (CAETHG_3932) and one of the xylulokinases (CAETHG_3933) by the xylose and xylose-syngas cells indicated that these enzymes are highly driven by the presence of xylose and the potential for future energy release from the sugar is enough to offset the energy requirement for phosphorylation (Fig. 4.5a).

However, as the first bar in each graph shows for these proteins (CAETHG_3932 and CAETHG_3933), the presence of syngas in the mixed carbon fermentation had minimal effect on protein expression. While, the fact that another xylulokinase (CAETHG_3998) had higher expression when exposed to syngas (both xylose-syngas and syngas treatments) versus xylose as the only carbon source would indicate that *C. autoethanogenum* was able to bypass this phosphorylation reaction with another enzyme. Further analysis of CAETG_3998 in the KEGG database revealed that this protein is the autoinducer 2 kinase, LsrK. It phosphorylates 4,5-dihydroxy-2,3-pentanedione (DPD) (EC 2.7.1.189), the AI-2 signal molecule, and is part of the autoinducer 2 network used to transport xylose into the cell via the transporter, LsrABCD (Xavier et al., 2007; Zhu et al., 2013). The deoxyribose-phosphate aldolase/phospho-2-dehydro-3-deoxyheptonate aldolase protein, LsrF (CAETHG_4004), also showed up as significant in the experimental data with expression results (Table 4.2) similar to LsrA, LsrB, and LsrK (CAETHG_4000, CAETHG_4003, and CAETHG_3998; Table 4.1 and 4.2). Specifically, higher expression was observed in the syngas treatment with minimal gas effects shown in the xylose-syngas treatment because xylose was causing down-regulation as a result of pH stressed cultures and imminent sugar exhaustion. LsrF catalyzes the terminal step in the autoinducer 2 network by transferring the acetyl group from the AI-2-phosphate termination product, 3-hydroxy-2,4-pentadione-5-phosphate, to coenzyme A to form two intermediates in central carbon metabolism, dihydroxyacetone phosphate and acetyl-CoA (Marques et al., 2014). Since the syngas treatment did not contain xylose for substrate uptake, the cells obviously used LsrF activity to turn off the autoinducer 2 complex and yield acetyl-CoA as a substrate for further reactions.

Another transporter of interest from the experimental data was the sugar transporter, CAETHG_3935 (Fig. 4.5b and Table 4.1). It is located on an operon with the genes for xylose conversion (CAETHG_3932 and CAETHG_3933) and aldose 1-epimerase (CAETHG_3934) and is also directly upstream of a xylose operon transcriptional regulator (CAETHG_3936). Similar to xylose isomerase (CAETHG_3932) and xylulokinase (CAETHG_3933), the up regulation of this sugar transporter was triggered by the presence of xylose which could mean that this protein was a probable xylose transporter. The uncharacterized membrane protein, CAETHG_ 2280, is located in the genome in close proximity to other genes that are annotated as membrane proteins, thus as a result, the role of this protein is likely associated with membrane transport activity. Similar to permease proteins, this protein may be located in the inter-membrane region where it assists in conformation changes or substrate binding associated with ABC transport (White, 2007). Since CAETHG_ 2280 (Table 4.1) had significantly higher expression when xylose was a carbon source (both xylose and xylose-syngas fermentations), it possibly played a role in xylose transport during culture growth.

Carbon metabolism

Although none of the proteins used in the transketolase, transaldolase, sugar-phosphate isomerase, or ribulose-phosphate 3-epimerase reactions of the pentose phosphate pathway showed a significant change in expression between the xylose, xylose-syngas, and syngas carbon source treatments, there were protein regulation differences further along in the path of central carbon metabolism. Examination of the experimental protein data for reactions related to the conversion of glucose-6-phosphate and fructose-6-phosphate to pyruvate and vice versa revealed that treatments consuming xylose had higher expression of glycolytic proteins (catabolism) while syngas usage was associated more with proteins expressed for the purpose of gluconeogenesis

reactions (anabolism). Six different glycolysis pathway reactions demonstrated strong protein up regulation when xylose was present in the culture broth (xylose and xylose-syngas fermentations). As shown in Figure 4.6 and Table 4.2, these enzymatic reactions and proteins include: fructose-6-phosphate conversion to fructose-1,6-bisphosphate by ATP-dependent 6-phosphofructokinase (CAETHG_2439), interconversion between glyceraldehyde-3-phosphate and dihydroxyacetone phosphate by triosephosphate isomerase (CAETHG_1758), 1,3-bisphosphoglycerate conversion to 3-phosphoglycerate by phosphoglycerate kinase (CAETHG_1759), 3-phosphoglycerate conversion to 2-phosphoglycerate by phosphoglycerate mutase (CAETHG_1757), 2-phosphoglycerate conversion to phosphoenolpyruvate by enolase (CAETHG_1756), and finally phosphoenolpyruvate conversion to pyruvate by pyruvate kinase (CAETHG_2441). The proteins in these reactions did not have a significant fold difference between the xylose-syngas and xylose treatments so the gas effect on glycolytic carbon metabolism was minimal. Since xylose is a relatively rich energy source, it is not a surprise that these six reactions yield a net ATP gain (Fig. 4.6) for *C. autoethanogenum* which contributes to the higher biomass and end products generated by the xylose and xylose-syngas treatments (Fig. 4.1). The protein, CAETH_1761, is a transcriptional regulator for the DeoR family of proteins which control sugar catabolism, and in this case, it probably regulated glycolysis given that not only is its gene transcribed just upstream of an operon containing genes for proteins used in glycolysis (CAETHG_1756, CAETHG_1757, CAETHG_1758, CAETHG_1759, and CAETHG_1760) but it also showed the same xylose triggered expression pattern and fold differences as these glycolytic proteins (Table 4.2).

Expression of glyceraldehyde-3-phosphate dehydrogenase showed an interesting experimental result depending on whether the treatment cultures were dependent on xylose or the

carbon in syngas for carbon fixation (Fig. 4.6 and Table 4.2). The glyceraldehyde-3-phosphate dehydrogenase, CAETHG_1760, demonstrated an expression pattern similar to the six glycolytic proteins mentioned above; where the presence of xylose induced up regulation of CAETHG_1760 so that it could participate as a key enzyme in catabolic carbon metabolism. Meanwhile, the glyceraldehyde-3-phosphate dehydrogenase, CAETHG_3424, was repressed by the presence of xylose as the syngas treatment had significantly higher protein levels than either the xylose or the xylose-syngas fermentation treatments. This indicates that CAETHG_3424 enabled gluconeogenesis to occur within the cell since the *C. autoethanogenum* treatment with syngas as the sole carbon source was able to express the protein without any negative effects and, given the reactions of the Wood-Ljungdahl pathway, the syngas-grown cell would need to use gluconeogenesis to transform pyruvate into phospholipids, amino acids, and sugars required for the cell to survive (White, 2007). In addition, if the CO in syngas is used as an electron donor, the availability of NADH is not limited. The reaction from 1,3-bisphosphoglycerate to glyceraldehyde-3-phosphate catalyzed by glyceraldehyde-3-phosphate dehydrogenase, CAETHG_3424, would also allow the cell to gain back needed NAD^+ along with releasing a phosphate ion that could be used to create ATP (Fig. 4.6). In a similar study, Marcellin et al. (2016) evaluated heterotrophic growth on fructose versus autotrophic growth on a gas mix (35% CO, 10% CO_2, and 2% H_2 to represent basic oxygen furnace gas, 25 psi) with *C. autoethanogenum* and found 1) phosphoenolpyruvate carboxykinase (CAETHG_2721) controls the rate-limiting step of gluconeogenesis, and 2) identified a specialized glyceraldehye-3-phosphate dehydrogenase (CAETHG_3424) that may enhance anabolic capacity by reducing the amount of ATP consumed by gluconeogenesis. Although our work used xylose as the key sugar, it also found that phosphoenolpyruvate carboxykinase had a significant expression difference

between treatments. Phosphoenolpyruvate carboxykinase (CAETHG_2721), which catalyzes the conversion of oxaloacetate to phosphoenolpyruvate during gluconeogenesis, was down regulated in the presence of xylose and xylose-syngas versus syngas as the only carbon source (Table 4.2). This is important as the flow of phosphoenolpyruvate in the gluconeogenic direction allows the cells to build sugars for cell wall metabolism which would be needed when the cells are growing solely on syngas. The phosphoenolpyruvate carboxykinase reaction is ATP dependent; however, it does release CO_2 which can be fixed by *C. autoethanogenum* through the Wood-Ljungdahl pathway if hydrogen is available to reduce it. Another protein repressed by the presence of xylose but not syngas was fructose-1,6-bisphosphatase class 3 (CAETHG_0897) which also participates in gluconeogenesis by releasing energy in the form of a phosphate ion through the hydrolysis of fructose-1,6-bisphosphate. While some gluconeogenesis reactions are beneficial for the syngas-grown *C. autoethanogenum* cell, several more deplete the cell's energy stores and provide metabolites (e.g.. fructose-6-phosphate is a precursor to amino sugars) at a cost such that the organism has a reduced capacity to produce new cells as evidenced by the lower growth results for the syngas-grown cultures in Figure 4.1.

Of the proteins involved in the Wood-Ljungdahl pathway, only those used in the interconversion between CO and CO_2 and formation of H_2, as shown in Figure 4.7, seemed to be affected by the three carbon source treatment conditions. Carbon-monoxide dehydrogenase (CODH) catalyzes the reversible reduction of CO_2 to CO with ferredoxin used as the electron carrier. In acetogens, CODH forms a tight complex with acetyl-CoA synthase (ACS) which allows the assembly of acetyl-CoA following CO formation, and in some organisms, such as *Moorella thermoacetica*, these two enzymes are actually a bifunctional protein (Darnault et al., 2003). The xylose-only treatment had significantly higher protein expression of two CODH,

CAETHG_1621 and CAETHG_1620, than either of the treatments in which syngas was provided as a carbon source (xylose-syngas and syngas). Although one might believe that growth on syngas would lead to higher expression of this protein as a result of *C. autoethanogenum*'s need to process CO_2 as a carbon source or to generate reducing equivalents from CO, the experimental results actually showed that CODH was used to a greater extent to reassimilate the CO_2 produced as a result of xylose metabolism (e.g. pyruvate conversion to acetyl-CoA). The additional reducing equivalents produced by sugar metabolism also contributed to making the reaction of CO_2+H_2 to CO possible. Besides providing intermediates to fuel the creation of acetyl-CoA and other metabolites via the Wood-Ljungdahl pathway, the reassimilation of CO_2 from xylose metabolism also prevents pH decay by sequestering CO_2 and preventing its reaction with water to form carbonic acid. A third CODH, CAETHG_0455, appeared to be upregulated by syngas while also downregulated by xylose. Syngas enhanced expression of CAETHG_0455 in the xylose-syngas treatment, and the presence of just syngas in the syngas-only treatment increased this protein expression even further. Additional details on CAETHG_0455 in the KEGG database show that it is a quinone-dependent CODH that catalyzes the oxidation of CO to CO_2 under aerobic conditions in carboxydotrophic bacteria and is enzymatically comparable to the anaerobic reaction. While in the UniProt database CAETHG_0455 has similar sequence identity to a xanthine dehydrogenase, iron-sulfur cluster and FAD-binding subunit A protein in *C. ljungdahlii*, so its sensitivity to syngas may be the result of its oxidoreductase activity and relate to the reduced ability to deal with oxidative stress in *C. autoethanogenum*.

Between the xylose, xylose-syngas and syngas treatments, no significant differences in expression were observed among the phosphate acetyltransferase and acetate kinase proteins

involved in acetate production; however, both of the proteins used to produce ethanol from acetyl-CoA had significant expression changes between the treatments (Figure 4.8). Two acetaldehyde dehydrogenases (CAETHG_3747 and CAETHG_1819) both had higher expression in the syngas-only treatment as the result of probable down regulation by xylose in the other treatments (xylose and xylose-syngas). As mentioned earlier the cultures were late exponential when samples were harvested, so acetaldehyde formation from acetyl-CoA may have been a lower priority for cells consuming xylose in relation to other biochemical reactions such as amino acid formation that could occur. Yet, for the energy hungry syngas-only treatment, acetaldehyde dehydrogenase action regenerated coenzyme A so that it could work with tetrahydrofolate to fix more C1 molecules and also liberated electrons from NADH so that the electron carrier could participate in further energy transfer. Considering the alcohol dehydrogenase expression observed, the experimental evidence showed that *C. autoethanogenum* used different isozymes depending on whether xylose or syngas was providing carbon and energy. Two alcohol dehydrogenases (CAETHG_3954 and CAETHG_3604) were highly up regulated in the presence of xylose (xylose and xylose-syngas) regardless of whether syngas was also in the system and a third alcohol dehydrogenase (CAETHG_1841) had higher protein expression in the syngas only treatment with the effect of xylose in the xylose-syngas treatment being too small to be significant (Fig. 4.8). As mentioned earlier, pyruvate formation (CAETHG_2441) was upregulated in the presence of xylose (xylose and xylose-syngas treatments, Fig. 4.6) which indicates that the majority of the acetyl-CoA formation as a precursor to acetate/ethanol production was possibly being fueled by the sugar metabolism as opposed to C1 gases. Pathway Tools showed that the uncharacterized protein, CAETHG_3030 (Table 4.2), is transcribed downstream of a pyruvate ferredoxin oxidoreductase so it may have a related

function in redox reactions related to pyruvate formation and conversion under a single carbon source (xylose-only or syngas-only treatments).

C. autoethanogenum is believed to possess an aldehyde ferredoxin oxidoreductase (AOR) to allow the conversion from acetate to acetaldehyde in order to accept excess electrons and prevent the formation of more harmful acetic acid. Although neither the KEGG database nor Pathway Tools contain a curation of this exact reaction for *C. autoethanogenum*, Marcellin et al. (2016) and Mock et al. (2015) indicated that *C. autoethanogenum* proteins, CAETHG_0092 and CAETHG_0102, which belong to enzyme class 1.2.7.5 perform the AOR reaction. Per the KEGG database, enzyme 1.2.7.5 catalyzes the reduction of a carboxylate to an aldehyde using ferredoxin as the electron carrier. A different enzyme, 1.2.1.3 or NAD-dependent aldehyde dehydrogenase, catalyzes the same carboxylate to aldehyde reaction using NAD^+/NADH instead of ferredoxin and may be the reason why the database curations for *C. autoethanogenum* are incorrect as generalized pathways in the KEGG database list EC. 1.2.1.3, and not EC. 1.2.7.5, as the appropriate reaction for acetate to acetaldehyde interconversion. Out of the two AOR specified by Marcellin et al. (2016) and Mock et al. (2015), only CAETHG_102 had an expression change between the carbon source treatments in the experimental data (Table 4.2). CAETHG_102 had higher expression in exclusively the syngas treatment, and was down regulated by the xylose and xylose-syngas treatments, which reveals that following the creation of acetyl-CoA from syngas metabolism, the cells created acetate to generate ATP and then converted the acetate to acetaldehyde to dispose of electrons. This result agrees with the observation for the alcohol dehydrogenase, CAETHG_1841, which showed drastically higher expression with syngas as the only carbon source even though the upstream acetaldehyde dehydrogenase had a lower fold difference. From this it can be deduced that CAETHG_102 and

CAETHG_1841 work together to produce ethanol from acetate which is more energetically efficient for the cell when the syngas is the only substrate. Work by Abubackar et al. (2015) also supports this deduction as they witnessed minimal accumulation of acetate, but healthy cultures and ethanol production, from *C. autoethanogenum* growth on CO as the sole carbon source.

Energy metabolism

Figure 4.9 and Table 4.3 show the protein expression differences for enzymes related to the notable electron carriers: nicotinamide adenine dinucleotide (NAD^+/NADH) and nicotinamide adenine dinucleotide phosphate ($NADP^+$/NADPH). The reduced form of these electron carriers is used for energy storage while interconversion to the oxidized form allows the release of energy. Figure 4.9a illustrates that during NAD^+ biosynthesis and/or salvage that the NAD^+ synthetase, CAETHG_2782, showed better expression under mixed carbon, xylose-syngas conditions. Since the xylose-syngas treatment provided the most carbon to the cells, it had wider metabolic options available and could take advantage of both sugar and C1 gases to provide energy. Reactions involving NADP(H) are correlated with biomass- or growth-associated energy. One particular NADPH dehydrogenase (CAETHG_0482) was expressed to a greater extent during conditions with syngas as the sole source of carbon (Fig. 4.9b and Table 4.3). Since syngas-grown cultures were not as dense as those grown on xylose or xylose-syngas (Fig. 4.1), the result seen with CAETHG_0482 was probably linked to the NADP(H)-dependent reactions required for *C. autoethanogenum* to metabolize CO and CO_2+H_2 in the Wood-Ljungdahl pathway rather than biomass production. Mock et al. (2015) found that the only active hydrogenase in *C. autoethanogenum* cells grown on CO_2+H_2 was NADP- and ferredoxin-dependent. This [FeFe]-hydrogenase (CAETG_2794-2799) is electron bifurcating as it catalyzes the reversible oxidation of H_2 to H^+ with Fd_{ox} and $NADP^+$, and it forms an enzyme complex with

the formate dehydrogenase (CAETHG_2789) that reduces CO_2 with H_2 to formate in the Wood-Ljungdahl pathway (Mock et al., 2015; Wang et al., 2013). Mock et al. (2015) and Wang et al. (2013) also showed that the methylene-H_4F dehydrogenase (CAETHG_1616, also in the Wood-Ljungdahl pathway) used by *C. autoethanogenum* is NADP(H)-dependent. Another NADP(H)-dependent reaction is that of flavin mononucleotide (FMN) reductase (CAETHG_0716) which takes part in one and two-electron transfers. Since FMN reductase can catalyze the removal of two electrons, its expression would be beneficial in scenarios where there is a high demand for reductant. CAETHG_0716 demonstrated highest expression in the syngas-only treatment (Fig. 4.9c) which was the most reductant-limited condition of the three treatments because it did not contain sugar as a source of energy.

Riboflavin is a precursor to the redox cofactors flavin mononucleotide (FMN) and flavin adenine dinucleotide (FAD). It is synthesized from one molecule of guanosine triphosphate (GTP) and two molecules of ribulose-5-phosphate (Bacher et al., 2001). Given that ribulose-5-phosphate is an end product of the pentose phosphate pathway, it was not unexpected that riboflavin biosynthesis protein RibBA (CAETHG_0305, 3,4-dihydroxy-2-butanone-4-phosphate synthase) which catalyzes the conversion of ribulose-5-phosphate in the first step of riboflavin biosynthesis was more highly expressed in the xylose and xylose-syngas treatments (Fig. 4.10 and Table 4.3). The next step in the biosynthesis pathway is carried out by 6,7-dimethyl-8-ribityllumazine synthase (CAETHG_0304), and the expression of this protein was also positively influenced by the presence of xylose as a carbon source since the xylose-only treatment was upregulated compared to the syngas-only treatment by a fold difference (a.k.a. $\log_2$ fold change) of 5.42.

It has been demonstrated previously that *C. autoethanogenum* possesses an Rnf complex to translocate protons across the cell membrane (Marcellin et al., 2016; Mock et al., 2015). Of the six subunits that comprise the RnfABCDGE type electron transport complex, proteins for all subunits except subunit A were present in the experimental results (Fig. 4.11a and Table 4.3). Overall, the fold differences observed for Rnf subunits B, C, D, G, and E (CAETHG_3232, CAETHG_3227, CAETHG_3228, CAETHG_3229, and CAETHG_3230, respectively) revealed that the components of syngas (CO, CO_2, and H_2) as found in the xylose-syngas and syngas treatments enhance Rnf expression. The presence of sugar (xylose and xylose-syngas treatments) induced either slight repression (CAETHG_3232, CAETHG_3227, and CAETHG_3229) or no repression (CAETHG_3228 and CAETHG_3230) of the Rnf complex proteins. The use of an Rnf complex is essential for electrons to move, and if the proton motive force created by the complex is also used to drive ATP synthesis with F_1F_O ATP synthase (Allegretti et al., 2015), this creates an even more energetically favorable situation for the cell. Syngas metabolism is considered to be bioenergetically inferior compared to sugar metabolism, so a culture fed syngas as a substrate will have a greater need to express any mechanism (such as an Rnf complex paired with ATP synthase) that improves its energy dynamics.

Several electron transport flavoproteins were differentially expressed between the three carbon source treatments. Two electron transfer flavoprotein alpha/beta-subunits (CAETHG_0115 and CAETG_0116) and a cytochrome *c* dependent lactate dehydrogenase (CAETHG_0117) which are located in the same transcription unit (Fig. 4.11b) had better protein expression when xylose was used as substrate. The flavoprotein alpha/beta-subunits appeared to be negatively affected by the use of syngas as the xylose-only treatment showed higher expression than both the xylose-syngas and the syngas-only conditions. As for the expression of

the lactate dehydrogenase, it was affected more strongly by the use of xylose in the growth media. Conversely, two other flavoprotein couples as depicted in Figures 4.11c and 4.11d may have been repressed by xylose since the syngas-only treatment had the highest protein expression in both cases. The first protein set contains an electron transfer flavoprotein alpha/beta-subunit (CAETHG_0245) and a cytochrome *c* dependent lactate dehydrogenase (CAETHG_0244) (Fig. 4.11c), while the second set consists an electron transfer flavoprotein alpha/beta-subunit (CAETHG_0246) and an uncharacterized protein (CAETHG_0247) that is probably another flavoprotein (Fig. 4.11d). Ultimately, these flavoprotein comparisons make it clear that certain proteins for electron transport will have favorable expression when xylose is used as a substrate while other proteins will have favorable expression when syngas is a substrate. This difference in flavoprotein expression under different substrates is likely correlated to the fact that xylose and syngas are metabolized in dissimilar pathways and the active sites of the enzymes used in each pathway will vary.

Additional observations

A few additional proteins had markedly high fold differences between the carbon source treatments (Table 4.4). The first, CAETHG_2212, a putative conserved protein, was highly expressed in the presence of xylose (xylose and xylose-syngas) with a fold difference of 9.32 between the xylose-only and syngas-only treatments. CAETHG_2212 is transcribed next to two proteins used for amino acid metabolism: CAETH_2210, an aminotransferase used in the degradation of alanine, and CAETHG_ 2211, a phosphoglycerate dehydrogenase used to biosynthesize serine. As a result, it can be assumed that CAETHG_2212 supports a key role in amino acid biosynthesis. The second protein was translation elongation factor G, CAETHG_1979, which had a fold difference of 5.35 between the syngas-only and xylose-only

treatments and a fold difference 7.14 between the syngas-only and xylose-syngas treatments. Translation elongation factor G is a translocase that assists in protein formation (Savelsbergh et al., 2003) and may be a vital contributor to conformational stability during a syngas-only fermentation condition when energy supplies are limited. Another over-expressed protein which has a hypothesized role in how well *C. autoethanogenum* uses different carbon sources was the aldo/keto reductase, CAETHG_0821. This protein has a coding region for transcription which overlaps with that of CAETHG_0822, a sugar diacid utilization regulator which may indicate that this protein also plays a role in the rate of sugar utilization. Further support for this hypothesis is given by the strong expression of CAETHG_0821 during xylose metabolism (fold difference = 6.04 between the xylose-only and syngas-only treatments) when the cell would be in a state of enhanced sugar utilization. Finally, CAETHG_0817, a glucarate dehydratase, had higher expression in the presence of xylose (fold difference = 8.01 between the xylose-only and syngas-only treatments) which showed the enhanced ability for carbohydrate metabolism when a sugar substrate such as xylose is used as a substrate. Although these observations may appear disconnected, they demonstrate the full extent of variation in protein regulation between the three carbon source treatments. In addition, these proteins play notably important roles in cell function (amino acid biosynthesis, protein formation, and sugar metabolism) which further stresses the effect that sugar or gaseous carbon can have on cellular homeostasis.

Conclusion

C. autoethanogenum exhibited differences in its physiology when it was grown on xylose as the only carbon source versus syngas or a co-fermentation of xylose and syngas. These differences manifested as changes in protein expression under each of the three carbon source options. *C. autoethanogenum* expressed an autoinducer 2 network (LsrABCD, LsrK, and LsrF)

for xylose transport which interestingly is not in found in its phenotypic biovar, *C. ljungdahlii*. Cultures containing xylose downregulated this network during late stage exponential growth to halt xylose transport when the environment was too acidic, even though xylose was still available, while cultures with only syngas maintained expression because the cell wanted the potential energy provided by sugar. Other work has shown that limited xylose uptake and cell growth was the result of *C. autoethanogenum*'s pH sensitivity and that xylose transport and metabolism were prolonged when cultures were maintained at a growth-optimal pH. Proteins used in the glycolytic pathway were highly expressed when xylose was available as a source of energy for catabolism with no detriment introduced by the effect of syngas in the mixed xylose-syngas treatment. Several additional proteins assisted in gluconeogenesis when syngas was the sole carbon source. Most notably, it was confirmed that CAETHG_3424, a glyceraldehyde-3-phosphate dehydrogenase, functions in an anabolic capacity in *C. autoethanogenum*. The Wood-Ljungdahl pathway is active regardless of the carbon source used with xylose metabolism actually upregulating two versions of carbon monoxide dehydrogenase to assist in the fixation of end product CO_2. Another inference was that *C. autoethanogenum* expressed different mechanisms for electron transport depending on what type of carbon (sugar or gaseous) was supplied to the cell. Of particular interest were the proteins of the Rnf complex which had higher expression during syngas metabolism and specificity for one flavoprotein over another during xylose versus syngas metabolism. Ultimately *C. autoethanogenum*'s protein expression is dictated by cell survival. If the organism can metabolize a particular substrate it will activate the necessary pathways to ensure the highest energy yields possible can be attained. If the energy provided by that substrate is limiting, the organism will upregulate alternate mechanisms for energy metabolism that can supplement the existing energetics.

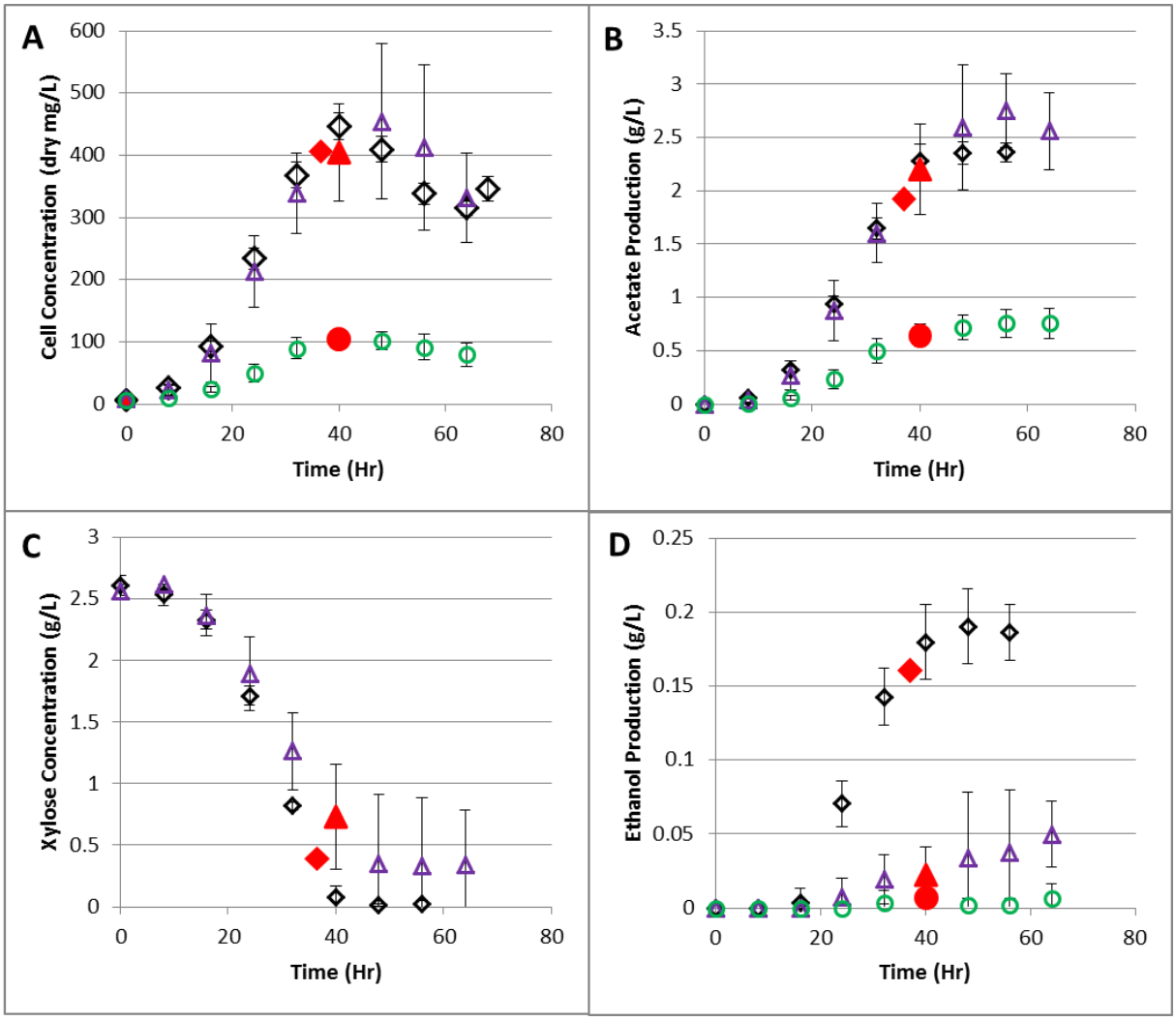

Figure 4.1. Performance of *C. autoethanogenum* fermentations with xylose only, xylose-syngas, and syngas only as the carbon source. Responses over time: A) cell concentration, B) acetate production, C) xylose concentration, and D) ethanol production. Diamond: xylose fermentation, Triangle: mixed xylose-syngas fermentation, Circle: syngas fermentation. Sample collection points for proteomic analysis are indicated by the solid red symbols. Error bars represent standard deviation.

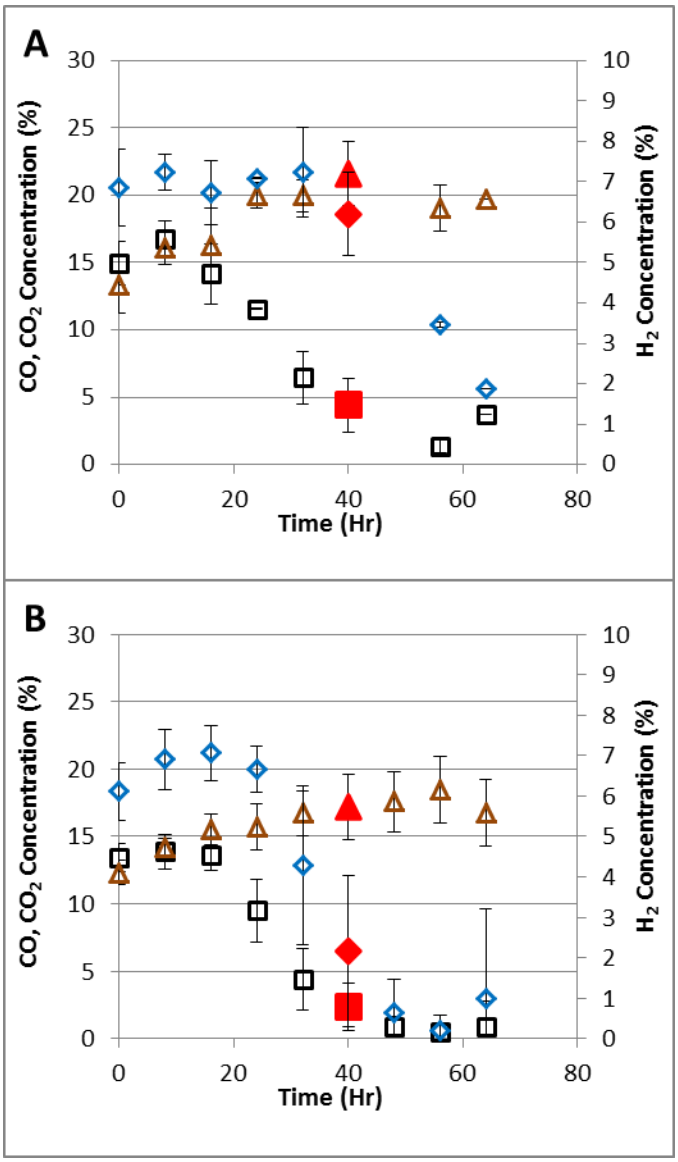

Figure 4.2. Headspace composition during *C. autoethanogenum* fermentations with A) xylose-syngas and B) syngas only as the carbon source. Headspace data not collected for xylose fermentation. Square: CO, Triangle: CO_2, Diamond: H_2. Sample collection points for proteomic analysis are indicated by the solid red symbols. Error bars represent standard deviation.

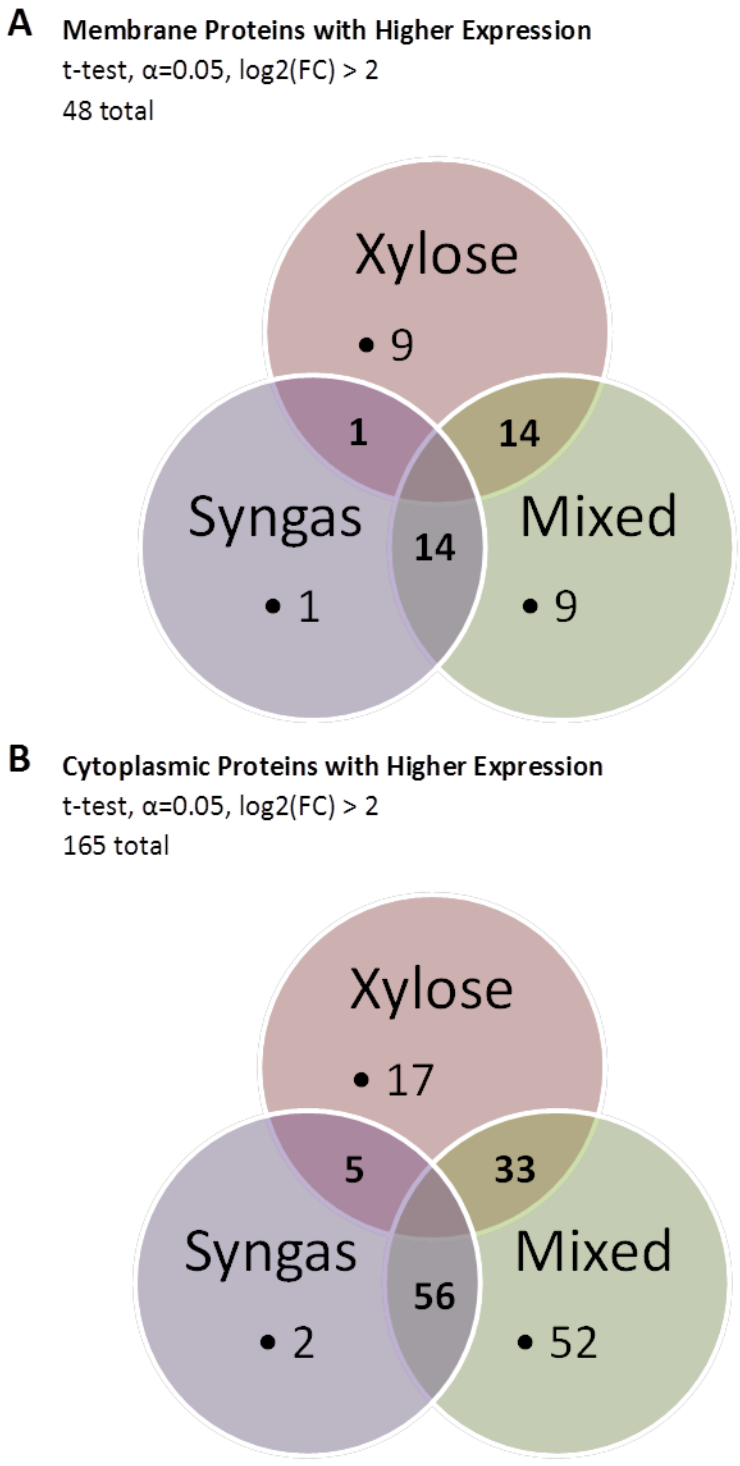

Figure 4.3. Number of significant proteins in either the A) cell membrane or B) cytoplasmic fraction that showed higher expression in the xylose, xylose-syngas (mixed), or syngas carbon source treatment of *C. autoethanogenum*.

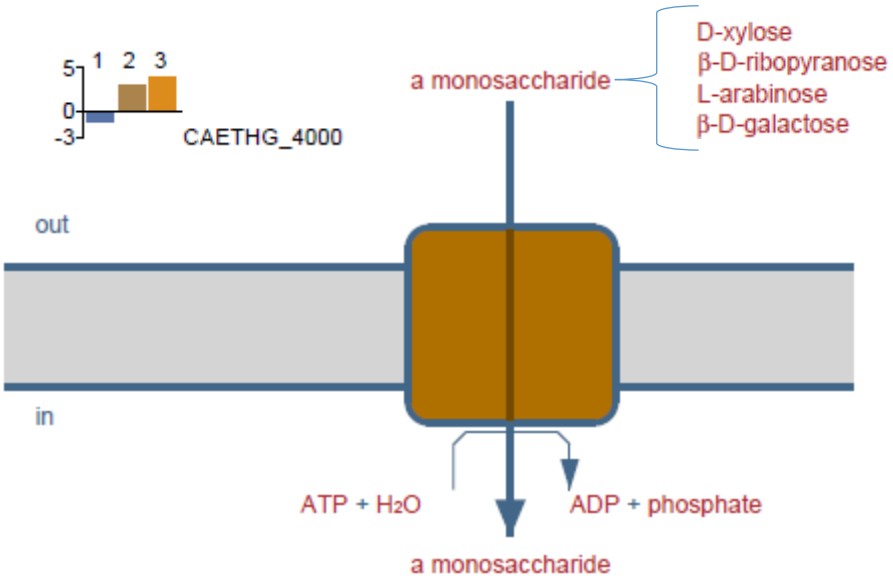

Figure 4.4. Xylose transport via a monosaccharide-transporting ATPase (CAETHG_4000). Bar graph labels represent the fold difference between 1) xylose-syngas versus xylose, 2) syngas versus xylose, and 3) syngas versus xylose-syngas treatments.

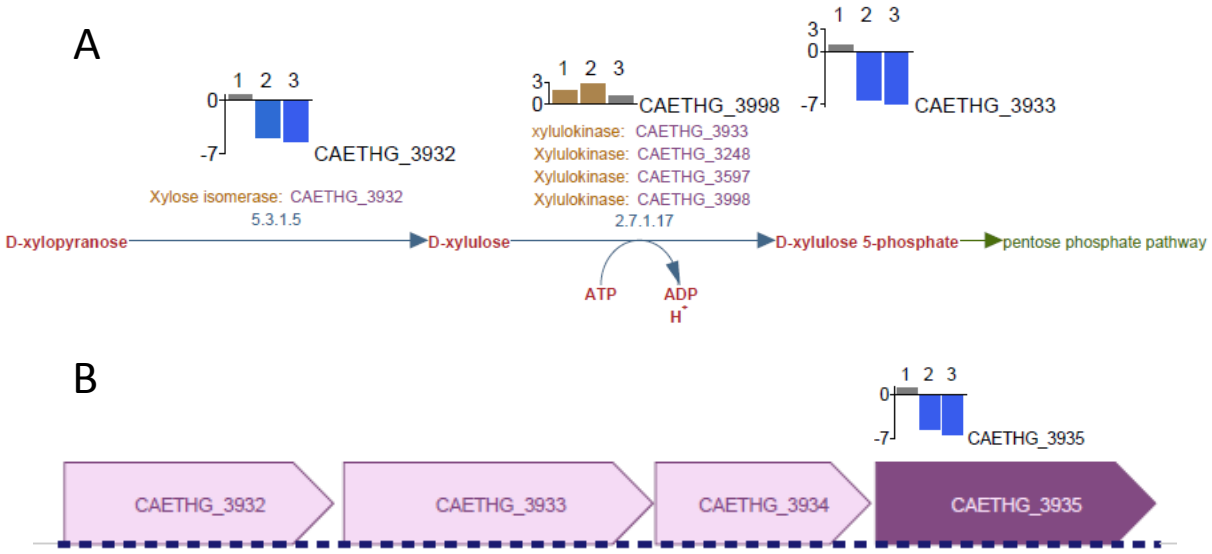

Figure 4.5. A) Xylose conversion before entry into the pentose phosphate pathway. B) Transcription of a sugar transporter (CAETHG_3935) with genes for xylose conversion (CAETHG_3932 and CAETHG_3933). Bar graph labels represent the fold difference between 1) xylose-syngas versus xylose, 2) syngas versus xylose, and 3) syngas versus xylose-syngas treatments.

Table 4.1. Key membrane transport proteins differentially expressed by *C. autoethanogenum* during xylose (XYL), xylose-syngas (MIX), or syngas (SYN) carbon source treatments. Significant results (t-test, α=0.05) with a fold difference (log2 fold change) greater than two are in bold.

Pathway	Gene	Protein (Membrane)	Fold Difference			Peptides	Sequence Coverage
			log2 FC = B-A A=XYL, B=MIX	log2 FC = C-A A=XYL, C=SYN	log2 FC = C-B B=MIX, C=SYN		(%)
ABC Transporters							
	CAETHG_1131	Cobalt ABC transporter ATPase (Sulfate-transporting ATPase) (EC 3.6.3.25)	-0.05	**-3.32**	**-3.27**	7	27.4
	CAETHG_1219	Cobalamin (Vitamin B12) biosynthesis CbiM protein	**-5.31**	**-5.04**	0.27	2	5.4
	CAETHG_2280	Uncharacterized protein	1.00	**-5.48**	**-6.48**	3	57.6
	CAETHG_3833	ABC-type transporter periplasmic subunit (ABC-type transporter, periplasmic subunit)	**-2.62**	**-2.94**	-0.31	5	20.1
	CAETHG_3835	ABC transporter related protein (ABC-type transporter ATPase component)	**-3.82**	-1.61	**2.21**	4	13.5
	CAETHG_3838	ABC-type transporter periplasmic binding protein (ABC-type transporter, periplasmic subunit)	-1.74	**-2.14**	-0.40	17	60.1
	lsrA CAETHG_4000	Monosaccharide-transporting ATPase (EC 3.6.3.17)	-1.04	**2.93**	**3.97**	2	6.3
	lsrB CAETHG_4003	Periplasmic binding protein domain containing protein (Periplasmic binding protein domain-containing protein)	1.43	**4.38**	**2.95**	13	30.2
Electrochemical Transporters							
	CAETHG_0138	Sugar (Glycoside-Pentoside-Hexuronide) transporter	0.12	**3.62**	**3.50**	1	2.9
	CAETHG_0816	Gluconate transporter	0.97	**-7.07**	**-8.03**	6	19
	CAETHG_3935	Sugar transporter	1.00	**-5.49**	**-6.48**	9	12.7
Phosphotranferase System (PTS)							
	No significant differences in protein expression						

Table 4.2. Key cytoplasmic carbon metabolism proteins differentially expressed by *C. autoethanogenum* during xylose (XYL), xylose-syngas (MIX), or syngas (SYN) carbon source treatments. Significant results (t-test, α=0.05) with a fold difference (log2 fold change) greater than two are in bold.

Pathway	Gene	Protein (Cytoplasmic)	Fold Difference			Peptides	Sequence Coverage
			log2 FC = B-A A=XYL, B=MIX	log2 FC = C-A A=XYL, C=SYN	log2 FC = C-B B=MIX, C=SYN		(%)
Pentose Conversion							
	xylA CAETHG_3932	Xylose isomerase (EC 5.3.1.5)	0.59	**-4.86**	**-5.45**	57	89.1
	CAETHG_3933	Xylulokinase	0.60	**-6.39**	**-6.99**	25	49.6
	lsrK CAETHG_3998	Xylulokinase (EC 2.7.1.189)	1.74	**2.70**	0.96	4	11.2
	lsrF CAETHG_4004	Deoxyribose-phosphate aldolase/phospho-2-dehydro-3-deoxyheptonate aldolase	1.88	**4.54**	**2.66**	9	38.1
Pentose Phosphate Pathway							
	No significant differences in protein expression, or proteins common with the pentose phosphate pathway and glycolysis.						
Glycolysis / Gluconeogenesis							
	fbp CAETHG_0897	Fructose-1,6-bisphosphatase class 3 (FBPase class 3) (EC 3.1.3.11) (D-fructose-1,6-bisphosphate 1-phosphohydrolase class 3)	0.40	**2.61**	**2.21**	8	18.8
	pfkA CAETHG_2439	ATP-dependent 6-phosphofructokinase (ATP-PFK) (Phosphofructokinase) (EC 2.7.1.11) (Phosphohexokinase)	0.24	**-4.82**	**-5.06**	17	54.1
	tpiA CAETHG_1758	Triosephosphate isomerase (TIM) (TPI) (EC 5.3.1.1) (Triose-phosphate isomerase)	0.26	**-3.27**	**-3.52**	27	87.1
	CAETHG_1760	Glyceraldehyde-3-phosphate dehydrogenase (EC 1.2.1.-)	0.29	**-3.46**	**-3.75**	39	89.9
	CAETHG_1761	Transcriptional regulator DeoR family (Transcriptional regulator, DeoR family)	0.14	**-6.58**	**-6.72**	9	29.3
	CAETHG_3424	Glyceraldehyde-3-phosphate dehydrogenase (EC 1.2.1.-)	-0.37	**6.87**	**7.25**	21	66.7
	pgk CAETHG_1759	Phosphoglycerate kinase (EC 2.7.2.3)	-0.05	**-3.38**	**-3.32**	33	75.9

Table 4.2. (continued).

Pathway	Gene	Protein (Cytoplasmic)	Fold Difference			Peptides	Sequence Coverage
			log2 FC = B-A A=XYL, B=MIX	log2 FC = C-A A=XYL, C=SYN	log2 FC = C-B B=MIX, C=SYN		(%)
	gpmI CAETHG_1757	2,3-bisphosphoglycerate-independent phosphoglycerate mutase (BPG-independent PGAM) (Phosphoglyceromutase) (iPGM) (EC 5.4.2.12)	-0.05	**-2.97**	**-2.92**	21	50.1
	eno CAETHG_1756	Enolase (EC 4.2.1.11) (2-phospho-D-glycerate hydro-lyase) (2-phosphoglycerate dehydratase)	-0.21	**-3.34**	**-3.12**	41	83.3
	CAETHG_2440	Pyruvate kinase barrel	-0.12	**-3.31**	**-3.19**	1	45
	CAETHG_2441	Pyruvate kinase (EC 2.7.1.40)	0.41	**-4.01**	**-4.42**	28	65.5
	pckA CAETHG_2721	Phosphoenolpyruvate carboxykinase [ATP] (PCK) (PEP carboxykinase) (PEPCK) (EC 4.1.1.49)	0.77	**4.31**	**3.54**	25	48.1
Ethanol and Acetate Fermentation							
	CAETHG_3030	Uncharacterized protein	**-6.75**	0.46	**7.21**	2	20.9
	CAETHG_1819	Acetaldehyde dehydrogenase (Acetylating) (EC 1.2.1.10)	0.41	**3.12**	**2.71**	6	20.9
	CAETHG_3747	Aldehyde-alcohol dehydrogenase	-0.88	**2.59**	**3.47**	27	42.2
	CAETHG_1841	Alcohol dehydrogenase (EC 1.1.1.1)	1.41	**7.66**	**6.25**	33	79.5
	CAETHG_3604	Alcohol dehydrogenase (EC 1.1.1.1)	-0.04	**-5.27**	**-5.22**	7	21.7
	CAETHG_3954	Alcohol dehydrogenase (EC 1.1.1.1)	-0.19	**-4.05**	**-3.87**	27	72.2
	CAETHG_0102	Aldehyde ferredoxin oxidoreductase (EC 1.2.7.5)	0.13	**5.63**	**5.50**	14	24.2

Table 4.2. (continued).

Pathway	Gene	Protein (Cytoplasmic)	Fold Difference			Peptides	Sequence Coverage
			log2 FC = B-A A=XYL, B=MIX	log2 FC = C-A A=XYL, C=SYN	log2 FC = C-B B=MIX, C=SYN		(%)
Wood-Ljungdahl Pathway							
	CAETHG_0455	Carbon-monoxide dehydrogenase (Acceptor) (EC 1.2.99.2) (Molybdopterin-family oxidoreductase 2Fe-2S ferredoxin subunit)	**2.48**	**5.43**	**2.96**	4	31
	CAETHG_1620	Carbon-monoxide dehydrogenase (Acceptor) (EC 1.2.99.2)	**-5.79**	**-3.94**	1.85	18	82.8
	CAETHG_1621	Carbon-monoxide dehydrogenase (Acceptor) (EC 1.2.99.2)	**-5.22**	**-3.66**	1.56	34	73.2
	CAETHG_0371	Hydrogenase assembly chaperone hypC/hupF	0.83	**2.24**	1.41	3	44.1

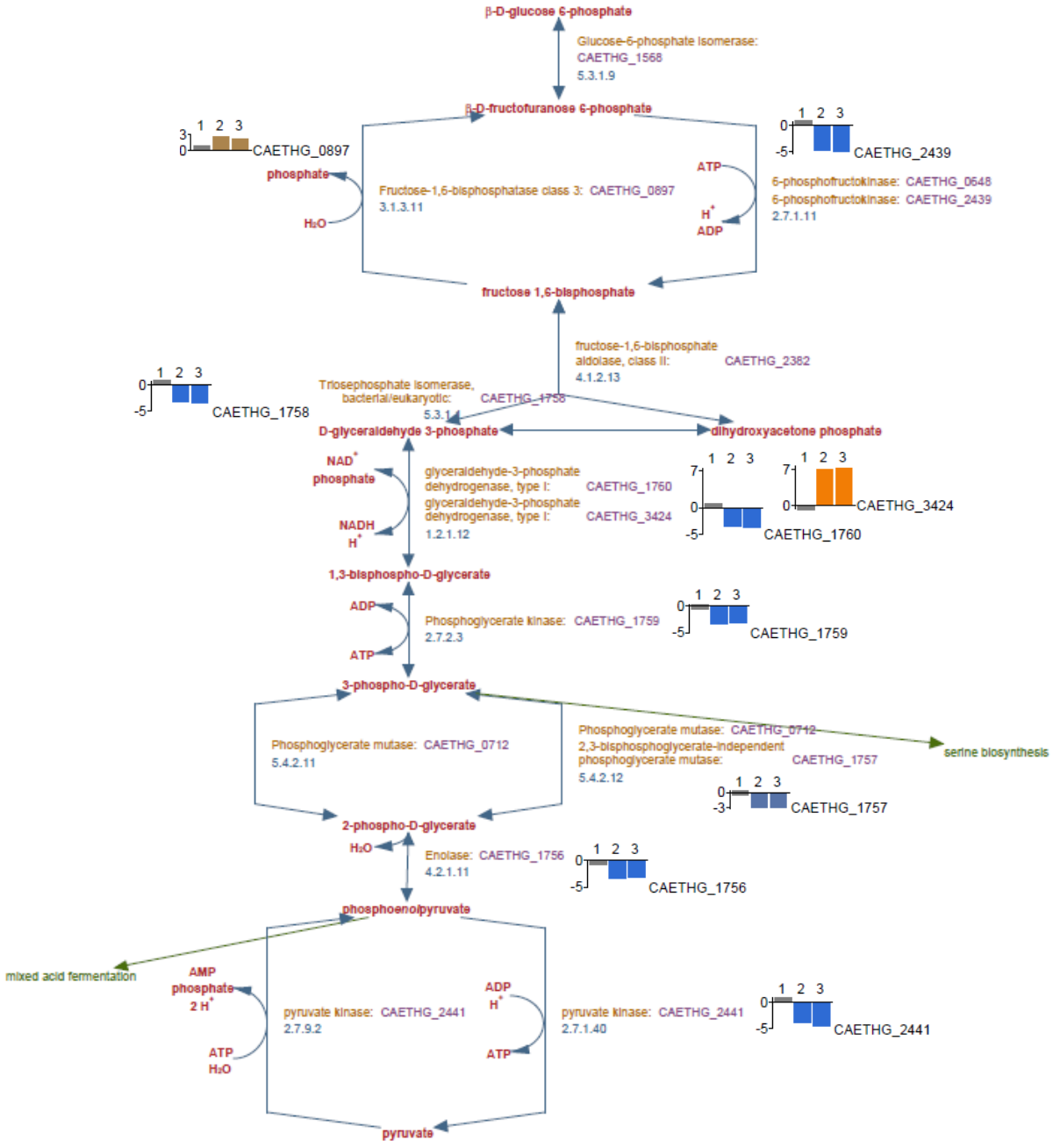

Figure 4.6. Glycolysis pathway from glucose-6-phosphate to pyruvate in *C. autoethanogenum*. Bar graph labels represent the fold difference between 1) xylose-syngas versus xylose, 2) syngas versus xylose, and 3) syngas versus xylose-syngas treatments.

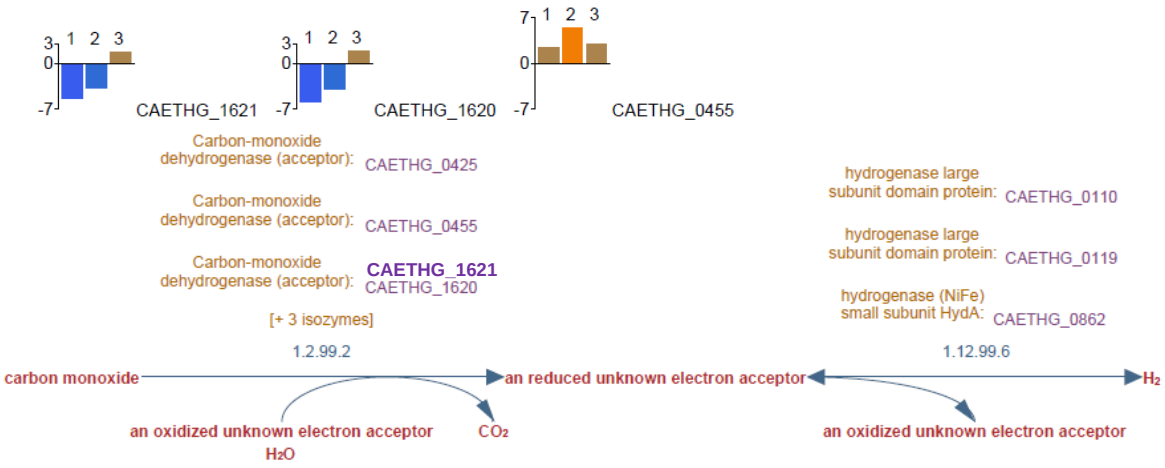

Figure 4.7. Interconversion between CO and CO_2, and production of H_2 in *C. autoethanogenum*. Bar graph labels represent the fold difference between 1) xylose-syngas versus xylose, 2) syngas versus xylose, and 3) syngas versus xylose-syngas treatments.

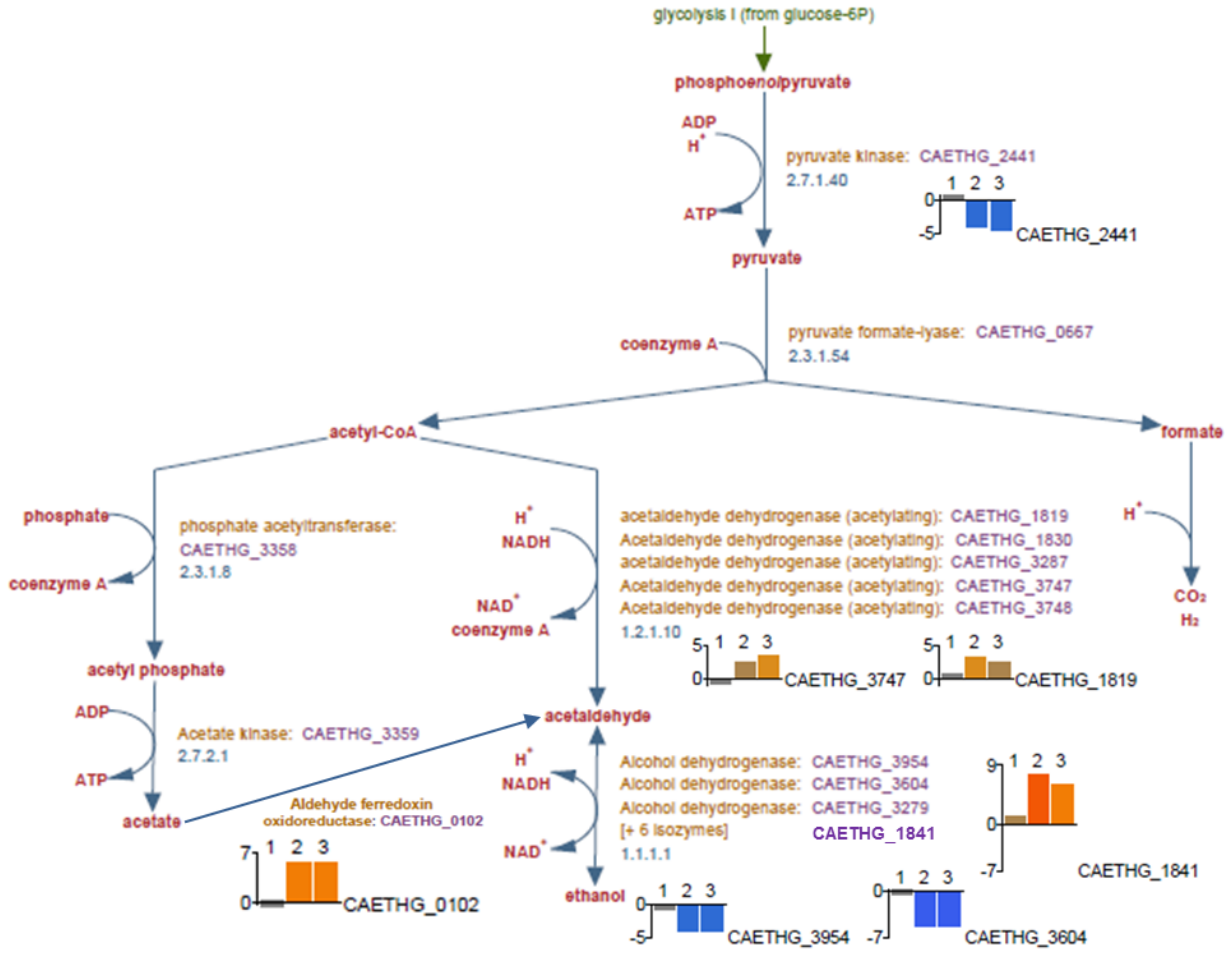

Figure 4.8. Acetate and ethanol fermentation pathway in *C. autoethanogenum*. Bar graph labels represent the fold difference between 1) xylose-syngas versus xylose, 2) syngas versus xylose, and 3) syngas versus xylose-syngas treatments.

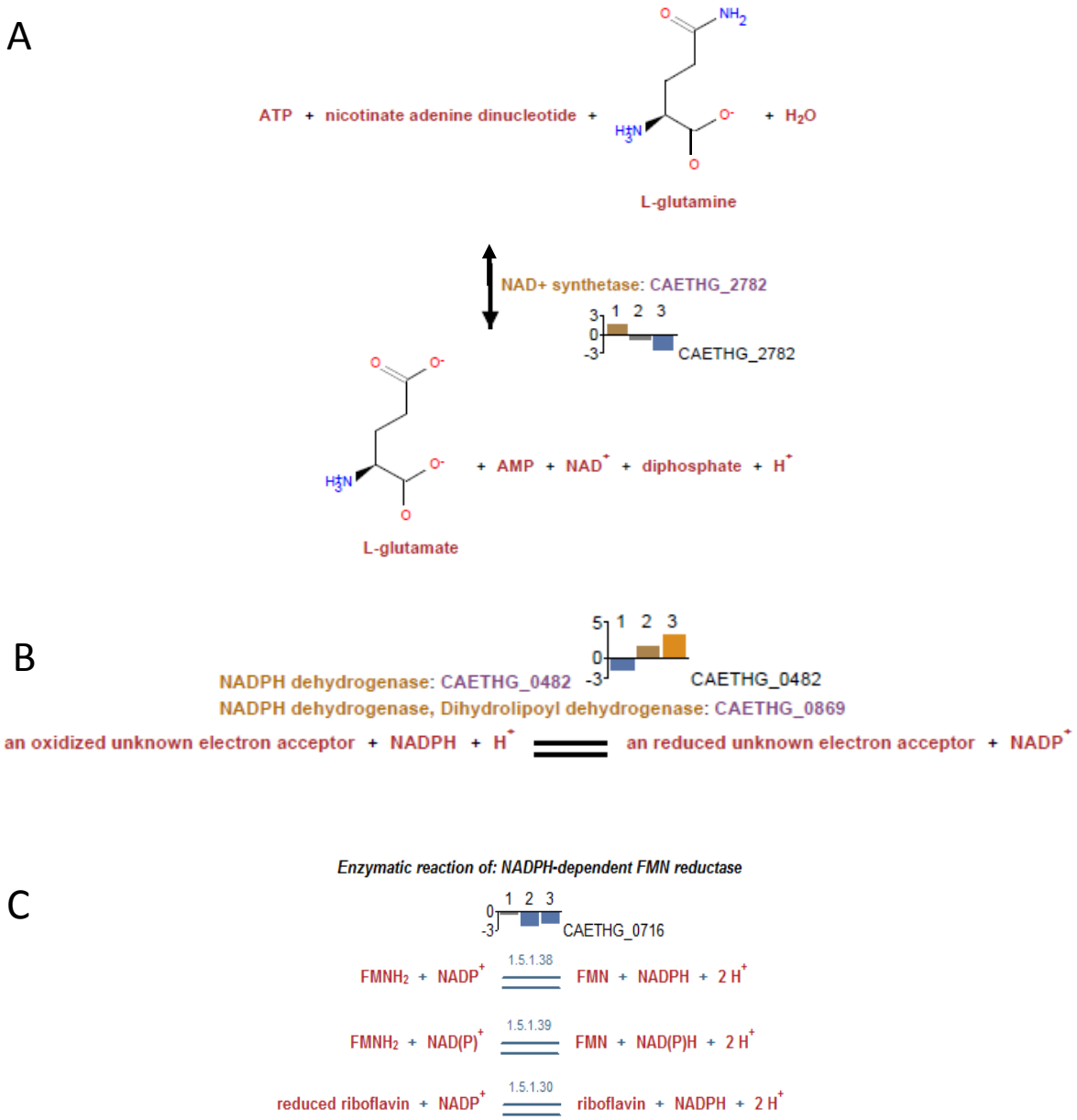

Figure 4.9. Energy metabolism in *C. autoethanogenum*: A) NAD biosynthesis and salvage, B) Reaction of NADPH dehydrogenase, C) Reaction of NADPH-dependent FMN reductase. Bar graph labels represent the fold difference between 1) xylose-syngas versus xylose, 2) syngas versus xylose, and 3) syngas versus xylose-syngas treatments.

Table 4.3. Key energy metabolism proteins differentially expressed by *C. autoethanogenum* during xylose (XYL), xylose-syngas (MIX), or syngas (SYN) carbon source treatments. Location: Cyt = cytoplasm and Mem = membrane. Significant results (t-test, α=0.05) with a fold difference (log2 fold change) greater than two are in bold.

Protein Location	Gene	Protein	Fold Difference			Peptides	Sequence Coverage
			log2 FC =B-A A=XYL, B=MIX	log2 FC =C-A A=XYL, C=SYN	log2 FC =C-B B=MIX, C=SYN		(%)
Cyt	ribH CAETHG_0304	6,7-dimethyl-8-ribityllumazine synthase (DMRL synthase) (LS) (Lumazine synthase) (EC 2.5.1.78)	-0.58	**-5.42**	**-4.84**	6	51.6
Cyt	ribBA CAETHG_0305	Riboflavin biosynthesis protein RibBA	-1.21	**-3.78**	**-2.57**	4	12.2
Cyt	CAETHG_0482	NADPH dehydrogenase (EC 1.6.99.1)	-1.55	1.65	**3.20**	4	16.9
Cyt	CAETHG_0716	NADPH-dependent FMN reductase	-0.43	**-2.38**	-1.96	1	11.2
Cyt	CAETHG_2782	NAD(+) synthetase (NAD+ synthetase) (EC 6.3.5.1)	1.61	-0.86	**-2.46**	3	6.3
Cyt	CAETHG_0115	Electron transfer flavoprotein alpha/beta-subunit	**-4.18**	**-3.80**	0.38	4	22.1
Cyt	CAETHG_0116	Electron transfer flavoprotein alpha/beta-subunit	**-2.18**	**-3.06**	-0.87	6	22
Cyt	CAETHG_0117	D-lactate dehydrogenase (Cytochrome) (EC 1.1.2.4)	-1.36	**-6.06**	**-4.70**	10	44
Cyt	CAETHG_0244	D-lactate dehydrogenase (Cytochrome) (EC 1.1.2.4)	1.31	**3.25**	1.93	11	22.8
Cyt	CAETHG_0245	Electron transfer flavoprotein alpha/beta-subunit	0.33	**4.14**	**3.82**	6	26.9
Cyt	CAETHG_0246	Electron transfer flavoprotein alpha/beta-subunit	-0.74	**3.10**	**3.84**	4	15.3
Cyt	CAETHG_0247	Uncharacterized protein	0.67	**4.31**	**3.64**	9	24.5
Mem	CAETHG_3227	Electron transport complex subunit C	1.24	**2.03**	0.79	38	84.2
Mem	CAETHG_3228	Electron transport complex subunit D	**2.61**	**2.69**	0.07	7	29
Mem	CAETHG_3229	Electron transport complex subunit G	1.81	**2.27**	0.46	13	65.9
Mem	CAETHG_3230	Electron transport complex subunit E	**2.31**	1.60	-0.71	2	3.8
Mem	CAETHG_3232	Electron transport complex subunit B (Electron transport complex, RnfABCDGE type, B subunit)	1.73	**2.35**	0.62	21	76.4

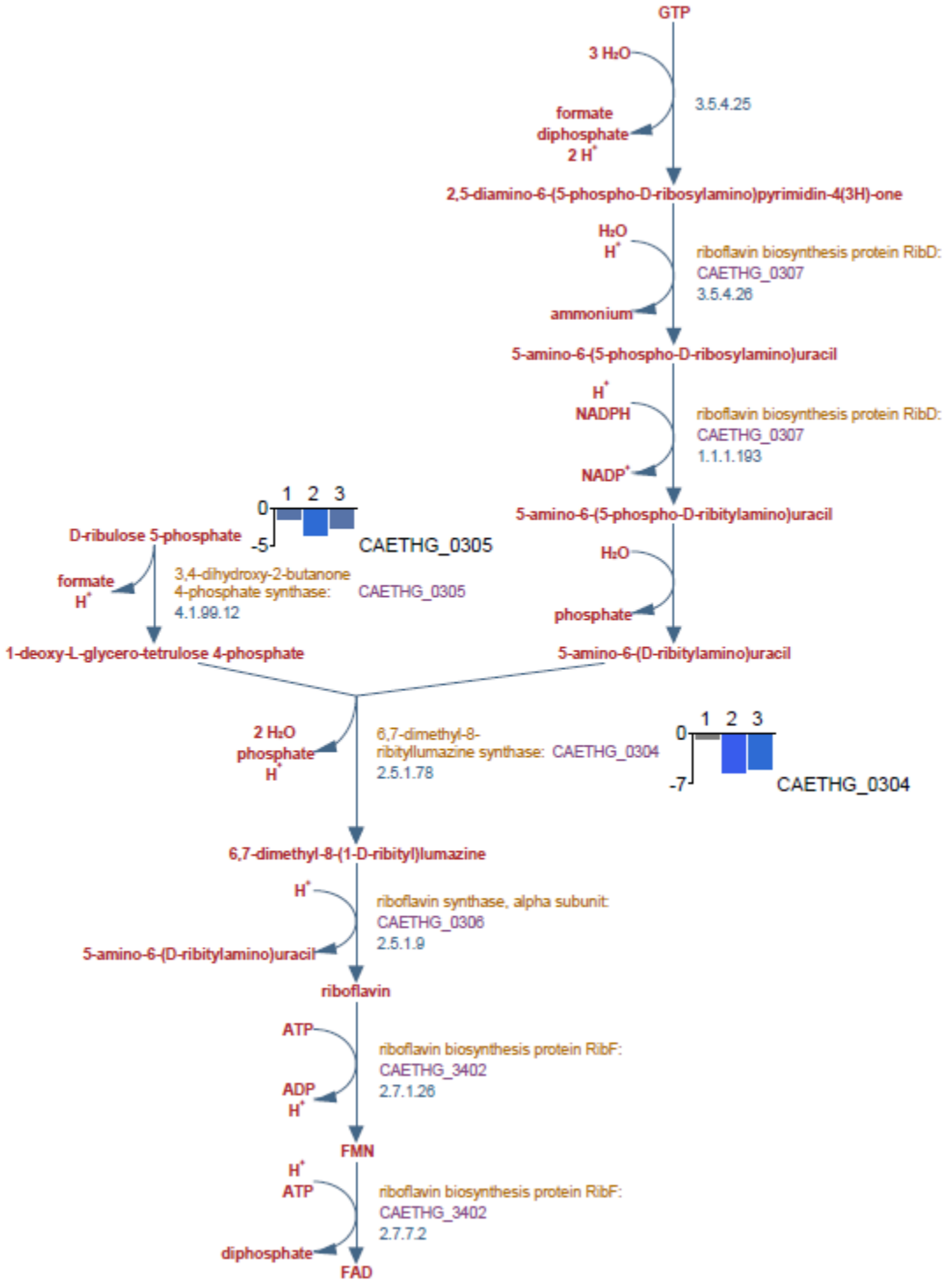

Figure 4.10. Energy metabolism in *C. autoethanogenum*: Flavin biosynthesis. Bar graph labels represent the fold difference between 1) xylose-syngas versus xylose, 2) syngas versus xylose, and 3) syngas versus xylose-syngas treatments.

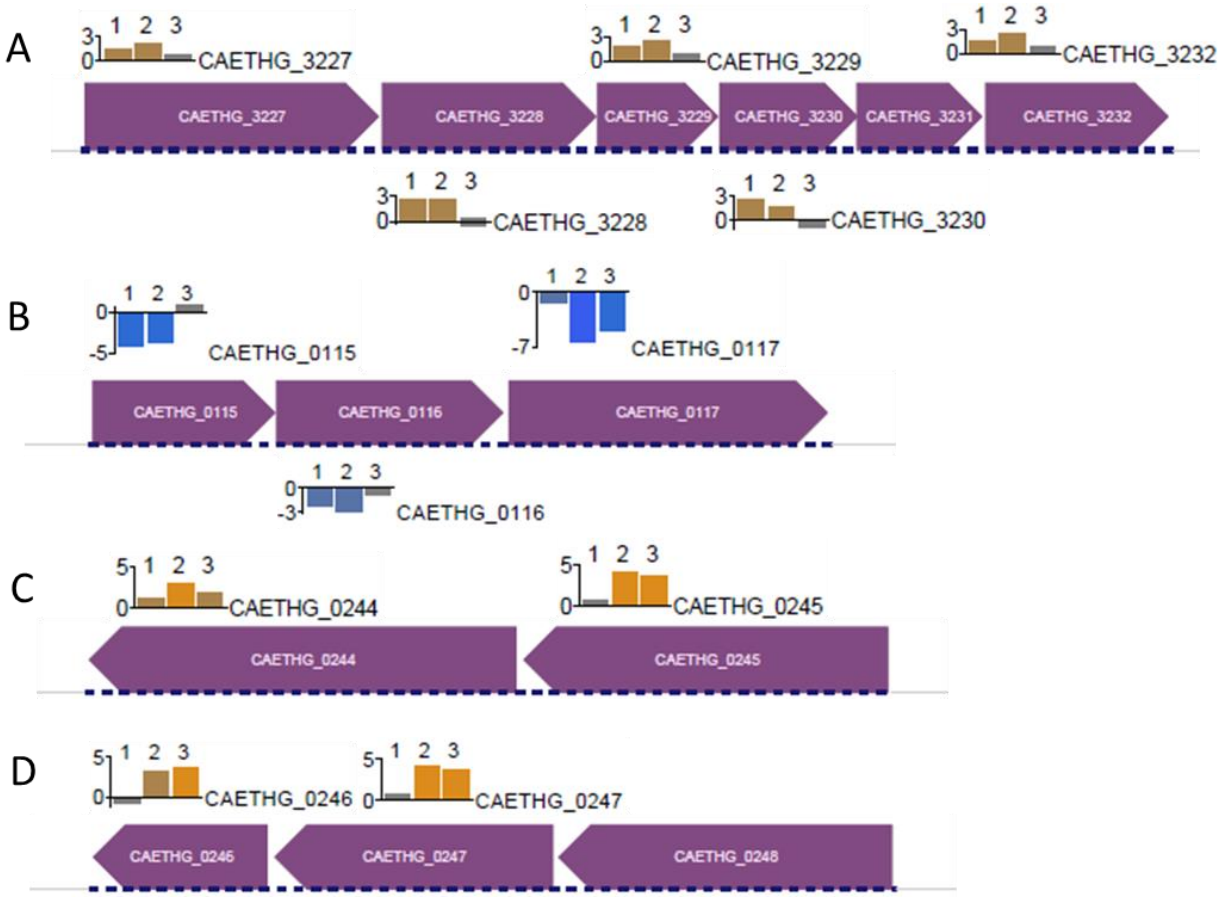

Figure 4.11. Energy metabolism in *C. autoethanogenum*: a) Transcription unit for electron transport complex, RnfABCDGE type; B, C, D) Transcription units for electron transfer flavoproteins. Bar graph labels represent the fold difference between 1) xylose-syngas versus xylose, 2) syngas versus xylose, and 3) syngas versus xylose-syngas treatments.

Table 4.4. Additional cytoplasmic proteins with notably high fold differences expressed by *C. autoethanogenum* during xylose (XYL), xylose-syngas (MIX), or syngas (SYN) carbon source treatments. Significant results (t-test, α=0.05) with a fold difference (log2 fold change) greater than two are in bold.

Pathway	Gene	Protein	Fold Difference			Peptides	Sequence Coverage
			log2 FC =B-A A=XYL, B=MIX	log2 FC =C-A A=XYL, C=SYN	log2 FC =C-B B=MIX, C=SYN		(%)
Amino Acid Biosynthesis and Degradation							
	CAETHG_2210	Alanine--glyoxylate transaminase (Alanine-glyoxylate transaminase) (EC 2.6.1.44)	-0.87	**-8.49**	**-7.62**	34	78.9
	CAETHG_2211	Phosphoglycerate dehydrogenase (EC 1.1.1.95)	-0.87	**-8.67**	**-7.79**	20	61.4
	CAETHG_2212	Putative conserved protein UCP033563	-0.56	**-9.32**	**-8.75**	11	59.4
Other							
	CAETHG_0817	Glucarate dehydratase (EC 4.2.1.40)	0.35	**-8.01**	**-8.36**	17	46.4
	CAETHG_0821	Aldo/keto reductase / Methylglyoxal reductase (NADPH-dependent) (Methylglyoxal reductase (NADPH-dependent)) (EC 1.1.1.283)	0.25	**-6.04**	**-6.29**	20	61.7
	CAETHG_1979	Translation elongation factor G	-1.79	**5.35**	**7.14**	21	38.3

REFERENCES

Abrini, J., Naveau, H., and Nyns, E.J. (1994). *Clostridium autoethanogenum*, sp. nov., an anaerobic bacterium that produces ethanol from carbon monoxide. Arch. Microbiol. *161*, 345–351.

Abubackar, H.N., Veiga, M.C., and Kennes, C. (2015). Carbon monoxide fermentation to ethanol by *Clostridium autoethanogenum* in a bioreactor with no accumulation of acetic acid. Bioresour. Technol. *186*, 122–127.

Abubackar, H.N., Fernández-Naveira, Á., Veiga, M.C., and Kennes, C. (2016). Impact of cyclic pH shifts on carbon monoxide fermentation to ethanol by *Clostridium autoethanogenum*. Fuel *178*, 56–62.

Allegretti, M., Klusch, N., Mills, D.J., Vonck, J., Kühlbrandt, W., and Davies, K.M. (2015). Horizontal membrane-intrinsic α-helices in the stator a-subunit of an F-type ATP synthase. Nature *521*, 237-240.

Bacher, A., Eberhardt, S., Eisenreich, W., Fischer, M., Herz, S., Illarionov, B., Kis, K., and Richter, G. (2001). Biosynthesis of riboflavin. In Vitamins & Hormones, (Academic Press), pp. 1–49.

Bruno-Barcena, J.M., Chinn, M.S., and Grunden, A.M. (2013). Genome Sequence of the Autotrophic Acetogen *Clostridium autoethanogenum* JA1-1 Strain DSM 10061, a Producer of Ethanol from Carbon Monoxide. Genome Announc. *1*, e00628-13.

Caspi, R., Billington, R., Ferrer, L., Foerster, H., Fulcher, C.A., Keseler, I.M., Kothari, A., Krummenacker, M., Latendresse, M., Mueller, L.A., et al. (2016). The MetaCyc database of metabolic pathways and enzymes and the BioCyc collection of pathway/genome databases. Nucleic Acids Res. *44*, D471–D480.

Clifton, M.C., Simon, M.J., Erramilli, S.K., Zhang, H., Zaitseva, J., Hermodson, M.A., and Stauffacher, C.V. (2015). In Vitro Reassembly of the Ribose ATP-binding Cassette Transporter Reveals a Distinct Set of Transport Complexes. J. Biol. Chem. *290*, 5555–5565.

Cotter, J.L., Chinn, M.S., and Grunden, A.M. (2008). Ethanol and acetate production by *Clostridium ljungdahlii* and *Clostridium autoethanogenum* using resting cells. Bioprocess Biosyst. Eng. *32*, 369–380.

Cotter, J.L., Chinn, M.S., and Grunden, A.M. (2009). Influence of process parameters on growth of *Clostridium ljungdahlii* and *Clostridium autoethanogenum* on synthesis gas. Enzyme Microb. Technol. *44*, 281–288.

Dale, J.M., Popescu, L., and Karp, P.D. (2010). Machine learning methods for metabolic pathway prediction. BMC Bioinformatics *11*, 15–15.

Darnault, C., Volbeda, A., Kim, E.J., Legrand, P., Vernède, X., Lindahl, P.A., and Fontecilla-Camps, J.C. (2003). Ni-Zn-[Fe_4-S_4] and Ni-Ni-[Fe_4-S_4] clusters in closed and open α subunits of acetyl-CoA synthase/carbon monoxide dehydrogenase. Nat. Struct. Mol. Biol. *10*, 271-279.

Guo, Y., Xu, J., Zhang, Y., Xu, H., Yuan, Z., and Li, D. (2010). Medium optimization for ethanol production with *Clostridium autoethanogenum* with carbon monoxide as sole carbon source. Bioresour. Technol. *101*, 8784-8789

Kanehisa, M., Furumichi, M., Tanabe, M., Sato, Y., and Morishima, K. (2017). KEGG: new perspectives on genomes, pathways, diseases and drugs. Nucleic Acids Res. *45*, D353–D361.

Kanehisa Laboratories (2018). KEGG GENOME: Clostridium autoethanogenum. https://www.kegg.jp/kegg-bin/show_organism?org=T02883.

Karp, P.D., and Paley, S. (1995). Automated drawing of metabolic pathways. Proceedings of the 3rd International Conference on Bioinformatics and Genome Research. pp. 225–238.

Karp, P.D., Paley, S., and Romero, P. (2002). The Pathway Tools software. Bioinformatics *18*, S225–S232.

Karp, P.D., Billington, R., Holland, T.A., Kothari, A., Krummenacker, M., Weaver, D., Latendresse, M., and Paley, S. (2015). Computational Metabolomics Operations at BioCyc.org. Metabolites *5*, 291–310.

Karp, P.D., Latendresse, M., Paley, S.M., Krummenacker, M., Ong, Q.D., Billington, R., Kothari, A., Weaver, D., Lee, T., Subhraveti, P., et al. (2016). Pathway Tools version 19.0 update: software for pathway/genome informatics and systems biology. Brief. Bioinform. *17*, 877–890.

Li, J., Attila, C., Wang, L., Wood, T.K., Valdes, J.J., and Bentley, W.E. (2007). Quorum Sensing in *Escherichia coli* Is Signaled by AI-2/LsrR: Effects on Small RNA and Biofilm Architecture. J. Bacteriol. *189*, 6011–6020.

Marcellin, E., Behrendorff, J.B., Nagaraju, S., DeTissera, S., Segovia, S., Palfreyman, R.W., Daniell, J., Licona-Cassani, C., Quek, L., Speight, R., et al. (2016). Low carbon fuels and commodity chemicals from waste gases – systematic approach to understand energy metabolism in a model acetogen. Green Chem. *18*, 3020-3028.

Marques, J.C., Oh, I.K., Ly, D.C., Lamosa, P., Ventura, M.R., Miller, S.T., and Xavier, K.B. (2014). LsrF, a coenzyme A-dependent thiolase, catalyzes the terminal step in processing the quorum sensing signal autoinducer-2. Proc. Natl. Acad. Sci. *111*, 14235–14240.

Mbeunkui, F., and Goshe, M.B. (2011). Investigation of solubilization and digestion methods for microsomal membrane proteome analysis using data-independent LC-MSE. Proteomics *11*, 898–911.

Mitra, S.K., and Goshe, M.B. (2009). Cysteinyl-Tagging of Integral Membrane Proteins for Proteomic Analysis Using Liquid Chromatography-Tandem Mass Spectrometry. In Membrane Proteomics, (Humana Press), pp. 311–326.

Mock, J., Zheng, Y., Mueller, A.P., Ly, S., Tran, L., Segovia, S., Nagaraju, S., Köpke, M., Dürre, P., and Thauer, R.K. (2015). Energy Conservation Associated with Ethanol Formation from H_2 and CO_2 in *Clostridium autoethanogenum* Involving Electron Bifurcation. J. Bacteriol. *197*, 2965–2980.

National Center for Biotechnology Information (2018). Home - Gene - NCBI. https://www.ncbi.nlm.nih.gov/gene.

Norman, R.O.J., Millat, T., Winzer, K., Minton, N.P., and Hodgman, C. (2018). Progress towards platform chemical production using *Clostridium autoethanogenum*. Biochem. Soc. Trans. BST20170259.

Paley, S.M., and Karp, P.D. (2006). The Pathway Tools cellular overview diagram and Omics Viewer. Nucleic Acids Res. *34*, 3771–3778.

Sandoval-Espinola, W.J., Makwana, S.T., Chinn, M.S., Thon, M.R., Azcárate-Peril, M.A., and Bruno-Bárcena, J.M. (2013). Comparative phenotypic analysis and genome sequence of *Clostridium beijerinckii* SA-1, an offspring of NCIMB 8052. Microbiology *159*, 2558–2570.

Savelsbergh, A., Katunin, V.I., Mohr, D., Peske, F., Rodnina, M.V., and Wintermeyer, W. (2003). An Elongation Factor G-Induced Ribosome Rearrangement Precedes tRNA-mRNA Translocation. Mol. Cell *11*, 1517–1523.

Slivka, R.M., Chinn, M.S., and Grunden, A.M. (2011). Gasification and synthesis gas fermentation: an alternative route to biofuel production. Biofuels *2*, 405–419.

The UniProt Consortium (2017). UniProt: the universal protein knowledgebase. Nucleic Acids Res. *45*, D158–D169.

Wang, S., Huang, H., Kahnt, J., Mueller, A.P., Köpke, M., and Thauer, R.K. (2013). NADP-Specific Electron-Bifurcating [FeFe]-Hydrogenase in a Functional Complex with Formate Dehydrogenase in *Clostridium autoethanogenum* Grown on CO. J. Bacteriol. *195*, 4373–4386.

White, D. (2007). The Physiology and Biochemistry of Prokaryotes (New York: Oxford University Press).

Xavier, K.B., Miller, S.T., Lu, W., Kim, J.H., Rabinowitz, J., Pelczer, I., Semmelhack, M.F., and Bassler, B.L. (2007). Phosphorylation and Processing of the Quorum-Sensing Molecule Autoinducer-2 in Enteric Bacteria. ACS Chem. Biol. *2*, 128–136.

Zhu, J., Hixon, M.S., Globisch, D., Kaufmann, G.F., and Janda, K.D. (2013). Mechanistic Insights into the LsrK Kinase Required for Autoinducer-2 Quorum Sensing Activation. J. Am. Chem. Soc. *135*, 7827–7830.

APPENDICES

Appendix A

Stability of the cell membrane

After ruling out additional growth factors and trace elements as the limiting factor impacting *C. autoethanogenum* cells (Chapter 3), attention was turned to the stability of the cell membrane and deficiencies that may exist. One trait that is critical to proper proton transfer and membrane maintenance is the availability of divalent cations, specifically Ca^{2+} and Mg^{2+}. Since the DSMZ 640 basal medium used for *C. autoethanogenum* growth contains no Ca^{2+} and a sufficient quantity of Mg^{2+} at 1.97 mM (ideally these ions should be supplied to the cell at concentrations of at least 500 μM [Neidhardt et al., 1974]), the impact of 1 mM Ca^{2+} on cell function was evaluated. Compared to the control treatment with no Ca^{2+}, the presence of this divalent cation did not appear to have a significant effect on cellular metabolism as shown in Table A.1. However, when the intermittent addition of base (0.2M NaOH) was used to adjust the pH mid-growth and neutralize some of the acid present in the culture broth, it proved to circumvent the eventual decay of culture pH to toxic conditions ($pH \leq 4.0$) for a brief period and allow the cells to display both enhanced metabolism and a delay in cell death. As Table A.1 indicates, the intermittent pH adjustment of the culture with 0.2M NaOH significantly improved biomass production, xylose utilization, and end product generation. Specifically, xylose utilization by the cells increased from 3.3 g/L consumed with the control up to full consumption of the initial 5 g/L xylose for those cultures treated with pH adjustment.

Table A.1. Evaluation of factors impacting the *C. autoethanogenum* cell membrane. Superscripts indicate statistical differences between the treatments over time ($\alpha = 0.05$).

Treatment	Initial Xylose Concentration	Maximum Values Observed			
		Dry Cell Concentration	Xylose Consumed	Acetate Produced	Ethanol Produced
	g/L	dry mg/L	g/L	g/L	g/L
Control	5	401.11 [a]	3.29 [a]	2.95 [a]	0.2 [a]
1mM Ca^{2+}	5	390.22 [a]	3.27 [a]	2.94 [a]	0.206 [a]
pH Adjustment with 0.2M NaOH	5	441.63 [b]	5.16 [b]	3.27 [b]	0.233 [b]
1mM Ca^{2+} & pH Adjustment	5	422.89 [b]	5.07 [b]	3.16 [b]	0.24 [c]

*Superscripts a, b, and c are repeated for the response variable in each column.

REFERENCE

Neidhardt, F.C., Bloch, P.L., and Smith, D.F. (1974). Culture Medium for Enterobacteria. J. Bacteriol. *119*, 736–747.

Appendix B

A scaled lesson with pH

In an attempt to maintain a controlled pH environment for *C. autoethanogenum*, the organism was grown in 1.5 L fermenters with automatic pH control (New Brunswick Scientific BIOFLO 110, 3L vessel) which utilized initial sugar concentrations ranging from 5 to 30 g/L with either no pH control (5 g/L concentration only) or pH controlled at 5.0 via automated 3M KOH addition. Per good statistical methodology, the study aimed for at least three replicates for each treatment. However, given that only one fermenter unit was available for use and growth runs lasted two weeks, each replicate had to be grown separately with attempts made to maintain and use each batch of source inoculum that was grown up from frozen stock at least twice if possible. Although *C. autoethanogenum* cultures grown in serum bottles could produce highly precise results with at times small standard deviation, culture replicates grown at the larger fermenter scale yielded non-repeatable results beyond an elapsed fermentation time of 48 hours which indicated that there was a separate limiting issue at hand. Figure B.1 shows the extent of growth variability witnessed in 1.5 L fermentations with an initial xylose concentration of 10 g/L. This non-repeatability among replicates was witnessed for all treatments tested, and was not related to the pH control system as even the treatment with no pH control implemented showed maximum culture concentrations ranging from 126-317 mg dry cells/L on the low end to greater than 634 mg dry cells/L on the high end (Table B.1). Tunable fermenter parameters (100 rpm agitation, 10 mL/min N_2 gas sparging) may not have been optimal for *C. autoethanogenum* growth but they were consistent enough with other fermenter studies (ex. *C. ljungdahlii*) to be acceptable for the purpose of the study. Based on the results witnessed for intermittent, manual pH adjustment to 5.0 or 5.8 as a target in serum bottles (Chapter 3), the variability between

replicates could be connected to the pH control target used with the fermenter, especially if it compromised the ability of the cells to effectively control their internal pH relative to the external pH. Although the pH control setpoint was programmed at 5.0, the use of a 0.05 pH deadband for system response actually maintained the culture pH at 4.95. This slightly closer proximity to the acetate-acetic acid dissociation could have unintentionally created an environmental condition where it was harder to attain repeatable internal pH control of the cells from replicate to replicate due to the fastidious nature of *C. autoethanogenum*. However, the treatment with no pH control implemented was just as variant as the treatments with a pH control target, so the root cause of non-repeatability between replicates may just be that the required use of different inoculum for each replicate magnified the subtle differences between each seed culture set.

A second pH study was conducted in 250 mL modified spinner flasks to evaluate changes on a scale larger than serum bottles but with greater simultaneous replication than a single fermenter and also to address potential issues with system configuration. Since these reactors did not possess automatic pH measurement or base addition, all pH measurements were performed on collected samples and pH adjustments were made manually every 16 hours. The 250 mL flasks utilized incremented sugar addition with 2.5 g/L xylose doses added every 32 hours and manual adjustment to pH 5.0 with 3M KOH. Both batch and continuously sparging (10 mL/min) headspaces of inert, nitrogen were trialed. The batch headspace conditions led to higher culture densities for those replicates which showed healthy growth over 317 mg dry cells/L (1.0 OD). Figure B.2 presents the growth profiles for these runs. The biggest takeaway was that the batch headspace cultures appeared to display better energetics than the continuous headspace cultures. As mentioned in the Results and Discussion section of Chapter 3, it was

hypothesized that the batch headspace cultures may have utilized produced CO_2 for its buffering capacity and as a substrate in the Wood-Ljungdahl pathway. The continuous headspace cultures would not have been able to take advantage of the produced CO_2 as the continuous sparging and open exhaust vent probably swept the gas out of the reactors. Another takeaway was that the condition of the flasks used as reactors for this study may have impacted the results. If the cultures grew to concentrations greater than 317 mg dry cells/L, the results were repeatable enough to draw preliminary conclusions; however, 75% of the inoculated flasks either never grew or only showed mediocre growth (<317 mg dry cells/L) as shown in Table B.1. Some of the flasks may have had poorly sealing gaskets due to age and repeated use which prevented them from being gas-tight and thus oxygen was allowed into the system and killed the cells. All flasks were checked for leaks prior to use, but the expansion and contraction that occurred during autoclave sterilization could have caused some seals to fail. As a result of the issues with the flasks, further pH work with *C. autoethanogenum* was scaled back down to the serum bottle level as it was the only method to guarantee quality, precise results. Yet, knowledge and techniques learned during the flask study, as well as the fermenter study, were highly valuable for continued work with the organism.

Table B.1. Summary of culture performance in larger reactors.

Culture Performance	250 mL Flask				1.5 L Fermenter			
mg dry cells/L	Batch Headspace		Continuous Headspace		No pH Control		pH Control	
	# Reps	Percent	# Reps	Percent	# Reps	Percent	# Reps	Percent
Super: > 634 mg/L >2.0 OD	4	25.0%	0	0.0%	1	20.0%	2	22.2%
Good: 317-634 mg/L 1.0-2.0 OD	0	0.0%	3	18.8%	1	20.0%	2	22.2%
Mediocre: 126-317 mg/L 0.4-1.0 OD	4	25.0%	8	50.0%	3	60.0%	5	55.6%
Poor or No Growth	8	50.0%	5	31.3%	0	0.0%	0	0.0%
Total	16	100.0%	16	100.0%	5	100.0%	9	100.0%

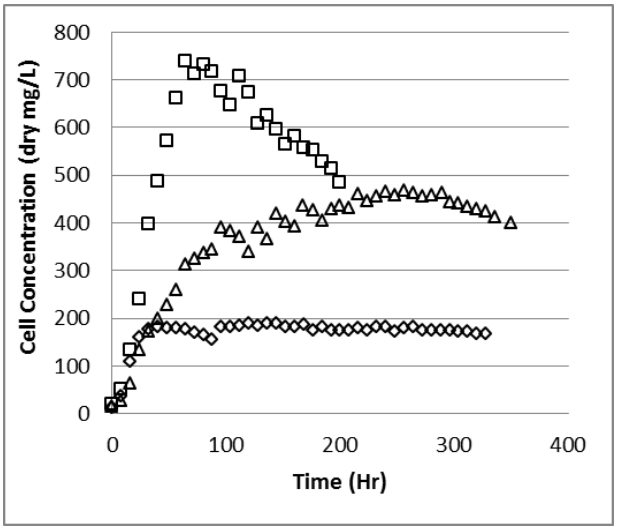

Figure B.1. Variable *C. autoethanogenum* growth in a 1.5 L fermenter with 10 g/L initial xylose and pH controlled at 5 via 3M KOH.

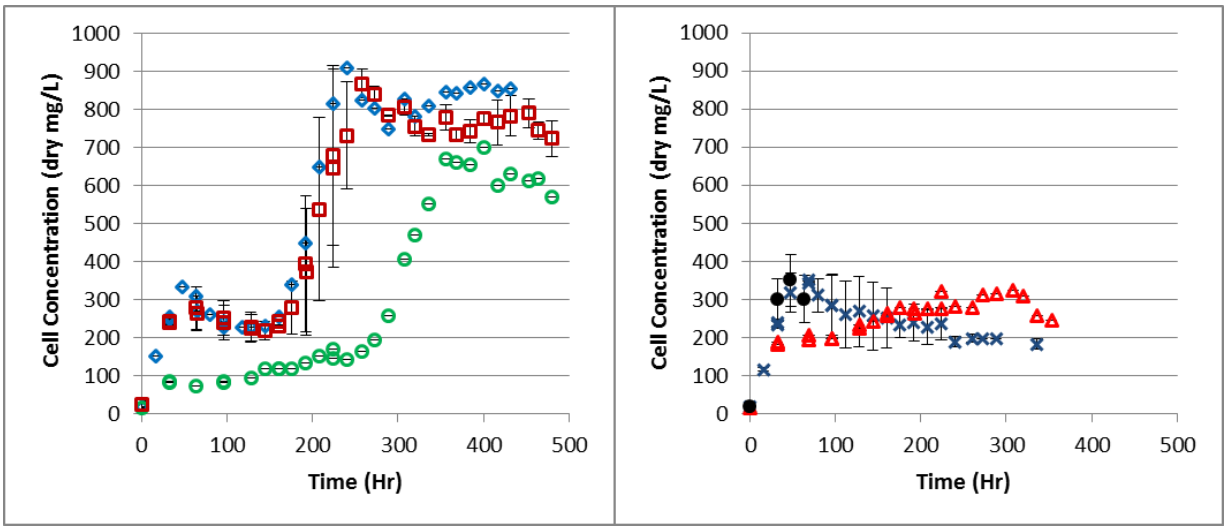

Figure B.2. Difference in *C. autoethanogenum* growth between A) batch and B) continuous (10 mL/min) headspace N_2 in a 250 mL modified spinner flask dosed incrementally by 2.5 g/L to the equivalent of 10 g/L or 20 g/L initial xylose and pH adjusted to 5 via 3M KOH every 16 hours. Note: cultures which achieved less than 317 mg dry cells/L in either headspace are not shown. Diamond: batch gas with 10 g/L, open circle: batch gas with 10 g/L and lag, square: batch gas with 20 g/L, X; continuous gas with 10 g/L, triangle: continuous gas with 20 g/L, solid circle: growth control with no pH adjustment.

Appendix C

Additional proteomic data

Table C.1. Cytoplasmic heme, nucleotide/nucleoside, and amino acid biosynthesis proteins differentially expressed by *C. autoethanogenum* during xylose (XYL), xylose-syngas (MIX), or syngas (SYN) carbon source treatments. Significant results (t-test, α=0.05) with a fold difference (log2 fold change) greater than two are in bold.

Pathway	Gene	Protein	Fold Difference			Peptides	Sequence Coverage
			log2 FC =B-A A=XYL, B=MIX	log2 FC =C-A A=XYL, C=SYN	log2 FC =C-B B=MIX, C=SYN		(%)
Heme Biosynthesis							
	CAETHG_0141	Uroporphyrinogen decarboxylase (URO-D)	-0.16	**2.73**	**2.89**	3	10.8
	CAETHG_0192	Uroporphyrinogen decarboxylase (URO-D) (EC 4.1.1.37)	0.36	-1.87	**-2.23**	12	38.8
	CAETHG_0197	Uroporphyrinogen decarboxylase (URO-D) (EC 4.1.1.37)	1.40	**-3.51**	**-4.91**	4	17.5
	CAETHG_0786	Radical SAM domain protein	1.20	-1.36	**-2.55**	17	41.3
	CAETHG_2300	Radical SAM domain protein	0.35	-1.89	**-2.25**	11	29.3
	CAETHG_2845	Uroporphyrinogen decarboxylase (URO-D)	**2.51**	1.45	-1.06	8	39.7
	CAETHG_2850	Uroporphyrinogen decarboxylase (URO-D)	**3.15**	**2.19**	-0.96	4	20.6
Nucleotide / Nuceloside Biosynthesis and Degradation							
	CAETHG_0456	Molybdopterin-family oxidoreductase molybdopterin binding subunit (Xanthine dehydrogenase) (EC 1.17.1.4)	1.06	**3.88**	**2.82**	16	37.1
	pyrE CAETHG_1476	Orotate phosphoribosyltransferase (OPRT) (OPRTase) (EC 2.4.2.10)	-1.32	**-5.36**	**-4.04**	12	58.9
	pyrF CAETHG_1479	Orotidine 5'-phosphate decarboxylase (EC 4.1.1.23) (OMP decarboxylase)	-0.94	**-4.72**	**-3.78**	7	32.5
	CAETHG_1480	Aspartate carbamoyltransferase regulatory subunit	-1.49	**-5.20**	**-3.71**	5	26.9
	purA CAETHG_2059	Adenylosuccinate synthetase (AMPSase) (AdSS) (EC 6.3.4.4) (IMP--aspartate ligase)	0.65	-1.56	**-2.22**	26	56.8
	CAETHG_2775	Ribonucleoside-diphosphate reductase, adenosylcobalamin-dependent (Ribonucleotide reductase) (EC 1.17.4.1)	**2.11**	-0.97	**-3.08**	11	15

Table C.1. (continued).

	purC CAETHG_2949	Phosphoribosylaminoimidazole-succinocarboxamide synthase (EC 6.3.2.6) (SAICAR synthetase)	0.70	**-2.37**	**-3.07**	13	45.5
	purM CAETHG_2951	Phosphoribosylformylglycinamidine cyclo-ligase (EC 6.3.3.1) (AIR synthase) (AIRS) (Phosphoribosyl-aminoimidazole synthetase)	0.87	-1.91	**-2.78**	11	30.2
	purH CAETHG_2953	Bifunctional purine biosynthesis protein PurH	1.53	-1.03	**-2.56**	23	48.3
	purD CAETHG_2954	Phosphoribosylamine--glycine ligase (EC 6.3.4.13) (GARS) (Glycinamide ribonucleotide synthetase) (Phosphoribosylglycinamide synthetase)	1.24	-1.67	**-2.91**	15	40
	CAETHG_3245	Phosphoribosylformylglycinamidine synthase (EC 6.3.5.3)	1.24	**-3.84**	**-5.08**	35	31.9
Amino Acid	**Biosynthesis and Degradation**						
	CAETHG_0213	Putative transcriptional regulator GntR family (Putative transcriptional regulator, GntR family) (EC 2.6.1.57)	-1.00	**-4.07**	**-3.07**	21	69
	CAETHG_0215	Aspartate transaminase (EC 2.6.1.1)	-0.83	**-2.15**	-1.31	26	62.6
	hutH CAETHG_0232	Histidine ammonia-lyase (Histidase) (EC 4.3.1.3)	0.29	**2.28**	1.99	19	37.3
	hutI CAETHG_0233	Imidazolonepropionase (EC 3.5.2.7) (Imidazolone-5-propionate hydrolase)	0.16	**3.52**	**3.36**	13	38.4
	hutU CAETHG_0234	Urocanate hydratase (Urocanase) (EC 4.2.1.49) (Imidazolonepropionate hydrolase)	0.01	**2.72**	**2.71**	28	46.1
	argJ CAETHG_0240	Arginine biosynthesis bifunctional protein ArgJ	0.82	-1.89	**-2.71**	3	10.6
	CAETHG_0406	Acetolactate synthase (EC 2.2.1.6)	-1.11	**-5.45**	**-4.34**	16	34.6
	CAETHG_0449	Carbamoyltransferase YgeW (EC 2.1.3.3)	1.49	**2.44**	0.95	14	47.2
	CAETHG_0477	Glutamate synthase (NADPH) (EC 1.4.1.13) (Pyridine nucleotide-disulfide oxidoreductase class-II)	**2.77**	-1.09	**-3.86**	17	48.8
	CAETHG_0478	3-isopropylmalate dehydratase (EC 4.2.1.33) (Aconitase/isopropylmalate dehydratase family) (EC 4.2.1.-)	**2.98**	-0.23	**-3.21**	5	10.9
	CAETHG_0823	Dihydrodipicolinate synthase (EC 4.3.3.7)	0.81	**-3.80**	**-4.62**	13	56
	proC CAETHG_1593	Pyrroline-5-carboxylate reductase (P5C reductase) (P5CR) (EC 1.5.1.2) (PCA reductase)	1.06	-1.39	**-2.45**	5	26.7

Table C.1. (continued).

	pdxS CAETHG_1804	Pyridoxal 5'-phosphate synthase subunit PdxS (PLP synthase subunit PdxS) (EC 4.3.3.6) (Pdx1)	0.47	**-4.72**	**-5.19**	14	54
	pdxT CAETHG_1805	Pyridoxal 5'-phosphate synthase subunit PdxT (EC 4.3.3.6) (Pdx2) (Pyridoxal 5'-phosphate synthase glutaminase subunit)	-0.02	**-4.32**	**-4.29**	2	10.1
	murC CAETHG_2010	UDP-N-acetylmuramate--L-alanine ligase (EC 6.3.2.8) (UDP-N-acetylmuramoyl-L-alanine synthetase)	0.70	**-4.80**	**-5.50**	5	13.6
	CAETHG_2024	Glutamine synthetase catalytic region	0.09	**-2.01**	**-2.09**	34	46.5
	CAETHG_2210	Alanine--glyoxylate transaminase (Alanine-glyoxylate transaminase) (EC 2.6.1.44)	-0.87	**-8.49**	**-7.62**	34	78.9
	CAETHG_2211	Phosphoglycerate dehydrogenase (EC 1.1.1.95)	-0.87	**-8.67**	**-7.79**	20	61.4
	CAETHG_2212	Putative conserved protein UCP033563	-0.56	**-9.32**	**-8.75**	11	59.4
	carB CAETHG_2510	Carbamoyl-phosphate synthase (glutamine-hydrolyzing) (EC 6.3.5.5)	-0.40	**-5.71**	**-5.31**	20	24.5
	CAETHG_2511	Amidohydrolase (EC 3.5.1.47)	0.74	**-2.10**	**-2.84**	4	16.2
	proB CAETHG_2697	Glutamate 5-kinase (EC 2.7.2.11) (Gamma-glutamyl kinase)	-0.39	**-2.23**	-1.84	2	11.7
	CAETHG_3247	L-threonine 3-dehydrogenase (EC 1.1.1.103) (Zinc-containing alcohol dehydrogenase)	**2.02**	**3.35**	1.33	2	12.6
	CAETHG_3249	Phosphoglycerate dehydrogenase (EC 1.1.1.95)	1.69	**4.43**	**2.74**	8	31.5
	CAETHG_3850	Glutamate synthase (Ferredoxin) (EC 1.4.7.1)	**-2.32**	**-3.50**	-1.17	24	21.7
	CAETHG_3851	Glutamate synthase NADH/NADPH small subunit (Glutamate synthase, NADH/NADPH, small subunit) (EC 1.4.1.14)	**-2.90**	**-2.52**	0.38	5	17
Other							
	CAETHG_0118	2-dehydropantoate 2-reductase (EC 1.1.1.169) (Ketopantoate reductase)	**-2.04**	**-3.49**	-1.45	3	9.9
	CAETHG_0738	Glycerol dehydrogenase (EC 1.1.1.6)	0.68	**-5.28**	**-5.96**	17	46.6
	hcp CAETHG_0812	Hydroxylamine reductase (EC 1.7.99.1) (Hybrid-cluster protein) (Prismane protein)	**-3.57**	1.12	**4.69**	17	37.7

Table C.2. Remaining proteins from the experimental data (not included in other tables) with significant expression by *C. autoethanogenum* during xylose (XYL), xylose-syngas (MIX), or syngas (SYN) carbon source treatments. Significant results (t-test, α=0.05) with a fold difference (log2 fold change) greater than two are in bold.

Pathway	Gene	Protein	Location	Fold Difference			Peptides	Sequence Coverage
				log2 FC =B-A	log2 FC =C-A	log2 FC =C-B		
				A=XYL, B=MIX	A=XYL, C=SYN	B=MIX, C=SYN		(%)
Carbon Metabolism								
	CAETHG_1899	Citrate lyase alpha subunit (Citrate lyase, alpha subunit) (EC 2.8.3.10)	Cytoplasm	0.75	**2.42**	1.68	12	30.6
	CAETHG_0480	Sorbitol operon regulator (Transcriptional regulator, DeoR family)	Cytoplasm	-0.20	**-2.30**	**-2.10**	2	8.9
Transport, Membrane Component, Signaling								
	CAETHG_1639	Putative secreted protein (Uncharacterized protein)	Cytoplasm	**3.84**	**2.38**	-1.46	2	11.2
	CAETHG_3898	Amino acid permease-associated region (Putative integral membrane protein)	Membrane	1.24	**-2.20**	**-3.45**	1	2.6
	mltG CAETHG_1284	Aminodeoxychorismate lyase (Uncharacterized protein)	Membrane	-0.62	**-3.36**	**-2.75**	3	11.4
	CAETHG_2784	Band 7 protein	Membrane	0.17	**-2.11**	**-2.28**	14	55.8
	CAETHG_2979	Beta-lactamase	Membrane	1.85	-1.02	**-2.87**	3	7.4
	CAETHG_2576	Cell wall binding repeat 2-containing protein	Membrane	**4.24**	1.24	**-3.00**	17	24
	CAETHG_2558	Cell wall binding repeat 2-containing protein	Membrane	1.78	-0.66	**-2.44**	38	39.4
	CAETHG_3917	Efflux transporter RND family MFP subunit (Efflux transporter, RND family, MFP subunit)	Membrane	**2.39**	-0.29	**-2.69**	14	42.4
	CAETHG_1778	Ig domain protein	Membrane	**2.43**	-0.14	**-2.57**	5	15.8
	CAETHG_2681	Ig domain protein	Membrane	**3.26**	-0.14	**-3.40**	3	8.3
	CAETHG_0672	Ig domain protein group 2 domain protein (Putative secreted protein containing bacterial Ig-like domain)	Membrane	-1.85	0.87	**2.72**	13	12
	CAETHG_2256	NLP/P60 protein	Membrane	1.66	-1.80	**-3.46**	3	11.5
	CAETHG_2255	NLP/P60 protein	Membrane	1.70	-0.62	**-2.32**	4	16.2
	CAETHG_2565	Peptidase M16C associated domain protein	Membrane	**2.20**	-1.38	**-3.58**	8	12.2
	CAETHG_3340	Peptidase membrane zinc metallopeptidase	Membrane	0.48	**-2.22**	**-2.69**	1	5.3
	CAETHG_0690	SNF2-related protein	Membrane	**-2.04**	**-2.68**	-0.65	5	18.5
	CAETHG_3199	Stage III sporulation protein AH-like protein	Membrane	0.17	**-4.60**	**-4.77**	9	37.1

Table C.2. (continued).

CAETHG_2644	Type IV pilin N-term methylation site GFxxxE family protein (Uncharacterized protein)	Membrane	0.42	-1.75	**-2.17**	3	32.6
CAETHG_2261	Uncharacterized protein	Membrane	0.03	**-4.18**	**-4.21**	2	18.4
CAETHG_2662	Uncharacterized protein (von Willebrand factor type A)	Membrane	-0.19	**-2.45**	**-2.26**	4	12.4
CAETHG_3883	Uncharacterized protein	Membrane	**2.01**	**-3.29**	**-5.30**	6	32.6
CAETHG_2941	Xanthine/uracil/vitamin C permease	Membrane	0.91	**-2.32**	**-3.22**	2	4.8
CAETHG_3916	Yip1 domain-containing protein	Membrane	**3.60**	1.01	**-2.59**	1	4.4
Cell Cycle, Stress, Sporulation							
CAETHG_2095	Heat shock protein Hsp20	Cytoplasm	**3.80**	**3.30**	-0.50	7	44.6
CAETHG_2094	Heat shock protein Hsp20	Cytoplasm	**4.04**	1.57	**-2.47**	5	27
CAETHG_3331	Stage IV sporulation protein A (EC 3.6.1.3) (Coat morphogenetic protein SpoIVA)	Cytoplasm	1.34	-1.89	**-3.23**	9	22.8
Redox, Electron Transport, Metal Ion Binding, Cofactors							
CAETHG_0205	2,4-dienoyl-CoA reductase (NADPH) (EC 1.3.1.34)	Cytoplasm	1.13	**2.15**	1.02	3	8.9
CAETHG_3603	2,4-dienoyl-CoA reductase (NADPH) (EC 1.3.1.34) (NADH:flavin oxidoreductase) (EC 1.6.99.1)	Cytoplasm	-1.31	**-4.13**	**-2.82**	8	18.4
CAETHG_0749	4Fe-4S ferredoxin iron-sulfur binding domain-containing protein	Cytoplasm	0.51	**-2.04**	**-2.55**	18	68.8
CAETHG_0083	4Fe-4S ferredoxin iron-sulpur binding domain-containing protein (4Fe-4S ferredoxin, iron-sulpur binding domain-containing protein)	Cytoplasm	-0.44	**2.18**	**2.62**	5	21.1
CAETHG_1059	Aldo/keto reductase (NADP-dependent oxidoreductase domain containing protein)	Cytoplasm	0.41	**-2.31**	**-2.72**	5	16.4
CAETHG_1900	Citryl-CoA lyase (EC 4.1.3.34)	Cytoplasm	1.14	**2.57**	1.43	13	53.4
CAETHG_0150	Cobalamin B12-binding domain protein	Cytoplasm	-0.52	**2.78**	**3.30**	7	32.5
CAETHG_0382	D-lactate dehydrogenase (Cytochrome) (EC 1.1.2.4) (FAD-binding oxidoreductase)	Cytoplasm	-0.61	**-2.24**	-1.63	5	17
CAETHG_2753	Isocitrate dehydrogenase (NAD(+)) (EC 1.1.1.41)	Cytoplasm	**-2.37**	**-5.06**	**-2.69**	9	24.7
CAETHG_0574	Molybdenum cofactor synthesis domain containing protein (Molybdenum cofactor synthesis domain-containing protein)	Cytoplasm	1.52	**2.67**	1.15	5	43.8

Table C.2. (continued).

	CAETHG_0454	Molybdopterin dehydrogenase FAD-binding protein (Molybdopterin-family oxidoreductase FAD-binding subunit)	Cytoplasm	1.16	**3.25**	**2.09**	3	14.3
	cobB CAETHG_2239	NAD-dependent protein deacetylase (EC 3.5.1.-) (Regulatory protein SIR2 homolog)	Cytoplasm	1.41	-1.40	**-2.81**	2	13.3
	CAETHG_0085	Nitrate reductase (EC 1.7.99.4)	Cytoplasm	-0.55	1.52	**2.06**	6	62.7
	CAETHG_0934	Nitroreductase	Cytoplasm	-0.14	**-2.34**	**-2.20**	3	12.5
	CAETHG_3628	Nitroreductase	Cytoplasm	-1.92	**2.97**	**4.90**	4	27.7
	CAETHG_3909	Nitroreductase	Cytoplasm	1.25	-1.87	**-3.12**	3	31.2
	pepT CAETHG_0008	Peptidase T (EC 3.4.11.4) (Aminotripeptidase) (Tripeptide aminopeptidase)	Cytoplasm	-1.13	**-2.43**	-1.30	9	28.9
	CAETHG_2844, CAETHG_2849	Putative cobalamin-binding protein (Uncharacterized protein)	Cytoplasm	0.14	**2.70**	**2.56**	1	5.7
	CAETHG_3907	Putative Fe-S cluster protein (Uncharacterized protein)	Cytoplasm	-0.06	**-3.20**	**-3.15**	4	12.5
	CAETHG_2060	Pyridine nucleotide-disulfide oxidoreductase FAD/NAD(P)-binding domain-containing protein (Pyridine nucleotide-disulfide oxidoreductase, FAD/NAD(P)-binding domain containing protein)	Cytoplasm	1.46	-1.39	**-2.85**	8	22.1
	CAETHG_0457	Selenium-dependent molybdenum hydroxylase 1 (Selenium-dependent molybdopterin oxidoreductase molybdopterin binding subunit)	Cytoplasm	1.07	**2.65**	1.58	10	15.3
	CAETHG_1482	CoA-substrate-specific enzyme activase (EC 1.3.7.8)	Membrane	-0.49	**-3.26**	**-2.77**	4	18.7
	CAETHG_3097	Ig domain protein (Ig domain-containing protein)	Membrane	**2.84**	-1.75	**-4.59**	32	31.1
Replication, Transcription, Translation								
	CAETHG_2401	Anti-sigma factor antagonist	Cytoplasm	0.00	**-3.36**	**-3.37**	2	28.7
	pyrD CAETHG_1477	Dihydroorotate dehydrogenase (DHOD) (DHODase) (DHOdehase) (EC 1.3.-.-)	Cytoplasm	**-2.28**	**-3.03**	-0.74	4	18.6
	glmE CAETHG_1905	Glutamate mutase epsilon subunit (EC 5.4.99.1) (Glutamate mutase E chain) (Glutamate mutase large subunit) (Methylaspartate mutase)	Cytoplasm	0.72	**2.30**	1.58	34	69.9
	glmS CAETHG_1907	Glutamate mutase sigma subunit (EC 5.4.99.1) (Glutamate mutase S chain) (Glutamate mutase small subunit) (Methylaspartate mutase)	Cytoplasm	-0.02	**2.23**	**2.26**	8	71.6
	def CAETHG_0293	Peptide deformylase (PDF) (EC 3.5.1.88) (Polypeptide deformylase)	Cytoplasm	**2.15**	-1.19	**-3.33**	1	5.8

Table C.2. (continued).

	cutC CAETHG_1829	Pyruvate formate-lyase PFL	Cytoplasm	-0.21	**2.31**	**2.52**	7	8.8
	rex CAETHG_1581	Redox-sensing transcriptional repressor Rex	Cytoplasm	-0.38	**-4.33**	**-3.95**	3	13.3
	CAETHG_1358	Single-strand binding protein (Single-strand binding protein/Primosomal replication protein n)	Cytoplasm	0.86	-1.80	**-2.66**	8	29.3
	CAETHG_0853	Small acid-soluble spore protein alpha/beta type	Cytoplasm	-1.62	**-4.35**	**-2.73**	1	15.4
	CAETHG_1908	Transcriptional regulator GntR family (Transcriptional regulator, GntR family)	Cytoplasm	1.39	**2.78**	1.39	8	28
	CAETHG_1840	Transcriptional regulator TetR family (Transcriptional regulator, TetR family)	Cytoplasm	-0.68	**-3.70**	**-3.02**	3	18.6
	CAETHG_2485	Transcriptional regulatory protein	Cytoplasm	1.72	**2.62**	0.89	1	5.6
Enzymatic Action								
	CAETHG_2751	(R)-citramalate synthase (EC 2.3.1.182)	Cytoplasm	**-2.90**	-1.68	1.22	4	10.7
	CAETHG_2752	Aconitate hydratase (EC 4.2.1.3)	Cytoplasm	-1.51	**-3.97**	**-2.46**	12	25.7
	clpP CAETHG_1192	ATP-dependent Clp protease proteolytic subunit (EC 3.4.21.92) (Endopeptidase Clp)	Cytoplasm	**2.56**	**2.58**	0.02	5	24.7
	CAETHG_1365	FolC bifunctional protein (EC 6.3.2.17)	Cytoplasm	0.42	**-2.06**	**-2.49**	3	8.9
	CAETHG_4037	Gamma-glutamyltransferase (EC 2.3.2.2)	Cytoplasm	0.68	**-2.42**	**-3.10**	7	18.9
	CAETHG_1902	Hydro-lyase Fe-S type tartrate/fumarate subfamily beta subunit (Hydro-lyase, Fe-S type, tartrate/fumarate subfamily, beta subunit) (EC 4.2.1.2)	Cytoplasm	0.89	**2.07**	1.18	11	58
	CAETHG_2267	Mannosyl-glycoprotein endo-beta-N-acetylglucosaminidase (EC 3.2.1.96)	Cytoplasm	-1.61	0.98	**2.59**	7	17.9
	CAETHG_1904	Methylaspartate ammonia-lyase (EC 4.3.1.2)	Cytoplasm	1.06	**2.44**	1.38	28	63.7
	nfo CAETHG_0108	Probable endonuclease 4 (EC 3.1.21.2) (Endodeoxyribonuclease IV) (Endonuclease IV)	Cytoplasm	0.13	**-2.27**	**-2.41**	1	4.7
	CAETHG_2503	Putative serine protein kinase, PrkA	Cytoplasm	1.95	-0.87	**-2.83**	3	5.7
	CAETHG_2224	Serine--pyruvate transaminase (EC 2.6.1.51) (Serine-pyruvate transaminase)	Cytoplasm	-0.40	**-2.52**	**-2.12**	5	17.6
	CAETHG_0736	Glycosyl transferase group 1	Membrane	-1.30	**-2.60**	-1.30	3	9.6
Others								
	CAETHG_0280	AroM family protein	Cytoplasm	0.42	**2.16**	1.75	6	37.1

Table C.2. (continued).

CAETHG_2068	Cupin 2 conserved barrel domain protein	Cytoplasm	1.13	**-2.25**	**-3.37**	4	45.9
CAETHG_3997	Cupin 2 conserved barrel domain protein	Cytoplasm	**2.42**	**4.45**	**2.03**	4	61.2
CAETHG_0484	Cyclase family protein	Cytoplasm	-0.12	**-4.64**	**-4.52**	6	32.4
CAETHG_0230	Formiminotransferase-cyclodeaminase (EC 4.3.1.4) (Glutamate formimidoyltransferase) (EC 2.1.2.5)	Cytoplasm	0.14	**2.79**	**2.66**	3	17.5
CAETHG_1906	GlmL (Uncharacterized protein)	Cytoplasm	**2.55**	**5.52**	**2.97**	12	40.6
CAETHG_1832	Microcompartments protein	Cytoplasm	1.77	**4.13**	**2.36**	1	13.3
CAETHG_0572	MOSC domain containing protein (Molybdenum cofactor sulfurase-like protein)	Cytoplasm	0.66	**2.05**	1.39	4	36.4
CAETHG_0019	Phenazine biosynthesis protein PhzF family	Cytoplasm	0.46	-1.80	**-2.27**	6	37.7
CAETHG_2335	Protein tyrosine phosphatase (EC 3.1.3.48)	Cytoplasm	1.90	-1.47	**-3.37**	1	7.9
CAETHG_0199	Uncharacterized protein	Cytoplasm	1.50	**-3.83**	**-5.34**	3	22
CAETHG_0751	Uncharacterized protein	Cytoplasm	0.37	-1.73	**-2.10**	2	5.7
CAETHG_0752	Uncharacterized protein	Cytoplasm	0.51	-1.65	**-2.16**	3	10.3
CAETHG_0886	Uncharacterized protein	Cytoplasm	0.52	-1.54	**-2.06**	8	66
CAETHG_1095	Uncharacterized protein	Cytoplasm	0.95	-1.63	**-2.58**	3	29.6
CAETHG_1096	Uncharacterized protein	Cytoplasm	1.18	**-3.34**	**-4.51**	3	19.1
CAETHG_1678	Uncharacterized protein	Cytoplasm	1.11	**3.98**	**2.87**	2	13.2
CAETHG_2281	Uncharacterized protein	Cytoplasm	1.20	**-3.55**	**-4.75**	7	17.4
CAETHG_2375	Uncharacterized protein	Cytoplasm	0.02	-1.99	**-2.01**	3	17.2
CAETHG_3155	Uncharacterized protein	Cytoplasm	0.58	-1.46	**-2.04**	5	25.7
CAETHG_3984	Uncharacterized protein	Cytoplasm	0.74	**-3.86**	**-4.59**	7	19.8
CAETHG_0067	UPF0597 protein CAETHG_0067	Cytoplasm	-1.10	**-4.80**	**-3.70**	15	41.8
CAETHG_1976	UvrB/UvrC protein	Cytoplasm	1.69	-1.42	**-3.11**	2	12.1
CAETHG_2768	XshC-Cox1-family protein	Cytoplasm	1.30	**2.57**	1.27	10	35.5
CAETHG_0156	Uncharacterized protein	Membrane	-1.14	1.46	**2.61**	4	13.8
CAETHG_0281	Uncharacterized protein	Membrane	**-3.79**	1.46	**5.25**	3	17.1
CAETHG_1603	Uncharacterized protein	Membrane	**-3.53**	-0.80	**2.73**	2	12.8
CAETHG_2313	Uncharacterized protein	Membrane	-0.69	**-2.77**	**-2.09**	3	7.8

Table C.2. (continued).

CAETHG_2682	Uncharacterized protein	Membrane	0.50	**-2.07**	**-2.57**	3	9.8
CAETHG_3360	Uncharacterized protein	Membrane	**-2.22**	**-2.66**	-0.44	1	8.4
CAETHG_3357	UPF0348 protein CAETHG_3357	Membrane	-1.46	1.95	**3.41**	4	10.5